INNOVATIVE METHODS FOR THE CHARACTERISATION OF FRACTURED ROCK AQUIFERS

BY

AKOACHERE RICHARD AYUK II

THESIS

Submitted in fulfilment of the requirement for the degree of

DOCTOR OF PHILOSOPHY

In the Faculty of Natural and Agricultural Science

Institute for Groundwater Studies (IGS)

University of the Free State,

Bloemfontein, South Africa.

November 28, 2008

Promoter: Professor Gerrit. J. Van Tonder.

INNOVATIVE METHODS FOR THE CHARACTERISATION OF FRACTURED ROCK AQUIFERS

BY

AKOACHERE RICHARD AYUK II

THESIS

Submitted in fulfilment of the requirement for the degree of

DOCTOR OF PHILOSOPHY

In the Faculty of Natural and Agricultural Science

Institute for Groundwater Studies (IGS)

University of the Free State,

Bloemfontein, South Africa.

November 28, 2008

Promoter: Professor Gerrit. J. Van Tonder.

ACKNOWLEDGEMENT

During the course of my research, many people gave me assistance of which a listing is not possible, but without which this difficult task would have become impossible. To all these people I say, "THANK YOU"

- I wish to state my profound gratitude to my promoter, Professor Gerrit van Tonder, for his kindness, guidance and the rigorous supervision of this work.
- I say thank you to the Director of the Institute for Groundwater Studies, Dr Ingrid Dennis for everything.
- Dr Brent Usher, thanks for all the assistance before and during my research
- Also to the entire staff of the Institute for Groundwater Studies (I.G.S); Dr Danie Vermeulen, Dr Rennie Dennis, Dr Jennifer Pretorius, Mr Lucas Elco, Catherine Blitzer, Professor Botha Jopie, Professor Hodgson Frank. Mmes; Jane Van den Heever, Lore-Mari Cruywagen, Hennie Hoffmann and Adri Van Wyke. For their comments, confrontations, criticisms, encouragements and assistance which made this research exciting and most times challenged me to work even harder.
- I wish to thank the entire staff of the Instrumentation department. Especially Mr Stephanes Piete Bothes, for making some of my apparatus and physical models.
- Thanks to my fellow post graduate students, Mehari Menghistu (PhD) and Sakhile Mndaweni (MSc) and my fellow Cameroonians, Georges Moukodi (MSc) and Stephen Nkafu (Hons) and Nkalle-Ngwese Sydoney (LLD), for their assistance during my field work.
- My gratitude goes also goes to the Department of Water Affairs and Forests, Water Research Commission (WRC/DWAF), for the opportunity given me to be included in the "Bulk Flow Project" under which this research was funded.
- My thanks go to Dr Allen Shapiro of the US Geological Survey for his personal communications.
- Thanks to Dr (Mrs.) Akoachere Jane Frances Kihla and Ms Eyong Mary Ayuk, for their support and taking care of the children while I was away.
- Thanks to the Minister of Higher Education Professor Fame Ndongo and the Vice chancellor of the University of Buea, Professor Vincent Titanji, for granting me a study leave.

Finally, a big "THANK YOU" to God Almighty, for his blessings and mercy.

CERTIFICATION

We the undersigned, wish to certify that;

We approve the submission of this thesis by, Akoachere Richard Ayuk II, a student at the Institute for Groundwater studies, Department of Geohydrology at the Faculty of Natural and Agricultural Sciences of the University of the Free State, Bloemfontein South Africa, who has carried out this research and wrote this thesis.

Also that, this thesis has not been submitted as a whole or partially to the examiners previously.

In witness whereof, we have appended our hand below

Promoter; ..... Date.....

Professor Gerrit Van Tonder

Head of the Institute for Groundwater Studies (IGS)

..... Date .....

Dr Ingrid Dennis

DECLARATION

I, the undersigned,

Akoachere Richard Ayuk II declare that, the thesis hereby submitted by me for the degree of Doctor of Philosophy at the Institute for groundwater Studies, Department of Geohydrology, Faculty of Natural and Agricultural Sciences, University of the Free State is my own independent work and has not previously been submitted by me at another university/faculty. I further more cede copyright of this thesis in favour of the University of the Free State.

..... Date .....
Akoachere Richard Ayuk II

DEDICATION

This work is dedicated to the entire Akoachere family.

Mbu, Ndip, Oben and Bessem.

Especially to;

Akoachere Vivian Öfậ Vïshy

Akoachere Vivien Önö Vïjüng

Akoachere Tábôt Erĕm Jaqueline

Akoachere Richard Ăýůk II jr.

Akoachere Vanessa Kĕñôkô

Akoachere Ekôm Ekĕǵę Della

Akoachere Ălőrr Idwĕh Coraçon

Lastly, to my late mother Akoachere Alice Tábôt Erĕm.

CONTENT

LIST OF FIGURES

LIST OF TABLES

ABSTRACT

Bulk flow is regional flow. The word region is used in two ways viz; i) A region may be a hydrogeologically and geographically distinct area. Ex: the Karoo basin. ii) A region maybe discontinuous but widespread encompassing related non adjacent aquifer systems such as surficial aquifers, coastal aquifers or as in our research project study case, some selected fractured rock aquifers in South Africa. In case (ii) regions, topical investigations are optimized for regional applications. In such investigations, focus is on processes rather than properties of specific aquifers (Groundwater science). Characterization tends towards common processes (drivers of the various processes) rather than geographical locations and particularities. Two new methods have been developed to determine inclined and horizontal fracture apertures **b**, in fractured rock aquifers. These methods are; i) The SLUG-TRACER (ST) TEST ; ii) The NAPL ENTRY PRESSURE (NEP) TEST/ NAPL INJECTION PRESSURE (NIP) TEST. Mathematical formulations were developed from laboratory experimentation using transparent Perspex parallel plate physical models and 27 apertures of 0.008 mm to 6 mm, created by using aluminum foil and thickness gauges between 20 mm thick clamped Perspex plates. The ST test uses a slug in which is added NaCl as tracer (500mg-5000 mg/l) and an EC meter is used to detect breakthrough in the observation boreholes. The NEP test uses a NAPL (Sunflower oil) hydraulic head and transducers to get the entry pressure. Using these mathematical formulae, fracture apertures are then determined for horizontal and inclined apertures. The NIP test uses the entry pressure recorded by transducers, of a NAPL (Sunflower oil) by injection and its volume to determine the fracture aperture for horizontal and inclined fractures. Results from smooth and rough (Buffed to 10x20 microns) fracture surfaces gave accurate results for 96-98 % aperture determinations of twenty six (26) apertures from 0, 04 mm to 6.3 mm.

The Phreatic Hydraulic Conductivity (PHC) apparatus was developed to measure

the hydraulic head gradient of samples. The PHC apparatus was made of a solid body divided into three chambers, mounted on a ten liter capacity water reservoir, with a pump. Three types of samples can be used; Consolidated (*in-situ*), loose/friable (*in-situ*), and unconsolidated samples (Drill/auger cuttings, Mine tailings/ash etc.). The apparatus was used to determine hydraulic conductivities of samples ranging from coarse gravel to very fine clayey dam tailings. The values ranged from 2.81E-03 to 4.32E+03 (m/d). The results were reproducible and compared well with those of other methods. The PHC apparatus' advantages are: Can be used in the field and laboratory (compact); Simple to use and needs limited maintenance (Three components); Economical, needing small volumes of water (ten liters); Light (6kg) and compact (0.16 m^3); Rapid results (Complete determination for a sample within tens of minutes); This apparatus is particularly suited to determine the hydraulic conductivity of clastic formations for non-confining flow under atmospheric conditions.

Laboratory experiments on the small (cm) scale aimed at determining the effect of variable thickness of formations on the hydraulic conductivity, determine the effect of composition, layering ,spatial disposition and develop a tool for predicting bulk hydraulic conductivity in phreatic aquifers were carried out. From these, the partial hydraulic conductivity formulation was developed empirically, to determine the bulk hydraulic conductivity of the samples, irrespective of the spatial disposition. With geologic insight, the bulk hydraulic conductivities were determined using the partial hydraulic conductivity theory. When the thicknesses of the layered sequences varied, the laws of composition broke down.

The Trigger-tube is an apparatus developed for mixing solutes and tracers for injection tests in boreholes. It is a simple cap-trigger tube segment and the technique mixes solutes in boreholes in two minutes. Solutes are introduced into the well and the trigger is released. The tube is withdrawn and the solute mixes instantaneously to give

a homogeneous mixture of solute with the borehole groundwater. Field tests using this method and apparatus for point dilution tests gave a Darcy velocity of 4.06 m/day, Seepage velocity of 122.89 m/day and effective porosity of 0.33. Natural gradient tests gave a Darcy velocity of 4.06 m/day and natural velocity of 123 m/day using NaCl for the same fracture at 21m in borehole UO5. This apparatus takes comparatively a shorter time to carry out SWIW tests than using the pump mixing method. Field tests gave 13 minutes for the trigger-tube method and 25 minutes for the pump mixing method for a point dilution test using NaCl. This apparatus can be used for any test that needs the introduction of a homogenous mixture in single well tests.

The thermal dilution test is a test developed to determine the position, number and groundwater (Darcy) velocity of fractures found in a single borehole drilled into a fractured rock aquifer using temperature as a tracer. Using a trigger-tube apparatus, cold at 2 degrees Celsius is introduced into a single well. The rate at which warmer groundwater flows into the well is measured as the change in temperature and used to determine flow zones, the position of fractures, their depths and the Darcy velocity of the various lithologies and fractures with flow present, from top to bottom of the borehole the method was used in a single well test on borehole UO5 to determine fractures at 14m, 15m, 16.8m, 18m, 19.4m, 21m, 22.4m, 24.2m,26m and 27.5m below the surface. These fractures had Darcy velocities ranging from 1.54m/day to4.17m/day, with the largest fracture contributing to flow in the borehole being that at 21m. This was confirmed by acoustic scan and borehole camera images of the borehole. This method is very useful to determine the hydraulic properties of fractures and formations under natural conditions (Without pumping) using a single well.

1.0 *INTRODUCTION*

Darcian flow assumes flow through unconsolidated particulate matrix but where there are fractures in a formation and these are saturated, the fractures become conduits for flow of groundwater. Being easier flow paths, fracture or conduit flow becomes dominant and flow by-passes the denser, tortuous unconsolidated or consolidated matrix. Such aquifers are referred to as fractured rock aquifers. To characterize such fractured rock aquifers entails to identify, describe and define the components of their flow systems which are;

- Geology and geometry of aquifer
- aperture size
- fracture distribution

According to EPA studies (EPA, 2001), fractured rock aquifers are among the most complex because of their considerable geologic heterogeneity and the nature of fluid flow and contaminant transport through fractured media. Relative to most unconsolidated deposits, characterization of contaminant migration in fractured rock usually requires more information to provide a similar level of understanding. The complexity of contaminant source conditions also makes remediation more difficult. Therefore, there is a need to improve and augment current technologies applicable to fractured rock aquifers.

For hydrogeological studies in fractured rock, it is the discrete fracture pathways, rather than the total fracture network, which are important. To be of hydraulic significance, fractures must be both conductive and sufficiently interconnected to serve as part of a pathway. Only some subsets of open fractures will have active groundwater flow, and a small number of transmissive fractures may dominate. The challenge in

application of innovative characterization technologies in fractured rock aquifers is to locate the significant fractures and apply technologies in a way such that measurements properly reflect in-situ conditions without perturbations.

Geological characterisation at fractured rock sites includes use of conventional techniques such as outcrop mapping, fracture trace analysis, drilling, coring, and, more recently, increased use of borehole geophysics. Drilling boreholes remains the principal means of geological characterization and, because it is generally slow and expensive, contributes significantly to characterization costs. The majority of holes are vertical; inclined drilling is also used, albeit less frequently, to intersect and sample vertical or near-vertical features. In addition, there is concern that drilling activities may create a conduit for cross-contamination by drilling through previously isolated fractures and, at DNAPL sites, may risk mobilisation

Collection and analysis of ground-water samples from monitoring wells is the most common method of chemically characterising the extent of contamination at fractured rock sites. Like hydraulic testing, chemical characterisation of fracture pathways involves collecting samples from specific vertical intervals of the borehole. These intervals may be isolated using packer assemblies in open boreholes, completion of monitoring wells over specific intervals in well clusters, or installation of multi-level monitoring assemblies. Multi-level monitoring assemblies designed for dedicated use in boreholes are commercially available. Non-permanent (re-usable) systems with inflatable packers or continuous borehole liner/sampling systems are among the most recent developments and are in the early stages of real-site application. The use of such techniques as temporary monitoring assemblies, or chemical profiling during drilling, may help to optimize sampling location and monitoring well design and significantly reduce the capital costs of sampling.

Conventional wire-line logging methods, such as calliper, fluid logs (temperature, conductivity), EM conductivity, and gamma logs, are the most commonly used geophysical tools. They are used in combination with core logging or optical and acoustic imaging methods to assist in mapping of geology and fracture zones, and to extend geologic correlation between boreholes. Recently, borehole applications have expanded to include improved methods of imaging the borehole and identifying which fracture zones have active flow. More recent techniques are television / tele-viewer methods (acoustic and tele-viewer), and flow meters (heat-pulse and EM

This research was carried out to create new knowledge and apparatus useful for the description of the characteristics or nature of fractured rock aquifers. Analysing their flow systems, flow processes, measuring their flow parameters and throwing more light on their bulk flow properties. This work was done in two parts;

- Laboratory experimentation. Here, the solution to some aspects of characterisation of fractured rock aquifers was sought from laboratory experimentation on samples using designed and built apparatus and physical models. The results of these experiments were then analysed to give new insight into the geohydrological phenomena. Some of the results were then tested in the field.
- Field experimentation. In this part of the work, the results of laboratory experiments and/or novel theoretical concepts were carried out in the field with designed field experiments, apparatus and/or with standard tests, to confirm or prove the validity and application of such concepts.

The results of this effort lead me to create two new apparatus and four new techniques/methods in the characterisation of fractured rock aquifers. These results

from the laboratory and field research are organised below in separate chapters in the order in which they were carried out and/or submitted for publication.

In chapter two, two new methods where developed to determine directly, fracture aperture in fractured rock aquifers important for flow parameter quantification.

In chapter three, a new apparatus was developed to determine the hydraulic conductivity of clastic formations associated with fractured rock aquifers over distances from meters to kilometres.

In chapter four, a new theory was proposed to determine large scale hydraulic conductivities from point measurements.

In chapter five, a new apparatus was developed to deliver in a clean manner, solutes into wells for carrying out point dilution tests (Tracer tests) more accurately.

In chapter six, a new method was developed to determine flow zones, fracture positions, their depth and the Darcy velocity of fractures in fractured rock aquifers using temperature as a tracer.

Chapter six gives the conclusion on the research and recommendations.

FIELD TEST SITE

1.1 Geology of the Campus Test Site

The Campus Test Site at the University of the Free State is the test site for postgraduate students covering an area of approximately 180x192m. To date thirty percussion and seven core-boreholes have been drilled (Fig.1). Many projects sponsored by the Water Research Commission of South Africa have used this site for research on (a) Karoo Aquifers (Botha *et al.*, 1998) and (b) tracer tests in fractured aquifers (Van Wyk *et al.*, 2000; Van Tonder et al (2000).

The Campus Test Site is underlain by a series of mudstones and sandstones from the Adelaide Subgroup of the Beaufort Group of formations in the Karoo Sequence. Mapping of geological outcrops around the Campus Site reveals the existence of extensional fractures (Mode I) and shearing fractures (Mode II). The dominant type of fractures recognized in the sediments includes sub-horizontal bedding-parallel fractures and orthogonal and diagonal fractures with dominant north-west, north-east and east-west rends.

Five of the seven core-boreholes were drilled vertically and two at an angle of 45 degrees. The two north-easterly fractures detected in core-boreholes CH6 and CH7 are the only sub-vertical structures intersected during the core drilling and both were calcified. The geological column of the Campus site can be subdivided into five different easily recognizable rock units, each characterized by a unique assemblage of rock types and structures. These litho logical units may be subdivided into different lithofacies.

The vertical lithofacies represent vertical accretion of deposits in flood-plains (mudstone and siltstone facies), shallow lakes (rhythmite facies) and channels (sandstone facies). A major feature of the core samples is the large number of bedding-parallel fractures whose frequency decreases downward from the upper, more weathered zone, as thicker and more competent units are encountered. The bedding plane fractures in the upper, more weathered part are often transected by large number of orthogonal, oblique and diagonal fractures. These fractures clearly represent secondary fracturing of the rock mass caused by the post-lithification process. The Mode I fracture is the most significant fracture on the Campus Site and all boreholes with high yields (11 have yields in excess of 3 l/s) intersected this bedding-plane fracture.

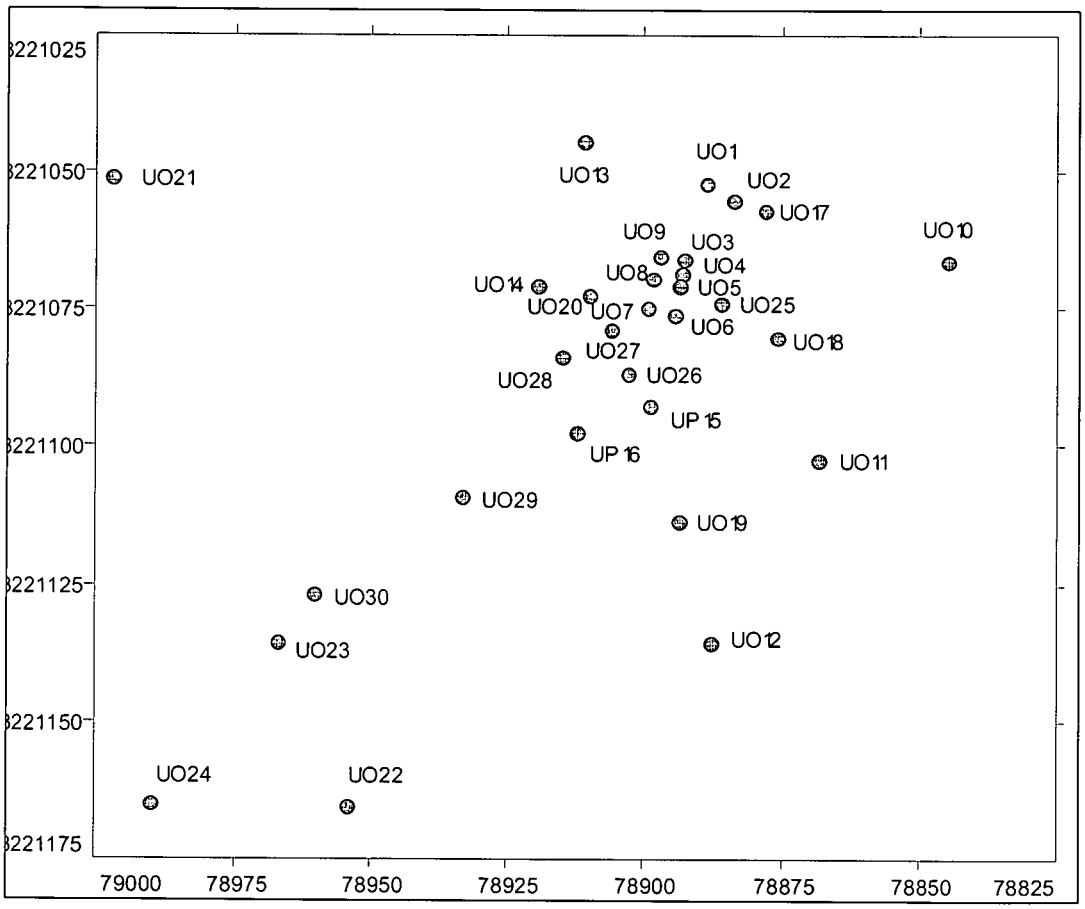

Figure1. Map of the University of the Free State Campus Test Site, showing borehole UO5 and borehole UO7. (Botha *et al.*, 1998)

The yields of the other 19 percussion boreholes are less than 0.6 l/s because the Mode I fracture was not intersected during drilling. The acoustic scan and borehole video of borehole UO5 show that the Mode I fracture, which is situated at about 21 m below surface, consists of a fracture zone with a thickness that varies between less than 1mm and 100 mm.

A very dominant layer of black shale at about 13 meters below the surface forms an aquitard between the top mudstone and the bottom sandstone layer (which could thus be viewed as semi-confined). There are three aquifers present on the Site. The top, a phreatic aquifer, occurs within the upper mudstone layers on the Site. This aquifer is separated from the middle and main aquifer, which occurs in a sandstone layer between 8 and 10 m thick, by a layer of carbonaceous shale with a thickness of 0.5 – 4 m. The bottom aquifer occurs in the mudstone layers (more than 100 m thick that underlies the sandstone unit (Botha *et al.*, 1998).

2.0 *TWO NEW METHODS FOR THE DETERMINATION OF HYDRAULIC FRACTURE APERTURES IN FRACTURE ROCK AQUIFERS*

2.1.0 INTRODUCTION

All aquifers can be considered to fall on a continuum between porous media systems and conduit systems. In porous media aquifers, groundwater flows through the voids in the formations. In fractured media groundwater flows mainly in conduits, and the aquifer matrix between the conduits is impermeable and has no porosity. In fractured porous media (formations in which the matrix is porous and the formation is fractured) water is also stored in the aquifer matrix between the conduits. In some cases, the matrix permeability is negligible, although in other cases it can contribute significantly to flow. In reality, most fractured rock aquifers are of the fractured porous media type. Models of groundwater flow, however, usually assume either homogeneous porous media or purely fractured media. Furthermore, models of groundwater flow in purely fractured systems usually assume that fractures are planar and parallel and many also assume that the fractures are identical. While these assumptions are unlikely to be true in reality, they provide a useful starting point for our understanding of groundwater behavior in fractured rocks. Fractured rock aquifers are comprised of a network of fractures that cut through a rock matrix. Characterization of fractured rock aquifers thus requires Information on the nature of both the fractures and the rock matrix. Fractures can be characterized in terms of their dimensions (aperture, length, width), their location (orientation, spacing, etc) and the nature of the fracture walls (e.g., surface roughness). The rock matrix is characterized by its pore size distribution, often expressed in terms of porosity. The fracture porosity (m_f) is defined as the total volume

of the aquifer occupied by open fractures. The matrix porosity (m) is the porosity of the rock matrix. In most csases, $m_f >> m$. The total porosity (m_t) is given by: $m_t = m_f + m$. Fractures are planes along which stress has caused partial loss of cohesion in the rock. Conventionally, a fracture or joint is defined as a plane where there is hardly any visible movement parallel to the surface of the fracture; otherwise, it is classified as a fault. In practice, however, a precise distinction may be difficult, as at times within one set of fractures some planes may show some displacement whereas others may not exhibit any movement. Fractures can be classified in several ways based on their geometric relationship with bedding or foliation. Strike joints are those that strike parallel to the strike of the bedding or foliation of the rock. In dip joints, the strike direction of joints runs parallel to the dip direction of the rock. Oblique or diagonal joints strike at an angle to the strike of the rock. Bedding joints are parallel to the bedding plane. Further, depending upon the strike trend of fractures with respect to the regional fold axis, fractures are designated as longitudinal (parallel), transverse (perpendicular) or oblique (Singhal & Gupta, 1999).

The relationship between fractures and the stresses that form them are discussed in most structural geology texts. Sheeting joints are generally flat, or somewhat curved and nearly parallel to the topographic surface, and often develop due to release of overburden stress in granitoid rocks. They are closely developed near to the surface and their spacing increases with depth. Columnar joints are generated due to shrinkage in rocks; igneous rocks contract on cooling, whereas mud and silt shrink because of desiccation. As a result, polygonal and columnar joints develop. The columns are often five- or six-sided, generally range from a few centimetres to a metre in diameter, and are several metres high. In some cases, fractures become filled with minerals or clay deposits. Where they remain open however, they can form channels for groundwater flow. If the hydraulic gradient is constant, then the mean water velocity through a

fracture (averaged over the fracture width) will increase as the distance between the walls increases. The mean velocity will also be greater if the fracture walls are flat and smooth, rather than irregular and rough.

While groundwater flow in fractured porous media occurs mainly through fractures, much of the water contained within these aquifers is stored within the matrix. This has important implications for the movement of contaminants or other dissolved substances. Even if the permeability of the matrix is very low, diffusion will cause mixing of solutes in water flowing through the fractures with those in the relatively immobile water in the rock matrix and pockets of no-flow-through fractures.

In practice, this means that dissolved substances usually appear to travel more slowly than water. Experimental studies have observed that very large particles (glass beads and bacteriophages) may travel very quickly (because they move through the fractures and do not readily enter the small pores within the matrix), while smaller solutes (including most ions) move more slowly. For example, in fractured shale near Oak Ridge, Tennessee, velocities of small glass beads have been measured to be up to 200 m d-1 (McKay *et al.*, 2000). In southern Ontario, Canada, bacteriophages have been observed to travel at 4 m d^{-1}, while dissolved bromide travels at only 0.04 m day^{-1} (McKay *et al.*, 1993). This movement of solutes between the fractures and the matrix is referred to as matrix diffusion. It causes smaller molecules to appear to move more slowly than larger molecules, depending on their diffusion coefficients.

Early attempts to simulate flow in fractures described them as consisting of two parallel plates. The term 'mechanical aperture' is used to describe the aperture of a fracture measured directly using various length determining devices, while hydraulic aperture is the aperture derived from tests using fluid flow properties in fractures. Renshaw (1995) concluded that, for large apertures, hydraulic and mechanical apertures have similar values, but the relationship between the two is non-linear and

breaks down for smaller fracture apertures, where fracture apertures approximate the scale of the fracture-surface roughness. Some other authors support the hypothesis that mechanical apertures and hydraulic apertures are not equal (National Research Council, 1996).

A number of authors have attempted to determine fracture apertures using two types of fracture aperture determinations:

a) Laboratory methods and,

b) Field methods.

2.1.1 LABORATORY METHODS

- Nuclear magnetic resonance imaging (NMRI) (Dijk *et al.*, 1999),
- Light transmission methods (LTM)(Nicholl *et al.*, 1999),
- Silicon injection (SIN) (Yeo *et al.*, 1998),
- Resin injection (RIN) (Hakami & Larsson, 1996; Konzuk *and Kueper*, 2004).
- Computer-aided tomography (CAT) (Keller, 1998),

2.1.2 FIELD METHODS

There are two types of field methods;

i) Direct Measurements, and

ii) Indirect measurements.

2.1.2.1 Direct Measurements

a) Fracture spacing - This is the measurement of the distances between fractures using rulers, callipers, sonar devices etc.

b) Fracture orientation - Measuring the characteristic orientation of the fracture plane. Dip, strike etc.

2.1.2.2 Indirect Measurements

i) The mass balance aperture.

This is derived from the mean residence time of a tracer, the flow rate, fracture geometry and the tracer test breakthrough (Tsang, 1992).

ii) Frictional loss aperture.

This is determined by expressing the mean residence time of the tracer in terms of the transport velocity.

iii) Hydraulic aperture.

-Measurements of bulk permeability were converted to equivalent hydraulic aperture in slug tests (Hvorslev,1951; Rutqvist,1996). This required assumptions regarding the number of fractures encountered.

-Injecting NAPLs and back-calculating the apertures from the entry pressure required to initiate flow (Steele et al, 2006).

-Hinsby *et al.*, (1996), Jorgensen *et al.*, (1998), Reitsma & Kueper, (1994), calculated aperture distribution for rough-walled fractures by correlating capillary pressures observed during NAPL injection, with local apertures in the fracture plane.

The mass balance aperture is greater than or equal to the hydraulic aperture, which in turn is greater than or equal to the frictional loss aperture (Tsang, 1992).

2.2.0 THE NEW METHODS

In our quest to completely characterize the University of the Free State campus test site, two new methods for the direct determination of the fracture apertures in fracture rock aquifers were developed. As of the time of writing this report, the two methods below are the only direct methods that can be used to determine the apertures of fractures in saturated fracture rock aquifers. The two new methods are;

a) The SLUG-TRACER TEST

b) The NAPL ENTRY PRESSURE TEST/ NAPL INJECTION TEST.

2.2.1 The Slug-tracer (ST) test

This test is for the determination of the hydraulic aperture of fractures in saturated fracture aquifers.

2.2.2 The NAPL entry pressure (NEP) test

This test is for the determination of the apertures of fractures in saturated fracture aquifers.

2.2.3 The NAPL injection pressure (NIP) test

This test is also used for the determination of the hydraulic aperture of fractures in saturated fracture aquifers.

2.3.0 MATHEMATICAL FORMULATIONS

2.3.1 The ST-TEST

Consider a borehole in a fracture aquifer with a horizontal saturated aquifer. For a cylindrical tube in the borehole of radius **r**, the volume of fluid in the cylinder of column height **h** is **V**.

$V = \pi r^2 h$ ..... (1)

Consider a cylindrical section of the fracture of radius **R**, with an aperture **b**, in the borehole. If the volume of this cylindrical slice of the fracture in our cylindrical section of the fracture above is V_b;

$V_b = \pi R^2 b$ ..... (2)

If a slug of fluid is released from the cylinder in the borehole and the fluid flows into the fracture with aperture **b**, at a certain time **t**, the fluid will be displaced to the point **R**, and there will be a change of height Δh of volume V_h in the cylinder in the borehole. At that time **t**, fluid flowing from the cylinder through the fracture, will reach the point **R** and there will be a change of head Δh of volume V_h.

$V_h = \pi r^2 \Delta h$ ..... (3)

At this time **t**,

$V_h = V_b$, $\pi r^2 \Delta h = \pi R^2 b$ ..... (4)

$[b = (r^2 / R^2) \Delta h.]$ ..... (5)

Where **b** is the fracture aperture, **r** is the radius of the borehole and **R** is the distance from the centre of the borehole to the point of observation of flowing liquid from borehole.

Principles

This is based on the principles of;

a) conservation of mass and

b) Volume transfer.

A fixed cylindrical volume of fluid is transferred and conserved from the cylindrical tube in the borehole on the left to, the cylindrical disk to the right in the fracture of thickness b. Fig2.1.

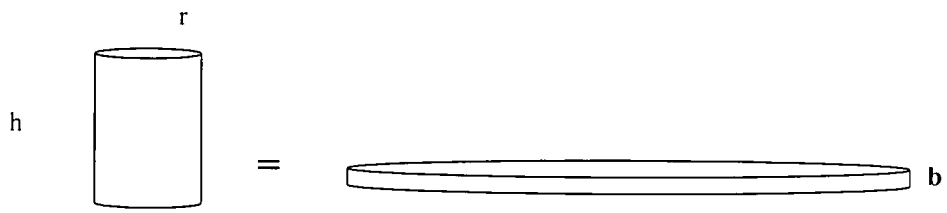

$V_h = \pi r^2 \Delta h.$ = $V_b = \pi R^2 b.$

2.3.1.1 ASSUMPTIONS

As with other measurements of the hydraulic properties of rock masses that assume radial symmetry, such as pump tests, the slug-tracer tests' results must be understood in terms of the model used. These tests are carried out with the following assumptions.

i) The fracture behaves as a parallel plate.

ii) Flow is radial and divergent

iii) There is only a single fracture within the test segment.

iv) The fracture and rock mass are rigid and the matrix is impermeable.

v) The fracture aperture varies along the radius and is radically symmetrical about the borehole.

vi) Advection, dispersion and diffusion are negligible due to the limited time and high velocities at play.

vii) Bulk flow with laminar, turbulent, preferred and non-preferred flow paths as in natural fractures.

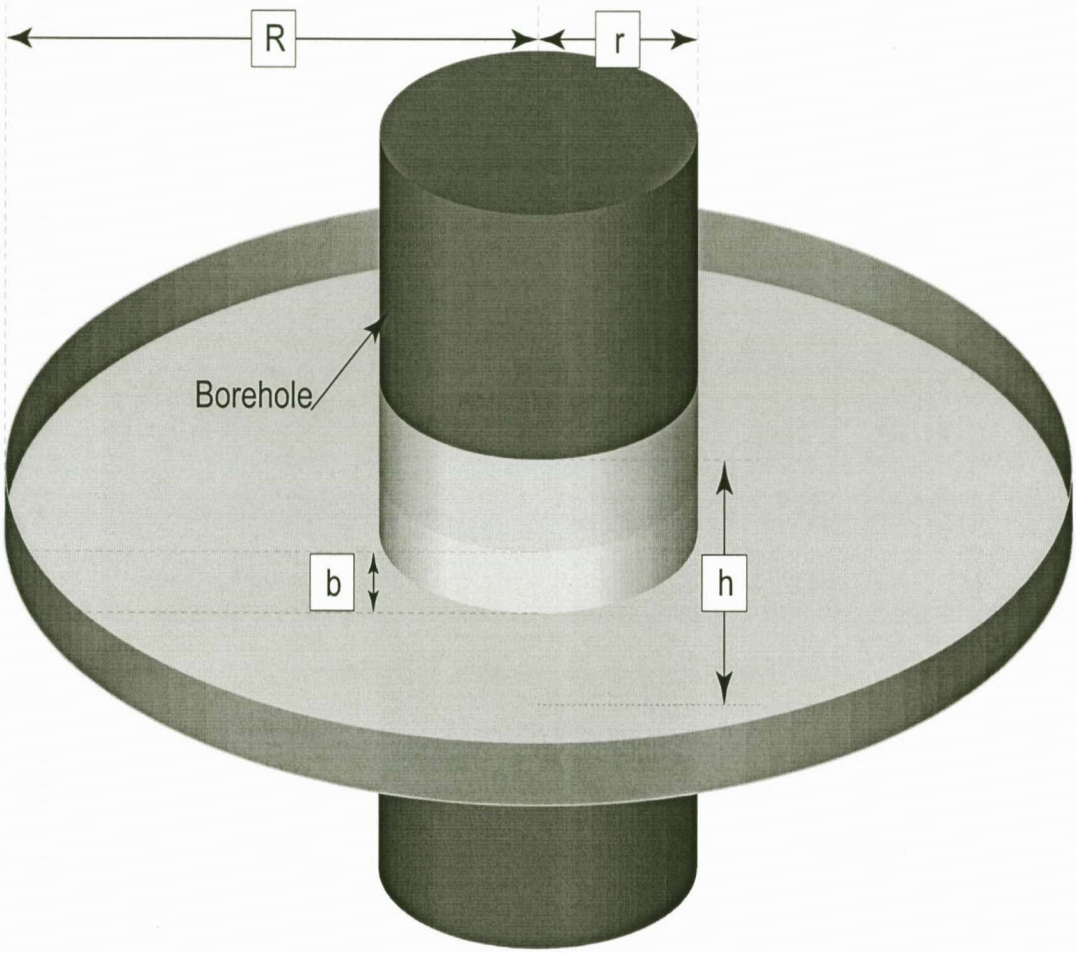

Figure2.1 Schematic diagram of fluid flow inside fracture and borehole; the sky-blue fracture volume corresponds to purple volume change in borehole. Aperture b, borehole radius and radius of flow at time t, R.

2.3.1.2 APPARATUS

i) Two packers.

ii) A pump or compressor.

iii) Two transducers.

iv) EC meter.

v) A segment of perforated cylindrical piping.

vi) An un-perforated cylindrical piping.

vii) A stopper valve.

viii) Water in which we add sodium chloride (slug-tracer). It is advisable to use water from the test borehole in order to reduce potential sources of pollution.

ix) A borehole camera.

2.3.1.3 PROCEDURES

Borehole parameters

Measure the observation and test borehole dimensions; Diameter, height above mean sea level, casing height, static water level and the depth of the fracture whose aperture is to be measured. Distance between test borehole and observation borehole and the inclination of the fracture to the horizontal.

Slug parameters

Measure the parameters of the slug and apparatus; The amount of tracer (NaCl) in the slug water is determined by considering the background EC value, the dilution rate in the borehole and the detection limit of the EC meter to be used. The diameter of

cylinder used to deliver the slug between the packers is D (= 2r), packer distance apart (L), length of perforated pipe between the packers below static water level, length of un-perforated pipe above the upper packer.

Process

At the sealed lower end of the cylinder, attach the packers with the required spacing to contain the transducer and isolate the fracture between them. Attach the outer transducer above the upper packer. Couple the necessary number of pipes to make up the depth of the borehole. Attach the stopper valve at the section between the un-perforated and the perforated cylinder. Place the inner transducer in the perforated cylinder. Couple the perforated and un-perforated cylinders. Insert the assembly above into the borehole. Fix the assembly solidly to the borehole. Inflate the packers. Allow the packers to equilibrate with the hydrostatic pressure within the borehole, seen from data logger of transducer. Using a large open ended funnel, fill the un-perforated cylinder with the salted water (slug-tracer). Record the water level in the un-perforated cylinder. Note the time, date, place coordinates and test number. Open the flow valve. Record the rate of fall of head versus time of slug-tracer. Simultaneously, at the observation borehole, place the EC meter adjacent to the fracture (on same side as the test the test borehole) in the borehole. Record the arrival time of tracer, by recording the time the EC meter records a sudden surge in value.

The time at which the EC meter records the change corresponds to a time in the test borehole for a certain change in height of slug-tracer (Δh). Using the value of the distance between the test borehole and the observation borehole as R, the radius of the cylinder with the

slug-tracer r, together with Δh. and equation (5) above, the hydraulic aperture of the fracture is calculated.

2.3.2 The NEP TEST

The pressure acting on a body is equals to the force over area.

P = F/A..... (1)

Force is the mass **M** multiplied by the acceleration **a**.

F = M*a..... (2)

If the acceleration is due to gravity, then, **a** = **g**. Thus, **P** = **M*a** / **A** = **M*g** / **A**. The mass of a fluid is the volume of the fluid multiplied by the fluid's density. Thus,

M = $V \bullet \rho$ ..... (3)

This gives,

P= V ρ g /A ..... (4)

However, if the volume of fluid in a borehole of radius **r** and height **h** is **V**,

V=π **r**^{2} **h**.

Replacing **V** in (4),

P =π r^{2}h. ρ g /A .....(5)

The area of entry of a fluid into the fracture of a borehole is the circular peel around the radius **r** of the borehole. If the said fracture has an aperture **b,** the area (**A**)

over which the fluid pressure is exerted is that of the circular peel of length **L**, and width **W**. **L** will be equal to the circumference of the borehole around the fracture.

Radius = **r** length = π **D** (**2** π **r**)

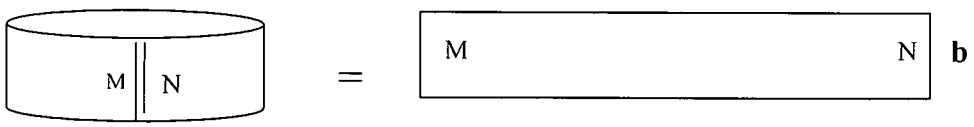

Circular peel of fracture opened circular peel

Thus,

A = Length (**L**)*Width (**W**). **L*** **W** ..... (6)

L = π *D = 2* π **r**, and **W** = **b**.

A = 2 π **r b** ..... (7)

Therefore, **P** = π r^2 **h.** ρ **g** / **2** π **r b**.

This gives,

$$\mathbf{P} = \frac{1}{2b}(\mathbf{r}\ \rho\ \mathbf{g}\ \mathbf{h}).$$

If the pressure **P** becomes equals to the entry pressure of the non wetting fluid, then **P** becomes $\mathbf{P_e}$

$$\mathbf{P_e} = \frac{1}{2b}(\mathbf{r}\ \rho\ \mathbf{g}\ \mathbf{h}).$$

$$[\mathbf{b} = \frac{1}{2Pe}(\mathbf{r}\ \rho\ \mathbf{g}\ \mathbf{h})] \quad \text{..... (8)}$$

This is the equation for the determination of the mechanical aperture of a fracture in a borehole using the entry pressure of a non wetting fluid.

$$Pe = Pnw - Pw \quad \text{..... (9)}$$

Pe is the entry pressure. Pnw is the pressure of the non-wetting fluid (NAPL), measured by transducer at entry into fracture. Pw is the pressure of the wetting fluid, water in the fracture, before the release of NAPL (Pankow and Cherry, 1996.)

2.3.2.1 APPARATUS

The apparatus are set up as in Figure2.2, with the exception of the fluid being a NAPL, Sunflower oil.

Process

The double packer assembly is set up as in the ST-TEST above, but without filling the cylindrical tube with fluid. The lower valve is removed. We pour oil into the cylinder by the use of a small tube. The oil level rises as more oil enters the cylinder. At a certain height h, the oil will enter the fracture and this will be recorded by the transducer in the cylinder and the oil level will start falling immediately entering the fracture.

The value of the entry pressure is gotten from the recorded pressures in the transducer in the packer, and **h** is gotten from the transducer in the cylinder. Using equations (8) and (9) above the aperture is calculated.

2.3.3 The NIP TEST

In certain settings, where the fracture is of shallow depth or very small, needing higher entry pressures than could not be provided by the height of fluid in the cylinder as in the NAPL test above, it is preferable for the oil injection method to be used. Pressure is the force acting over an area,

P = F/A, F = **M***a. **M** = ρ **V** and **a = g**.

F = ρ **g V** and **P** = ρ **g V/A** ..... (10)

If **A** = 2 π **r b** as in (7) above, then **P** = ρ **g V/** 2 π **r b**. Since at entry **P = Pe**, therefore, **Pe** = ρ **g V/** 2 π **r b**.

From which,

b = $\frac{1}{2Pe}$ (ρ **g V/ 2** π **r**). ..... (11)

And mass **M**, **M** = **V** ρ , thus

b = $\frac{1}{4Pe}$ (Mg / π r)..... (12)

This is the formula for the determination of the fracture aperture by injection of a NAPL.

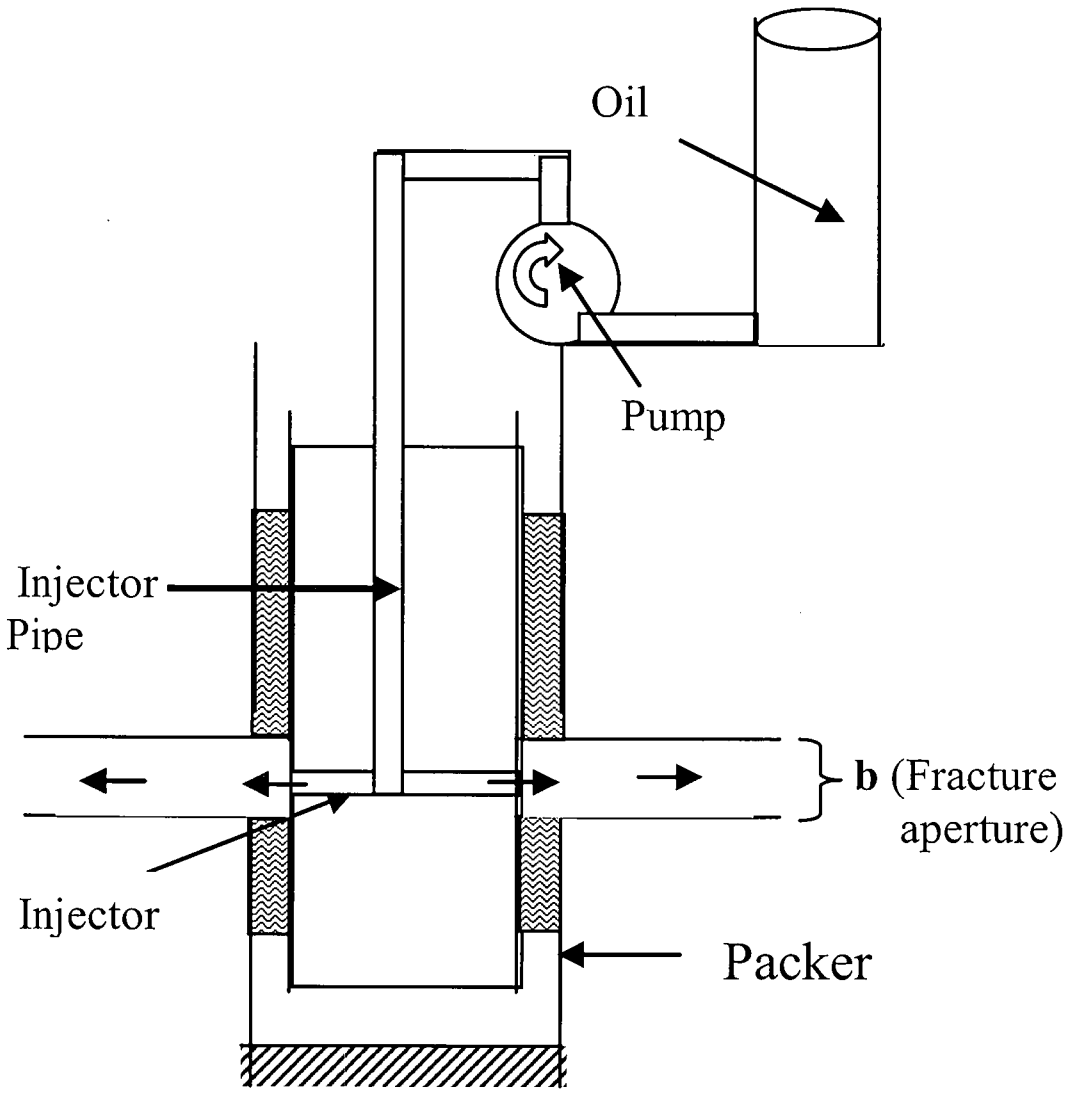

Figure2.2. Injection test using oil in NEP test.

2.3.3.1 APPARATUS

The set up is same as above with the exception that, an injector pump is used to pump the oil from the surface into the space between the double packers (Fig2.2).

Process

The injector is placed outside the open-ended un-perforated cylinder between the packers. A variable pressure oil-pump, pumps the oil from a container of known volume at a constant rate. The pressure in the inter-packer region will build up until it reaches the breakthrough entry value. The transducer will record the entry pressure value. The volume of fluid that has been pumped for the entry pressure is gotten by the difference in the volume from the container and put in (11), or by weighing the container and the difference in mass of the fluid is put in the values for the parameters in (12), to determine the value of the fracture aperture.

2.3.4 INCLINED FRACTURES

Horizontal fractures are common occurrences in fracture aquifers. Sometimes, fractures found in boreholes are inclined. The surface of the fracture in such boreholes is elliptical (Figure2.3). For the perimeter of an ellipse, there is no simple exact formula: There are simple formulas but they are not exact, and there are exact formulas but they are not simple (Jaleigh, 2000). However, there are two simple good approximations by Keppler and Ramajuan (Almkvist *et al.*, 1998) which give us accurate values within the

domain where we are applying the formula. For an ellipse with a minor axis **n**, and a major axis **m**, it has been found through laboratory experimentation that, if the inclination to the horizontal is less than forty-five degrees (45°), the value of the perimeter using Keppler's formula gives accurate values of aperture. While for inclinations above forty-five degrees to 89 %, the Ramajuan formula gives accurate results.

P = $2\pi\sqrt{mn}$ (Keppler).

P = 4m (Ramajuan).

Equation (7) above becomes, **A** = $2\pi\sqrt{mn}$ **b**, and **Pe** becomes,

Pe = π $\mathbf{r}^2$ **h.** ρ **g** / $2\pi\sqrt{mn}$ **.b.**

Thus,

b = $\frac{1}{2Pe}$ ($\mathbf{r}^2$ **h.** ρ **g** / $\sqrt{mn}$). ..... (12)

for fractures having inclinations less than forty-five degrees (45°) to the horizontal.

Or,

b = $\frac{1}{2Pe}$ (**V** ρ **g** / $\pi\sqrt{mn}$)..... (13)

for fractures with inclinations less than forty-five degrees (45°) to the horizontal by fluid injection. While, equation (7) becomes A = 4mb and Pe becomes,

Pe = π r^2 h. ρ g / 4mb.

Thus,

b = $\frac{1}{4Pe}$ (π $\mathbf{r}^2$ **h** ρ **g**) / **m**. ..... (14)

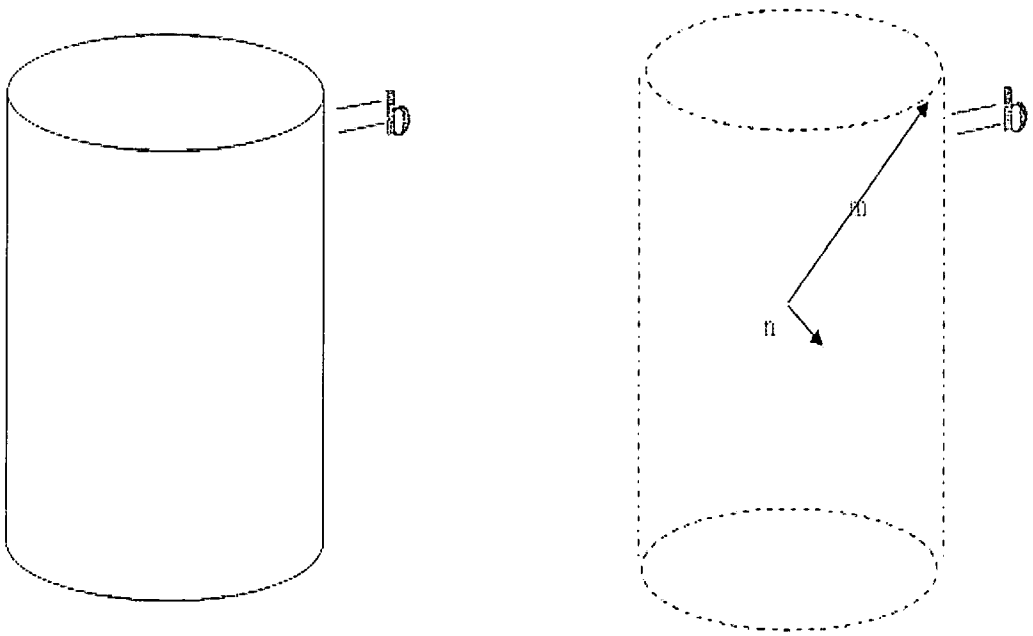

(a)Borehole with inclined fracture

(b) Surface of fracture

Figure2.3. Inclined fracture in borehole. Note the ellipsoidal surface resulting from the aperture of the fracture.

For fractures having inclinations more than forty-five degrees (45°) to the horizontal (NEP TEST)

Since $\mathbf{V} = \pi\ \mathbf{r}^2\ \mathbf{h}$,

$$\mathbf{b} = \frac{1}{4Pe}(\mathbf{V}\rho\ \mathbf{g}) / \mathbf{m} \quad \text{..... (15)}$$

The mass of fluid during injection is **M**, $\mathbf{M} = \mathbf{V}\rho$, where **V** is volume and ρ, is density of fluid. Equation (14) becomes,

$$[\mathbf{b} = \frac{1}{4Pe}(\mathbf{M}\ \mathbf{g}) / \mathbf{m}] \quad \text{..... (16)}$$

for fractures with inclinations more than forty-five degrees (45°) to the horizontal by fluid injection (NIP TEST).

A fracture in a borehole with an inclination of zero degrees (less than 45°), a minor axis **r** and a major axis **r**, will have a perimeter **P**. $\mathbf{P} = 2\pi\sqrt{rr} = 2\pi\mathbf{r}$. This is the perimeter of a horizontal circular fracture. The circle is a special form of an ellipse with its major and minor axis equal.

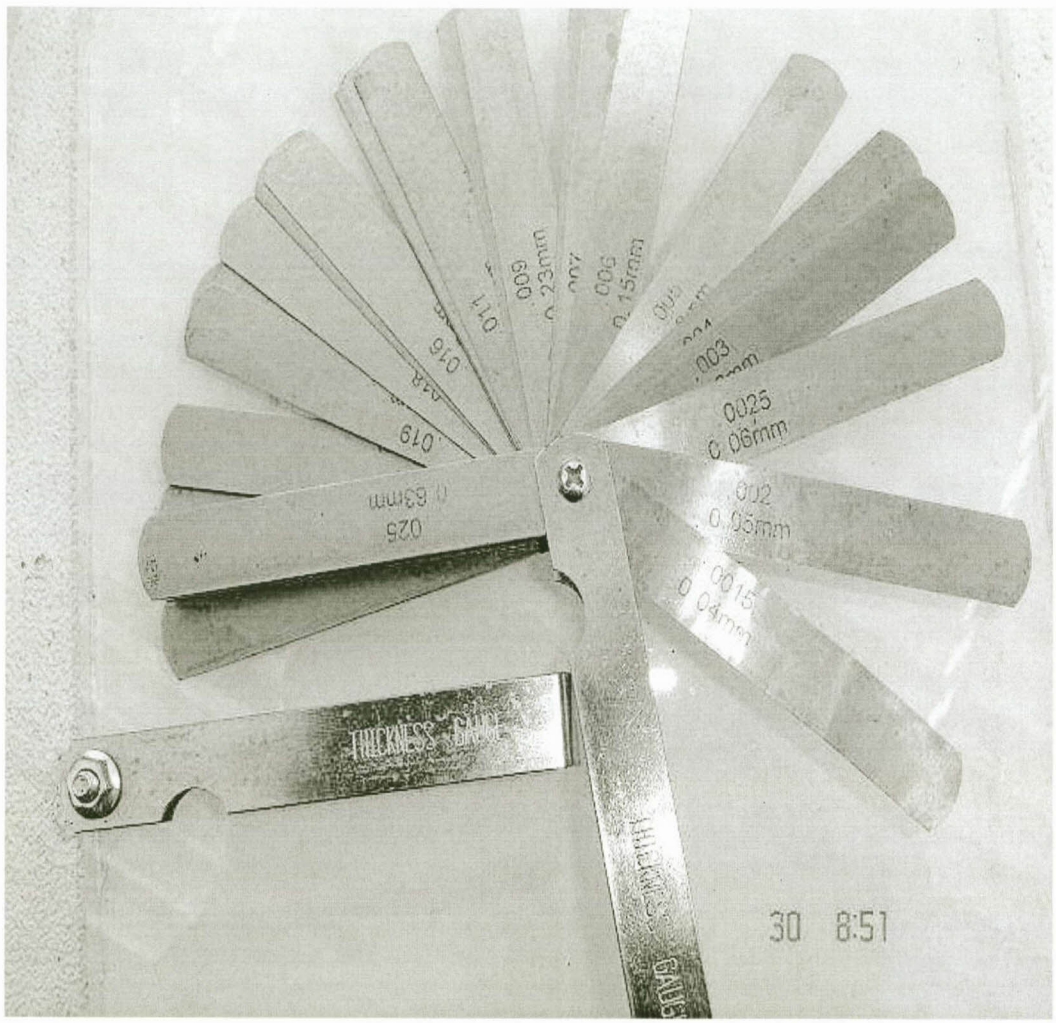

Figure2.4. Thickness (Feeler) gauge with the thickness of the blades printed on it. The blades are clamped between Perspex sheets to create fractures whose apertures are those of the blade.

2.4.0 LABORATORY EXPERIMENTS

2.4.1 APPARATUS

Parallel plate physical models to replicate fractures in fractured rock aquifers were built using two 20mm thick Perspex plates sand witching gauge blades of known thicknesses (Fig2.4). Two such models were constructed. One made of 100mm diameter circular Perspex plates (Figure2.5). The other was made of 100cm by 100cm square Perspex plates (Figure 2.7& 2.8).

A fracture of known aperture was created by clamping the Perspex plates together and sand-witching thickness gauge blades Figure2.4. On one of the two Perspex plates, a 10mm bore was drilled and a 10mm diameter Perspex tube was glued to the Perspex plate to represent the borehole. The whole apparatus now represented a fractured rock borehole. Using the above listed method and procedure, the aperture determination experiments were carried out.

The distance between test and observation borehole was taken as the diameter of the circular Perspex plate or the edge of the square plate (**R**). The radius of the Perspex tube was taken as the radius of the borehole (**r**). The change in fluid level in the tube was $\Delta \mathbf{h}$. The time taken for the water to move from the centre of the apparatus to the edge (**t**) was recorded.

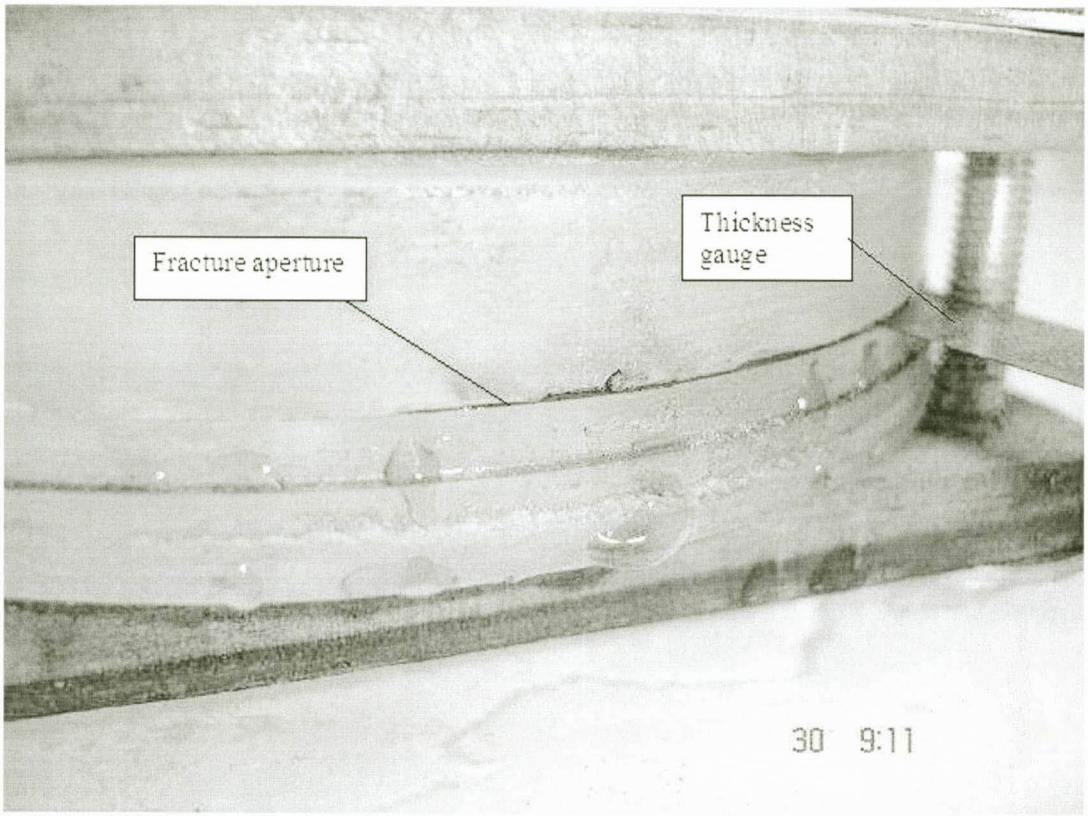

Figure2.5. Fracture aperture between two circular 100mm diameter Perspex plates Note the clamped thickness blade

Figure2.6. Laboratory apparatus for the fracture aperture determination experiment using blue colored water, Note the clamped thickness gauge blades to create the fracture aperture between two circular 100mm diameter Perspex plates.

Figure2.7. Laboratory apparatus for the fracture aperture determination experiment: Note the clamped thickness gauge blades to create the fracture aperture between two circular 100cm x100cm square Perspex plates.

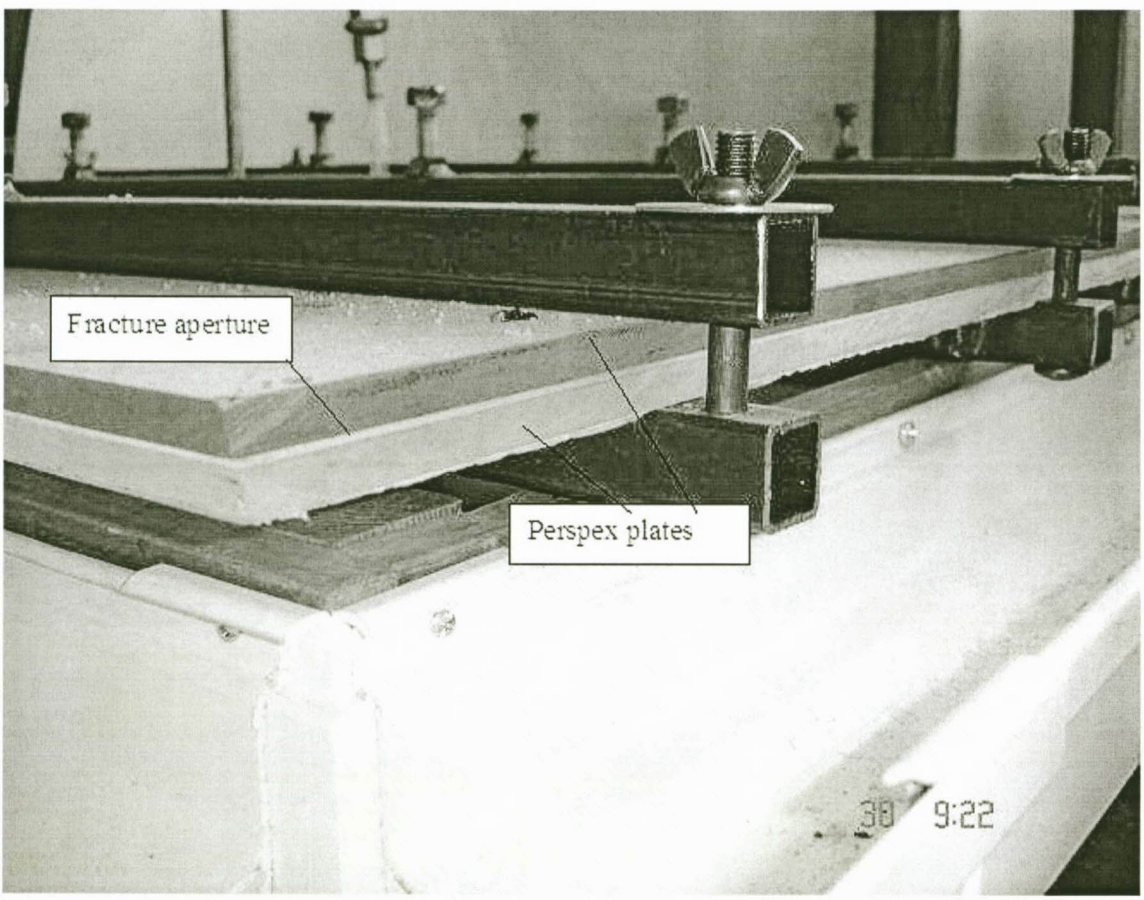

Figure2.8 Fracture aperture between two circular 100cmx100cm Perspex plates Note the clamps to keep the plates in place

2.4.2 RESULTS

From the experiments carried out in the laboratory on boreholes made from Perspex, smooth and rough (buffed to 10 by 20 microns) surfaced. We used this method to accurately determine 26 fracture apertures between 0.04mm to 6mm (Table2.1& 2.2, Figure2.9 and Figure2.10). The calculated and the actual apertures are the same with a maximum error difference of 0.02mm using water and 0.04 mm using oil.

Table2.1. Laboratory test results of aperture measurements of various gauge sizes using water

Gauge size mm	Distance	Radius	Δh	Time	Water mm	Aperture mm	Error diff
0.04	100	17.5	1.3	510.1	1.5	0.05	0.01
0.05	100	17.5	1.6	445.1	1.8	0.06	0.01
0.06	100	17.5	2.0	373.2	2.2	0.07	0.01
0.08	100	17.5	2.6	302.8	2.8	0.09	0.01
0.1	100	17.5	3.3	269.8	3.6	0.11	0.01
0.13	100	17.5	4.2	244.1	4.4	0.13	0.00
0.15	100	17.5	4.9	208.6	5.4	0.17	0.02
0.18	100	17.5	5.9	178.2	6.1	0.19	0.01
0.2	100	17.5	6.5	146.1	6.6	0.20	0.00
0.23	100	17.5	7.5	113.2	7.8	0.24	0.01
0.25	100	17.5	8.2	81.4	8.2	0.25	0.00
0.28	100	17.5	9.1	49.7	8.9	0.27	0.01
0.3	100	17.5	9.8	18.1	10.1	0.31	0.01
0.33	100	17.5	10.8	16.6	10.8	0.33	0.00
0.35	100	17.5	11.4	15.1	11.6	0.36	0.01
0.38	100	17.5	12.4	13.4	12.7	0.39	0.01
0.4	100	17.5	13.1	11.8	13.6	0.42	0.02
0.43	100	17.5	14.0	10.9	14.4	0.44	0.01
0.45	100	17.5	14.7	9.9	15.2	0.47	0.02
0.48	100	17.5	15.7	8.9	15.8	0.48	0.00
0.5	100	17.5	16.3	8.1	16.7	0.51	0.01
0.53	100	17.5	17.3	6.6	17.2	0.53	0.00
0.55	100	17.5	18.0	6.3	18.1	0.55	0.00
0.58	100	17.5	18.9	5.7	19.2	0.59	0.01
0.6	100	17.5	19.6	4.3	19.5	0.60	0.00
0.63	100	17.5	20.6	4.1	21.2	0.65	0.02

Table2.2. Laboratory test results of aperture measurements of various gauge sizes using oil

Gauge size mm	Distance mm	Radius mm	Δh(mm)	Time sec	Oil mm	Aperture mm	Error diff
0.04	100	17.5	1.3	37.4	1.4	0.04	0.00
0.05	100	17.5	1.6	32.8	1.6	0.05	0.00
0.06	100	17.5	2.0	27.5	1.9	0.06	0.00
0.08	100	17.5	2.6	22.1	2.5	0.08	0.00
0.1	100	17.5	3.3	19.2	3.5	0.11	0.01
0.13	100	17.5	4.2	18.1	4.4	0.13	0.00
0.15	100	17.5	4.9	15.3	4.8	0.15	0.00
0.18	100	17.5	5.9	13.2	6	0.18	0.00
0.2	100	17.5	6.5	10.7	6.6	0.20	0.00
0.23	100	17.5	7.5	8.1	7.7	0.24	0.01
0.25	100	17.5	8.2	6.1	8.3	0.25	0.00
0.28	100	17.5	9.1	4.1	9.3	0.28	0.00
0.3	100	17.5	9.8	1.8	9.9	0.30	0.00
0.33	100	17.5	10.8	1.4	10.7	0.33	0.00
0.35	100	17.5	11.4	1.1	11.5	0.35	0.00
0.38	100	17.5	12.4	0.98	12.6	0.39	0.01
0.4	100	17.5	13.1	0.82	13	0.40	0.00
0.43	100	17.5	14.0	0.81	13.8	0.42	0.01
0.45	100	17.5	14.7	0.74	14.6	0.45	0.00
0.48	100	17.5	15.7	0.71	15.2	0.47	0.01
0.5	100	17.5	16.3	0.64	16.4	0.50	0.00
0.53	100	17.5	17.3	0.61	17.4	0.53	0.00
0.55	100	17.5	18.0	0.48	18.2	0.56	0.01
0.58	100	17.5	18.9	0.42	19.1	0.58	0.00
0.6	100	17.5	19.6	0.34	20	0.61	0.01
0.63	100	17.5	20.6	0.31	22	0.67	0.04

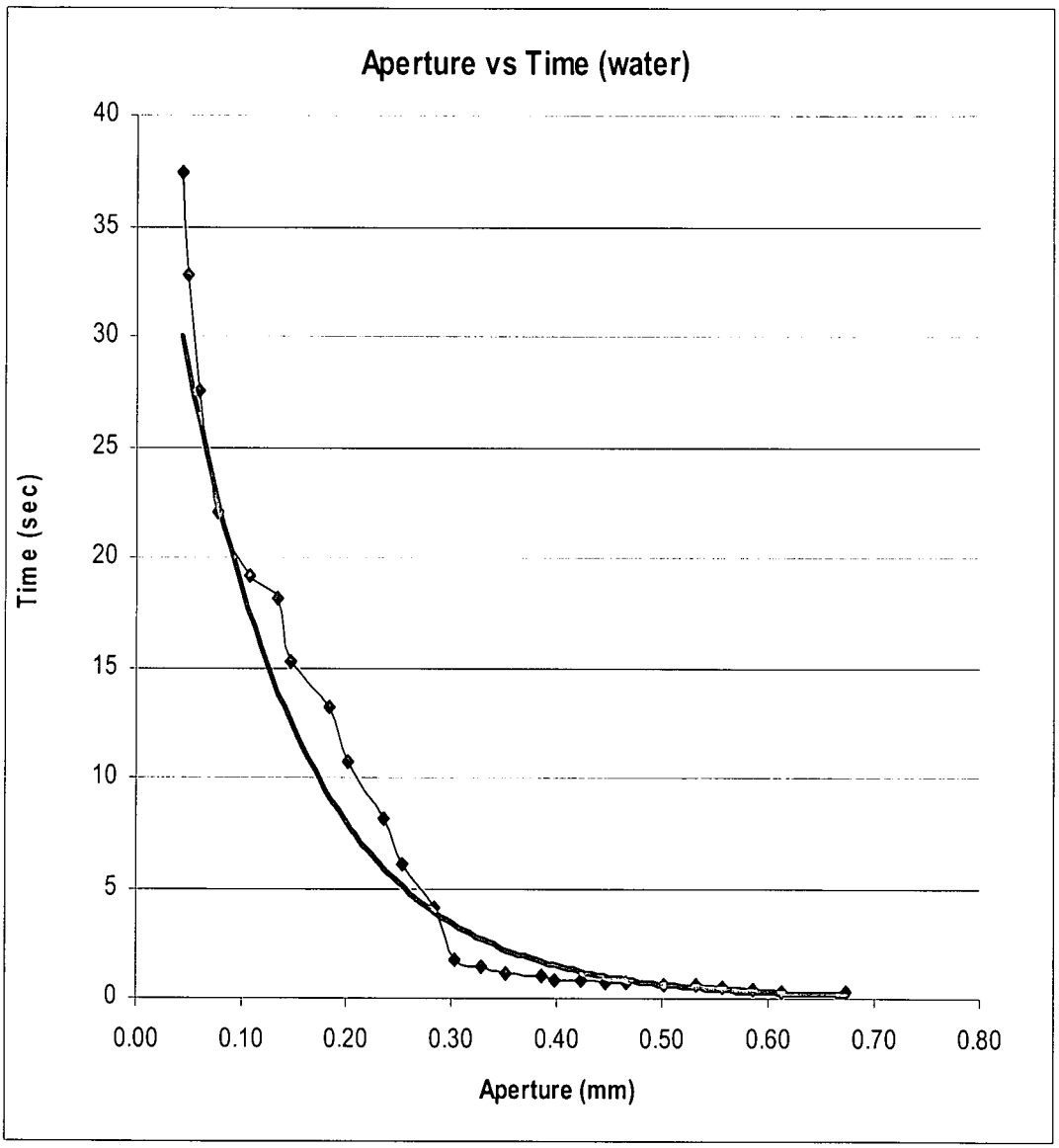

Figure2.9. Tests plot of aperture vs. time taken for fluid, (waters) to travel test distance of 100mm during the laboratory experiment.

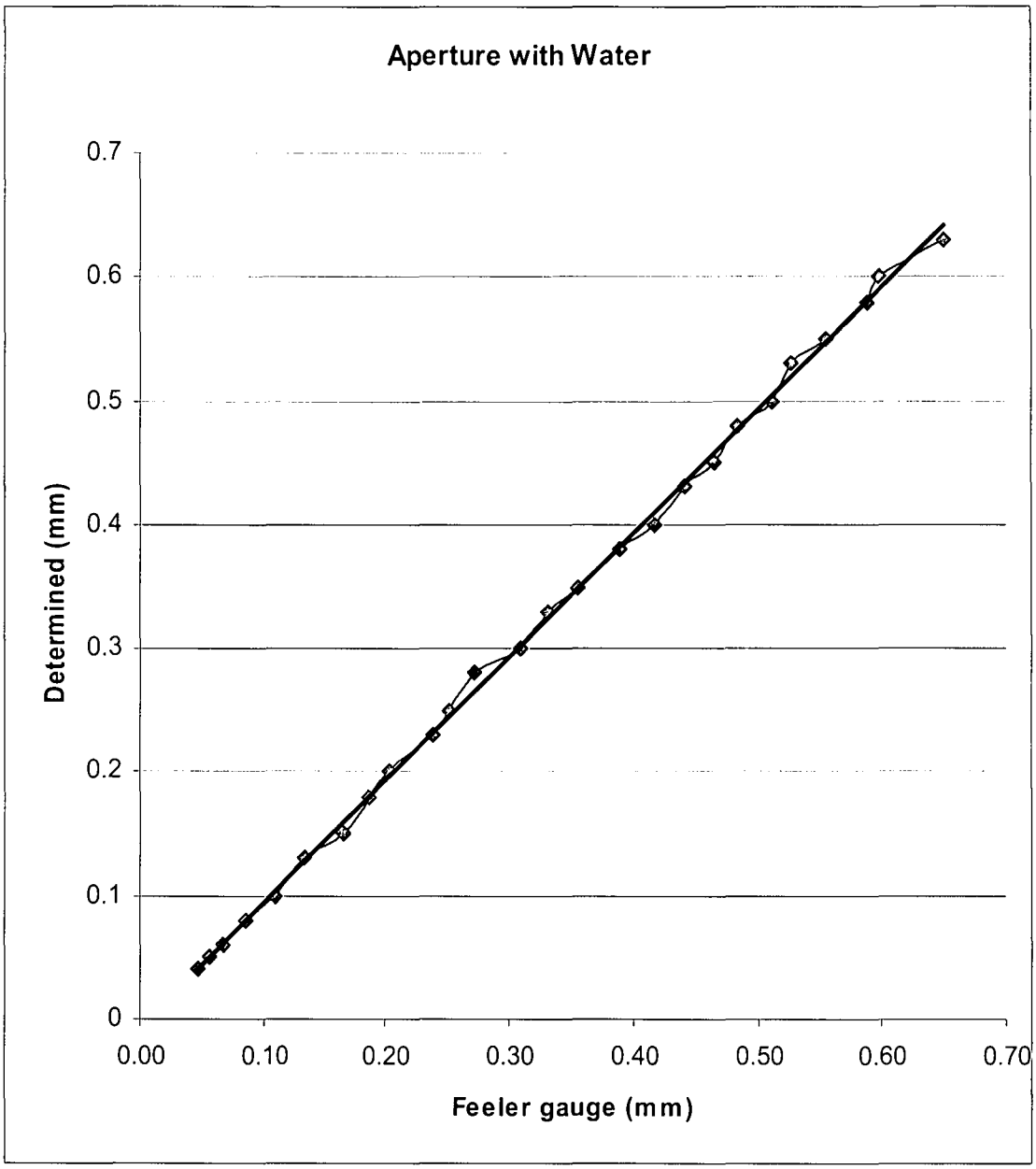

Figure2.10. Aperture determined using water. The results from the tests correspond to the feeler gage values.

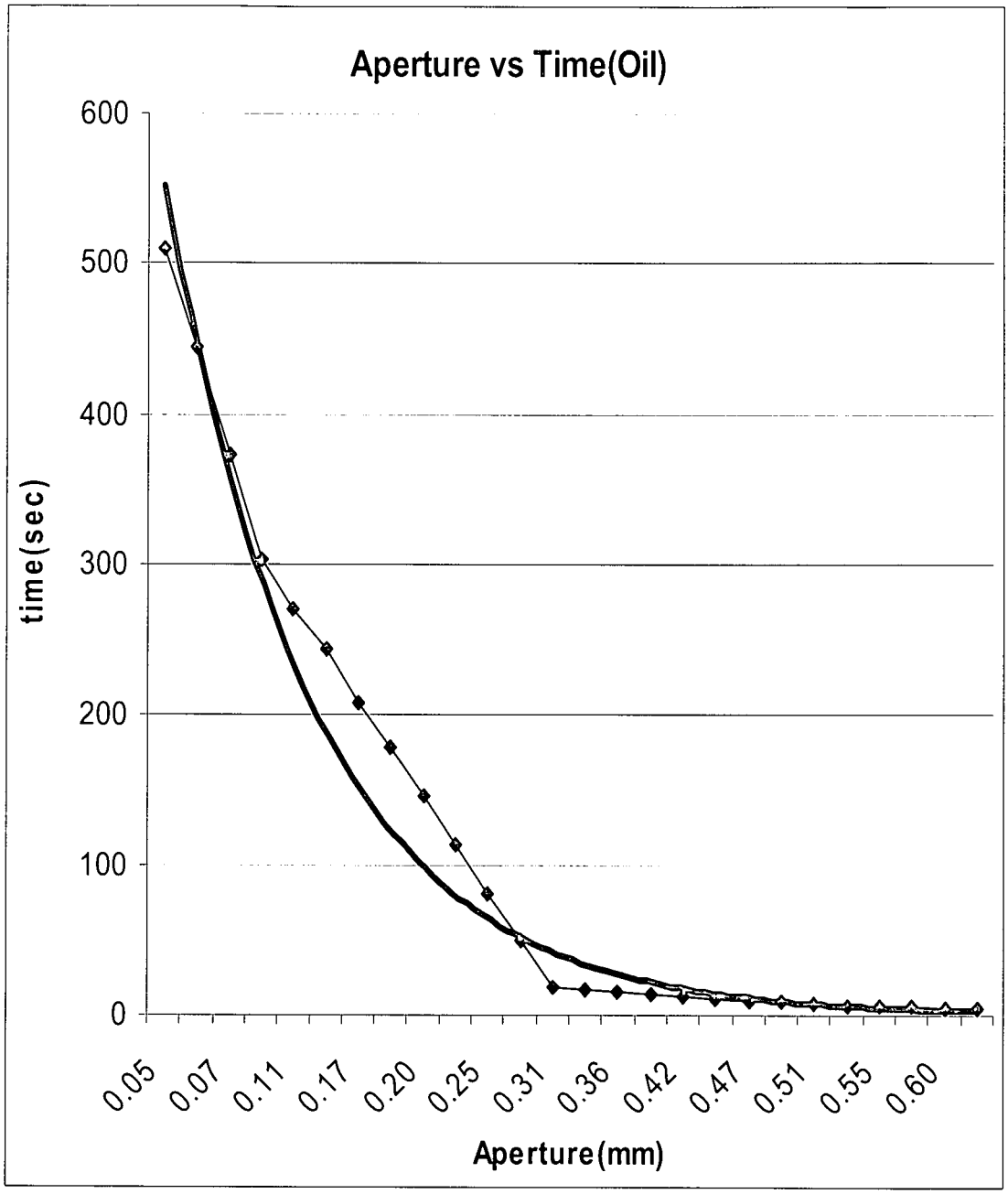

Figure2.11. Aperture vs time (oil). Note the longer period taken for the oil to travel in the fracture over the same tests distance (100mm) as in fig 2.9.

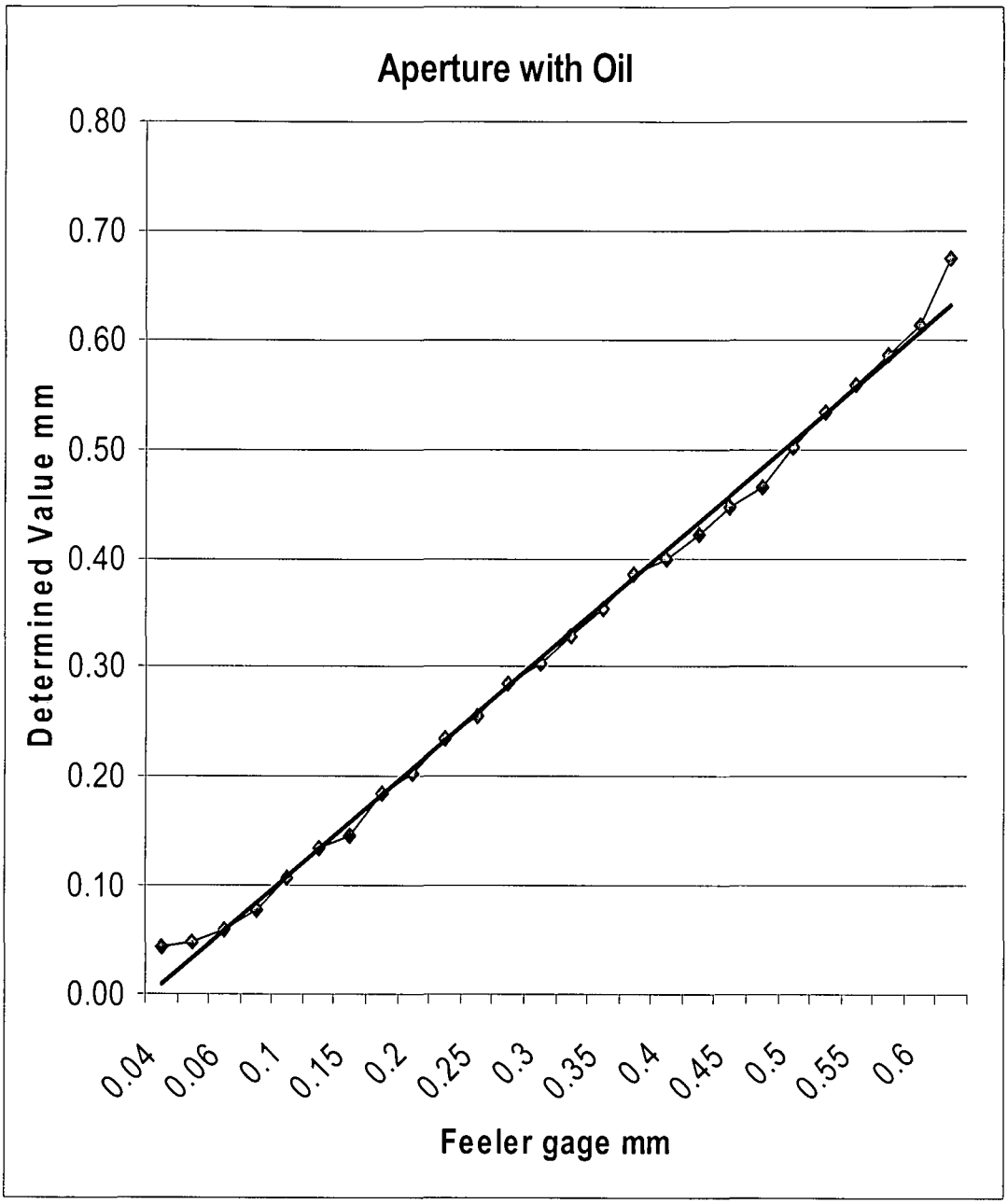

Figure2.12. Aperture determined using oil. The results from the tests correspond to the thickness gauge values.

2.4.3 DISCUSSION

Laboratory tests have given accurate values for the determination of 26 apertures between 0.04mm to 6mm on parallel plate Perspex fractures for the ST tests (Figure 2.8 & 2.9). Sunflower oil was also used to determine the apertures in the ST test (Figure 2.10 & 2.11). The sunflower oil results were less accurate compared to those of water and it took thirteen times more time for the oil to move across the same distance of 100mm, under the same conditions, although the oil is the non wetting fluid. Temperature affects the use of oil. At temperatures below eight degrees the time for the oil tests more than doubled due to the increased viscosity of the oil.

We can represent a fracture as a planar void with two flat parallel surfaces as in the set up above, to determine fracture flow parameters.

The hydraulic conductivity of this fracture K_f is defined as:

$$K_f = (2b)^2 \frac{\rho g}{12\mu}$$ (Cook and Simmons, 2000) ..... (1)

Where 2b is the fracture aperture, ρ is the density of water, g is acceleration due to gravity and μ is the dynamic viscosity of water. The mean groundwater velocity through the fracture, V_w, can be calculated as the product of the fracture hydraulic conductivity and the hydraulic gradient:

$$V_m = K_f \frac{\partial i}{\partial z}$$ (Cook and Simmons, 2000) ..... (2)

Where δi/δz is the hydraulic gradient

The transmissivity of an individual fracture is then:

$$T_f = (2b)^3 \frac{\rho g}{12\mu}$$ (Hvorslev, 1951; Cook and Simmons, 2000) ..... (3)

If the aquifer matrix is impermeable, then the transmissivity of any interval of aquifer is calculated by summing the transmissivities of the fractures within that interval. Where an interval contains only a single fracture, the transmissivity of the interval is simply equal to the transmissivity of that fracture. If the aquifer matrix is impermeable but has significant porosity, then solute transport is affected by matrix diffusion. Suppose that water within a fracture initially has a solute concentration of zero, and we then release a conservative tracer into the fractures, at a concentration that we will denote by C_o, and that this release continues over time t. The distance that the tracer would have moved after a given period of time, t, can be expressed:

$$x = V_w b \sqrt{\frac{t}{D\theta_m}}$$ (Cook and Simmons, 2000) ..... (4)

For freshwater at 20℃, β= 1.00 g cm-3, and μ = 1.00 m Pa s, and so ρg / μ = 7.4x 10^{11} m d^{-1}

Where V_w is the water velocity within the fractures and D is the effective diffusion coefficient within the matrix. Thus for a water velocity in the fractures of 35 m d^{-1}, fracture aperture of 2b = 250 μm, matrix porosity m = 0.05 and diffusion coefficient D = 10^{-4} m^2 yr^{-1}, the solute will travel 1386 m in 1 year. This is much less than the travel distance of the water, which is approximately 13 km (V_w *m* t). Whereas in porous media the distance traveled by a solute is directly proportional to the travel time, the distance traveled through a fracture is proportional to the square root of time. This means that if the solute travels 10 m in the first year, it will travel a further 4 m (and not 10 m) in the following year.

Consider a system of evenly spaced, identical, planar, parallel fractures in an impermeable rock matrix. The hydraulic conductivity of the medium in the direction parallel to the fractures can be expressed:

$$K = \frac{(2b)^3}{2B}\frac{\rho g}{12\mu}$$ (Cook and Simmons, 2000) ..... (5)

Where K is fracture permeability in m^2d^{-1}, 2B is the fracture spacing. In any other direction, the hydraulic conductivity is zero. This equation is sometimes referred to as the cubic law, because of the nature of the dependence of hydraulic conductivity on fracture aperture. A doubling of fracture aperture results in a factor-of-eight increase in hydraulic conductivity. For example, a fractured media with a fracture spacing of 2B = 1 m and fracture aperture of 2b = 250 μm, will have a hydraulic conductivity of approximately 10^{-5} m s^{-1}, similar to that of a coarse sand. It will also have the same hydraulic conductivity as a fractured media with a fracture spacing of 10 cm, and fracture aperture of 115 μm. If the rock matrix is impermeable, then solute transport will be characterized by advection through the fractures, with diffusion into the matrix. An understanding of the relationship between water velocities and apparent solute velocities can be gained by considering two end-member scenarios. Firstly, suppose that there is no diffusion into the matrix. In this case, the apparent velocity of a tracer is equal to the water velocity through the fractures. On the other hand, suppose that diffusion is very rapid and that fractures are spaced very closely together, so that after a period of time diffusion of solute into the matrix may result in the solute concentration throughout the matrix being identical to the concentration within the fracture. (We say that fracture and matrix concentrations have equilibrated.) Even though the water is moving only through the fracture, because of this

Equilibration it will appear as if the solute is moving evenly through the fracture and the matrix. In this case, the apparent tracer velocity, is related to the velocity of the water in the fractures, V_w, by the ratio of the total porosity, m, to the fracture porosity, mf, The tracer velocity will be equal to the groundwater flow rate divided by the total porosity. This condition is sometimes referred to as equivalent porous media (EPM) for solute transport, and will occur when Dt/B2 is large (Van der Kamp, 1992; Cook et al., 1996). In between these two end-members, the apparent solute velocities, will be less than the water velocity in the fractures, but greater than the EPM velocity. Such variation in hydraulic conductivity ranges is largely due to spatial variations in fracture aperture, fracture density, fracture length and fracture connectivity. There has been some discussion about how hydraulic conductivity in fractured rock aquifers varies with the scale of investigation. Consider a system of evenly spaced, identical fractures. Clearly, at very small scales the hydraulic conductivity varies between that of the matrix, Km, and that of the fractures, K_f depending on matrix porosity. However, when measurements are made at scales much larger than the fracture spacing, then the variability of hydraulic conductivity will be greatly reduced. At these scales, each measurement will return a value equal to the aquifer hydraulic conductivity. The scale beyond which the hydraulic conductivity approaches a constant value is referred to as the representative elementary volume (REV). However, when fractures are not evenly spaced and identical, then it is no longer clear that an REV exists. A number of people have argued that the hydraulic conductivity continues to increase as the scale of investigation increases because the probability of intersecting larger fractures increases. The basis of this proposition is that aquifers comprise a large number of very small fractures and a small

number of large fractures. However, others have argued that above a certain scale of measurement, permeability begins to decrease with increasing scale, as fracture connectivity is reduced. This proposed decrease in conductivity at large scales is a consequence of fractures having finite lengths. The maximum hydraulic conductivity occurs at the scale that is just great enough for a single large cluster of fractures to form, that spans the entire network (Renshaw, 1998).

As fracture networks become complex, it is no longer practical to characterize the system properties as the sum of individual fractures. Even for the simple parallel plate model, with identical planar fractures, characterization of groundwater flow and solute transport requires estimates of fracture orientation, fracture spacing, *fracture aperture*, matrix porosity and matrix diffusion coefficient. Many of these parameters are difficult to measure accurately.

Because of this, approaches that aim to measure large-scale properties that integrate the small-scale variability are more likely to be successful than those that aim to characterize the small-scale variation (Cook, 2003). Furthermore, field approaches should focus on measurement of aquifer properties that are most closely related to the properties of interest. For example, if the investigator is interested in knowing the groundwater flow rate, then it is preferable to use methods that measure groundwater flow directly, rather than infer it from indirect methods (such as measurements of velocity or hydraulic conductivity) other than using estimates from modeling techniques(Cook et al, 2003). Similarly, if the investigator is interested in predicting the velocity of contaminants, it is preferable to perform tracer tests that measure solute velocities than to attempt to infer solute velocities from measurements of groundwater flow rate. In many cases,

approximate direct methods may prove to be more useful than more accurate indirect methods. (Cook and Simmons, 2000)

Fracture aperture is one of the most important parameters for the quantification of flow parameters in fractured rock aquifers. Methods as those developed above are becoming increasingly more important for the characterization of fractured rock aquifers.

Steele et al (2006) carried out similar works for smaller fractures between 35 and 400 microns by carrying out traditional slug tests and using the slug test results in numerical simulations to estimate fracture aperture. Here direct measurements using the new methods above have been used to quantify the fracture apertures of fractures from 0.04mm (40 microns) to 63mm (63000 microns).

3.0 A NEW PHREATIC HYDRAULIC CONDUCTIVITY APPARATUS FOR THE DETERMINATION OF HYDRAULIC CONDUCTIVITY

3.1.0 INTRODUCTION

Groundwater flow is driven by four types of gradients (De Marsily, 1989), namely

i) Electric Potential Gradient (E.P.G).

ii) Chemical Potential Gradient (C.P.G).

iii) Thermal Potential Gradient (T.P.G), and

iv) Hydraulic Head Gradient (H.H.G)

Flow	Potential	Medium Property	Flux
Groundwater	Head, h(m)	Hydraulic conductivity, K(m/s)	$q = -K\nabla h$,(m/s)
Heat	Temperature, T(K)	Thermal conductivity, κ(W/°C.m)	$q_H = -\kappa\nabla T$,(W/m^2.s)
Solute	Concentration, C(g/m^3)	Diffusion coefficient, D_d(m^2/s)	$f = -D_d\nabla C$,(g/m^2.s
Charge	Electric, V(V)	Electrical conductivity, σ(1/Ω.m)	$j = -\sigma\nabla V$,(A/m^3)

3.1.1 Gradient of Electrical Potential

Water, consisting of bipolar electrically charged molecules, moves from high to low potentials. This principle is used for electro-kinetic drainage of soils with weak permeabilities (Terzaghi & Peck, 1967).

3.1.2 Gradient of Chemical Potential

Water moves from zones with high water concentration towards those with low concentrations (osmotic pump that makes life possible).

3.1.3 Gradient of Thermal Potential

Water flows from zones with high temperatures to those with low temperatures.

3.1.4 Hydraulic Head Gradient

Water flows from high hydraulic head to low hydraulic head.

All field or laboratory tests for the determination of groundwater flow velocity are carried out for the sole purpose of determining one or the other of the above gradients, from which all other parameters can be directly or indirectly determined. The direction and velocity of flow of water at any time is determined by the strongest gradient. Where the chemical, thermal or electrical gradient is stronger than the hydraulic gradients, water will flow against the hydraulic head gradient. Relatively, the most influential parameter in groundwater flow is the hydraulic head gradient (H.H.G). As such, the first step in understanding groundwater flow in any region is to understand the hydraulic conductivity characteristics or the ease and pathways of flow in the local formations (Akoachere *et al.*, 2007). In an attempt to shed more light on the "Bulk flow characteristics of some selected fracture rock aquifers in South Africa", a Water Research Commission (WRC) project, some alternative methods for the complete hydraulic characterisation (Figure3.1) of the

selected sites were developed. This chapter is based on the method developed to determine the hydraulic conductivity of clastic formations under phreatic saturated conditions, using the "Phreatic Hydraulic Conductivity" (PHC) apparatus. This apparatus is used to determine the hydraulic conductivity of a sample under atmospheric (phreatic) conditions, either in the field or the laboratory. Hydraulic conductivity (K) defines the rate of movement of water through a porous medium such as a soil or aquifer. It is the constant of proportionality in Darcy's Law (1856). The SI unit of K is m/d.

The unsuitable management and contamination of groundwater resources over the past century have damaged a substantial number of aquifer systems; some beyond repair. Contamination from the use, storage, and disposal of hazardous material needs to be tracked and removed from groundwater systems. This requires an understanding of the mechanisms governing the transport of contaminants in the subsurface, and will ultimately demand accurate predictions of the fate of contamination. A substantial number of field methods have been developed to measure hydraulic conductivity. These methods are divided into two broad categories: indirect methods and direct methods. Indirect methods require the measurement of hydraulic conductivity or transmissivity, an estimation of the effective porosity, and the measurement of the hydraulic gradient. Applying Darcy's Law, the average groundwater velocity can then be determined. Indirect methods include bail tests, pumping tests, and mapping hydraulic heads. The indirect calculation of the linear groundwater flow is limited by the difficulty in accurately measuring hydraulic conductivity. In the direct measurement of the groundwater flow velocity, an instrument is inserted into the porous medium or a

monitoring well, and is used to measure the rate of groundwater movement. This measurement can be directly related to the average linear flow velocity, or via a calibration constant, which is independently determined. Direct methods include thermal gradient measurements, concentration gradient tests such as a borehole dilution tests, and natural gradient tracer tests. There have been different approaches to estimating hydraulic conductivity, including:

1. Seepage meters, which directly measure the flux (Q) at the interface between the surface water feature and the aquifer. The basic method is to isolate part of the sediment-water interface with a chamber that is open at the base (surface area *A*) and measure the change in water volume contained in a bag attached to the chamber over a predetermined time period. When combined with head gradient measurements (dh/dl) between the sediment bed and the surface water body from mini-piezometer (Lee & Cherry, 1978), the vertical hydraulic conductivity K_v can be derived from Darcy's Law:

$$K_v = \frac{Q}{A}\frac{dl}{dh} \quad \text{..... (1)}$$

2. *Infiltration tests,* where infiltrometers (also known as permeameters) are used to measure the rate at which water infiltrates downwards through the sediment/soil profile, which is a function of vertical hydraulic conductivity. Two basic methods can be employed. In falling-head tests, water is added to reach a target level in the infiltrometer, after which the subsequent water level decline is recorded as infiltration occurs. In constant-head tests, the target level is maintained during the test by adding increments of water with known volumes. These tests are commonly used for unsaturated soils, but can also be carried out in calm, shallow water bodies (McMahon *et al.*, 1995; Duwelius, 1996; Lindgren &

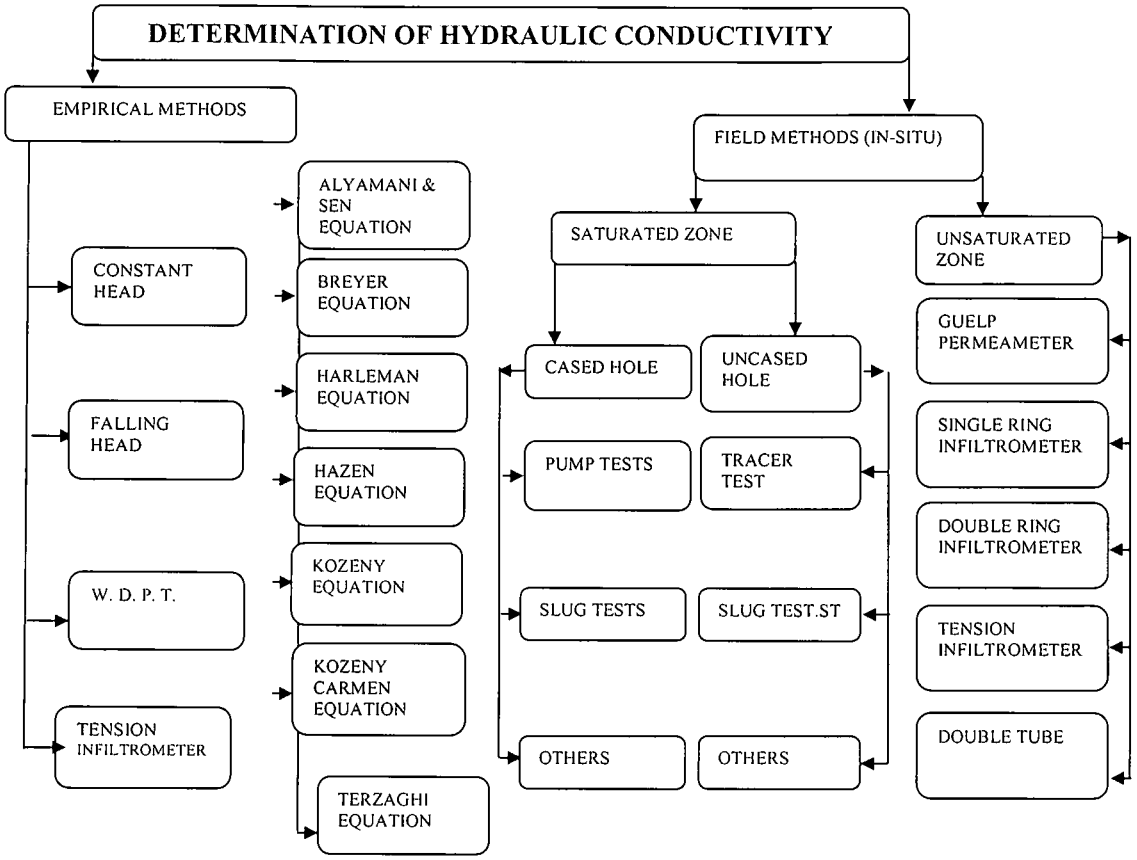

Figure3.1 Methods for the determination of hydraulic conductivity in the field and laboratory for the characterization of aquifers

Landon, 2000; Rosenberg, 2000). Various instruments are available based on measuring infiltration, including well, disc and ring (double and single) permeameters (ANCID, 2000). Similar tests using constant-head or falling-head configurations can be undertaken in the laboratory on core samples taken from the field site.

3. *Pump tests,* involving pumping groundwater from the piezometer and monitoring the pumping rate, as well as the groundwater level in the piezometer or in nearby piezometers. The pump test (also called aquifer test) indicates how the aquifer responds to groundwater withdrawals, with the data used to estimate aquifer characteristics such as hydraulic conductivity. A wide variety of formulas are available for the analysis of pump test data, based on differences in aquifer type and geometry, boundary conditions, and underlying assumptions. Pumping tests involve pumping water from a well for a predetermined period of time at a fixed rate. The drawdown of the water table is measured at the pumping well and selected observation wells in the vicinity. The data are used to calculate large-scale hydraulic conductivity values, which are then applied to the velocity estimation (EPA, 2000). Unfortunately, pumping tests require a considerable investment of time and can be expensive to perform.

4. *Slug tests* measure the rate of groundwater recovery after a small volume (slug) of water is suddenly displaced (Duwelius, 1996; Cey *et al.*, 1998; Springer *et al.*, 1999). Slug and bail tests are conducted sometimes through well screens and filter packs, which can make data analysis complex.

5. *Grain size analysis* involves determining the distribution of grain sizes within the sediment, using standard sieves. Empirical relationships are used to estimate

hydraulic conductivity from standard grain size parameters (Vukovic & Soro, 1992). The grain size diameter at which 10% of the sediment is finer (d_{10}) is applied in a commonly used empirical formula initially developed by Hazen (1893):

$$K = A_H C T d_H^2 \quad \text{..... (2)}$$

Where A_H is a dimension coefficient (= 1.0 for m/d), C is an empirical constant (=860) and T is a temperature correction factor (=1 at 10° C). Another empirical relationship developed by Alayamani & Sen (1993) uses the slope and intercept (I_0) of the grain size distribution curve between d_{10} and the median grain size (d_{50}):

$$K = 1300(I_0 + 0.025(d_{50} - d_{10}))^2 \quad \text{..... (3)}$$

However, the use of grain size for determining hydraulic conductivity could be very misleading, since the spatial disposition of the layers and grains play a vital role on the value of the hydraulic conductivity (Akoachere *et al.*, 2007).

6. *Point dilution tests* use the decay rate of the concentration of a tracer to determine the groundwater velocity using the formula (4) (Drost, 1968) which can then be used to determine the hydraulic conductivity:

$$v = \frac{\pi}{2t} r \ln\left(\frac{C}{Co}\right) \quad \text{..... (4)}$$

Where, v is groundwater velocity, t the time that elapsed, r the radius of the borehole, C the concentration after time t, and C_o is the initial tracer concentration.

3.2.0 RATIONALE

The multitude of methods above indicates that the determination of hydraulic conductivities is important. Hydraulic conductivity varies markedly in space, with changes in sediment characteristics and spatial disposition. Being direction dependent, hydraulic conductivity can be markedly different in the vertical from the horizontal directions. For the same lithologies, different spatial dispositions result in different hydraulic conductivities (De Marsilly, 1989; Akoachere *et al.*, 2007). Hydraulic conductivity is influenced by the properties of the transmitted fluid as well as the porous medium. Hydraulic conductivity also depends on scale. The use of laboratory experiments for understanding bulk flow characteristics is based on the principle of scaling from the small scale (isotropy) to medium scale (anisotropy), and finally to large scale or bulk flow (heterogeneity). Upscaling is the prediction of hydraulic conductivity based on the understanding of the heterogeneous structure of small-scale hydraulic conductivities. The converse is downscaling. Scaling has enjoyed increasing importance in regional groundwater flow studies, because measurements are easier to quantify at the small (laboratory) scale, while the problems to be solved occurs on the field (bulk) scale (Samouelien, 1999; Zijl, 1999). Scaling problems also include the issue of size. What should we consider as small scale? :

i) Local groundwater flow.

ii) Intermediate groundwater flow.

iii) Regional groundwater flow.

Another problem is the model flow direction. Is it one-dimensional (1D) as in fracture flow, two-dimensional as in lineament flow (2D), three-dimensional (3D) as in flow through porous media, or multi-dimensional as in regional (bulk) flow (nD)?

Another problem in regional groundwater flow is the derivation of the bulk effective hydraulic conductivity K_{eff} at any scale. Measurements taken at the (point scale) sample level may not be directly extrapolated to the bulk or aquifer scale (Akoachere *et al.*, 2007). Water and contaminant migration is critical to water resource development and management, agriculture, waste site restoration and waste disposal strategies. Regulations from the United States Environmental Protection Agency (2000) require the measurement of transport parameters for each geologic unit, soil horizon and engineered component for fracture and performance assessment needs. This necessitates new, simpler methods for the determination of hydraulic conductivity, which could reduced the length of time needed to carry out tests such as the PHC apparatus which measures the hydraulic conductivity of those geologic units that are not fractured. In our effort to shed more light on the "Bulk flow characteristics of some selected fractured rock aquifers in South Africa", some new methods for the complete hydraulic characterization of selected sites were developed. The chapter is based on the method that involves the PHC apparatus, which determines the hydraulic conductivity of clastic formations associated with fractured rock aquifers, under phreatic saturated conditions.

Fractured rock aquifers consist mainly of hard rock. However, most hard rocks over time have been weathered from the surface downward to some considerable depths. Other fractured rocks are overlain by formations that constitute good aquifers but comprising of essentially clasts in various spatial dispositions, due to facies changes and intrusions. Also most fractured rock aquifers are associated to clastic formations from which they receive or to which their groundwater flows. Considering bulk flow (flow through various formations

over distances of meters to kilometers, some of which are not fractured but whose hydraulic properties are interwoven to), understanding how groundwater will flow through the related but not fractured formations in any region, will help shed more light on the flow characteristics of these regions. Such zones may include, but are not limited to, coastal aquifers bordering or between fractured rock aquifers, weathered regoliths, large weathered veins, large weathered intrusives, wetlands and other formations which may overly or underly fractured rock formations and which may act as recharge or discharge zones, thereby acting in a deterministic way to contribute largely to bulk flow in such regions. At the campus test site and else where in the Karoo Basin, such formations abound. On the campus test site, fractured sandstones and other aquiferous formations are sandwiched between mudstones, siltstones and shales which by themselves have different properties. Often times, the hydraulic properties of the non-fractured-rock aquifers are not properly accounted for. Due to their areal extent, they should play an important role in the hydraulics of these regions. It is for this reason that this and the next chapter try to give an insight into the movement of water in these types of aquifers.

3.3.0 THE PHREATIC HYDRAULIC CONDUCTIVITY APPARATUS

This apparatus is made up of a solid body, divided into three chambers and mounted on a ten litre capacity water reservoir with a small pump. Figure3.2, displays the inlet chamber, sample cell chamber and outlet chamber.

The inlet chamber includes four bypass tubes on one side, placed at intervals of 0.25, 0.5, 0.75 and 0.9 of the total height of the chamber, and an inlet

tube at the topmost edge of the chamber. The bypass tubes maintain a constant head at the various levels.

The cell chamber (Figure3.2) is placed at the middle section of the apparatus. The sample cell is fitted here. The chamber is rimmed with a silicon seal to prevent leaks.

The outlet chamber includes five tubes on the outer side, placed at 0.1, 0.2, 0.3 0.45, 0.6 and 0.8 of the total height. These tubes can adjust the hydraulic gradient to accommodate all types of samples.

The sample cell is a 20cm x 10cm x 15cm open-sided cell. At each open end, there is a groove for fitting a fine sieve of hydraulic conductivity of 10^{23} m/d (Fig 3.3).

The sample cell is placed in the sample chamber of the hydraulic conductivity apparatus.

The water inlet valve is opened, allowing the submerged pump in the reservoir to pump water through the inlet tube into the inlet chamber, through the sample cell chamber to the outlet chamber, out of the apparatus through the water outlet tube, and back into the reservoir.

The apparatus is allowed to run for some minutes for the system to stabilize and attain a steady state.

The water levels in the outlet chamber (h_1) and the inlet chamber (h_2) on both sides of the sample cell are measured (Fig 3.3).

The flow rate Q is measured by the flow meter as outflow volume per time through the water outflow tube. The Dupuit-Forchheimer discharge formula (5) is used to determine the hydraulic conductivity.

$$Q=K\,W\,(h_2^2-h^2_1)/2L) \quad \text{..... (5)}$$

Where Q is the flow rate, K the hydraulic conductivity, h_1 and h_2 the height of water on either side of the sample cell, L the length of the sample cell (10cm) in the direction of flow and W the width (20 cm) of the sample cell in the direction perpendicular to the flow direction.

3.3.1 SAMPLES

The PHC apparatus measures the hydraulic conductivity of three types of samples;

a) Consolidated (*in-situ*) samples abstracted with the sample extractor.

b) Loose or friable *in-situ* samples.

c) Drill cuttings, auger samples or other unconsolidated samples.

In samples (a), a stainless steel extractor is rammed into the formation. With the aid of associated spatula, the formation around the extractor is carefully removed, leaving a representative sample in the extractor. The extractor containing the sample is then placed in the sample cell.

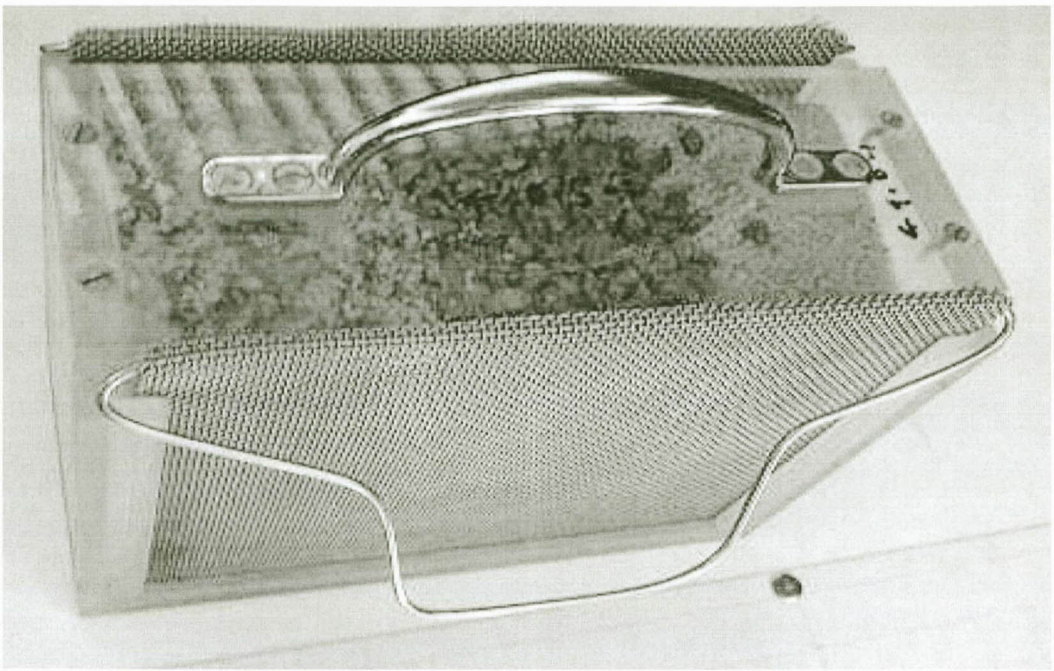

Figure3.2. Sample cell of hydraulic conductivity apparatus. Note vertically stripped spatial disposition of 1:1:1 for three samples of equal proportions.

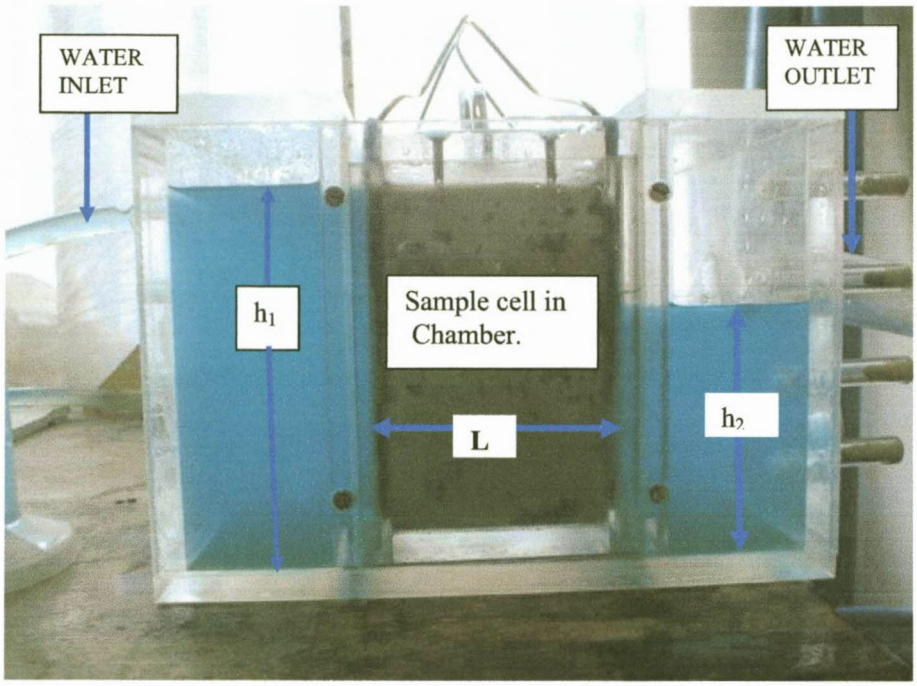

Figure3.3. The phreatic hydraulic conductivity apparatus. Note the height of water (h_1) in the inlet chamber; the height (h_2) in the outlet chamber; L (length of sample cell); the water inlet and water outlet tubes.

Samples (b) and (c) are recomposed to field densities in the sample cell by weighing the sample cell of known volume during compaction. The sample cell is then inserted into the sample cell chamber for the determination of the hydraulic conductivity.

3.3.2 RESULTS

Using the PHC apparatus, 140 samples from soils, drill cuttings, ash dams, mine tailings and sands were determined. The hydraulic conductivity values ranged from $1.76x10^{-2}$ m/d for clayey fine sands through $3.18x10^{3}$ m/d for medium sands to $8.10x10^{3}$ m/d washed grained sands (Table3.1). The results are reproducible and compare well with those from other methods in determining hydraulic Conductivity (Table3.2).

Table3.1. Average hydraulic conductivity of some soils, mine tailings, selected sands on campus building sites and sieved aquarium sands. For each sample, ten (10) repeated runs were averaged, K (1). Same samples using grain size analysis method of Alyamani &Sen (1993), K (2).

No.	SAMPLE LOCATION	SAMPLE DESCRIPTION	GRAIN SIZE	K(m/day) (1)	K(m/day) (2)
1	Dump-site Soil Secunda Mpumalanga	Brown CLAYEY fine sand	<106μ	$1.76x10^{-2}$	$2.21x10^{-2}$
2	Phalaborwa Limpopo	Mine Tailings Fine sand Black	0.1mm (20%)-1mm (85%)	$1.22x10^{0}$	$1.48x10^{0}$
3	Phalaborwa Limpopo	Mine Tailings Fine sand Black	0.1mm (15%) - 1mm (80%)	$1.33x10^{0}$	$1.97x10^{0}$
4	Campus Building gravel	Coarse gravel, dark grey	>4mm	$4.35x10^{3}$	$3.86x10^{3}$
5	Campus Building gravel	Medium gravel gray-brown	>2mm	$3.18x10^{3}$	$2.98x10^{3}$
6	Campus Building gravel	Fine gravel grey white	1.4mm - 2mm	$1.87x10^{3}$	$1.66x10^{3}$
7	Campus Building gravel	Medium gravel light brown	>2mm	$3.16x10^{3}$	$2.96x10^{3}$
8	Campus Building gravel	Medium gravel dark brown	>2mm	$2.65x10^{3}$	$1.82x10^{3}$
9	Aquarium gravel	Coarse washed white	4699μ	$8.10x10^{3}$	$8.50x10^{3}$
10	Aquarium Sand	Coarse washed white	2000 μ	$3.59x10^{3}$	$3.99x10^{3}$
11	Aquarium Sand	Medium washed white	1400 μ	$1.64x10^{3}$	$1.88x10^{3}$
12	Aquarium Medium sand	Medium washed white	1000 μ	$1.27x10^{3}$	$1.71x10^{3}$
13	Aquarium Fine sand	Fine washed white	250 μ	$5.87x10^{1}$	$6.27x10^{1}$
14	Aquarium very fine	Very fine washed white	106 μ	$2.39x10^{1}$	$2.91xs10^{1}$

Table3.2. Representative hydraulic conductivities for some grain types in meters per day (m/day).

No.	**Grain Type**	**Hydraulic Conductivity (m/day)**
1	**Gravel**	**$5x10^{1} - 5x10^{5}$**
2	**Coarse sand**	**$5x10^{0} - 5x10^{4}$**
3	**Medium sand**	**$5x10^{-1} - 5x10^{3}$**
4	**Fine sand**	**$5x10^{-2} - 5x10^{2}$**
5	**Silt**	**$5x10^{-4} - 5x10^{-1}$**
6	**Clay**	**$5x10^{-8} - 5x10^{-4}$**

3.3.3 DISCUSSION

The use of other methods for determining hydraulic conductivity is fraught with the following problems;

i) More or less cumbersome equipment needing specialized skills (Labaky *et al.*, 2007).

ii) Use of high power pumps with over- or under-pressures and other forces that do not tally with those found in the field (natural) conditions. These applied pressure techniques often cause flow to bypass portions of the sample because pressure unlike gravity is not a wholesome entity and will seek the path of least resistance, e.g. fractures, sandy areas and macrospores, and can affect the stabilities of common minerals like calcite, clays and gypsum.

iii) Measuring under confining conditions, in sealed pressurized tubes, samples that are under atmospheric conditions in the field in most cases.

iv) Measurement of over-compacted samples to meet equipment requirements.

v) For tracer tests (point dilution tests), there are a lot of problems, as it is very difficult to maintain a steady groundwater flow during tracer mixing; determine the rate at which the tracer flows out of the well; control the density gradients created by the tracer; exclude the distortion of flow fields around the well bore; mix the tracer homogeneously, in addition to predicting the hydraulic gradient (Halevy, 1967; Drost *et al.*, 1968; Malkki and Wihuri., 1980; Lamontagne *et al.*, 2002).

In spite of the obstacles mentioned above, the methods must be understood within the context of its assumptions. Each method is suited to some types of study and detail requirements, while a certain level of skill is necessary to obtain accurate results. An essential piece of information in assessing a

contaminant's fate is the hydraulic conductivity (USDIBR, 1985). Advection, defined as the component of solute movement attributed to transport by groundwater flow, is usually the dominant factor in the migration of dissolved contaminants in aquifers. Advection of a contaminant occurs at an equal rate to the average hydraulic conductivity. Therefore, accurately measuring the average hydraulic conductivity is important in predicting the rate of contaminant transport in a groundwater system. The U.S. Environmental Protection Agency (US-EPA, 2001) has established criteria for determining the groundwater vulnerability at hazardous waste facilities, based on groundwater velocity. The need to identify the average groundwater velocity and consequently the hydraulic conductivity is clear.

3.3.4 CONCLUSION

The PHC apparatus is a useful and handy tool for Agriculturists, Environmental scientists, Hydrogeologists, Water Resources Managers, Wetlands and River Basins / catchment Managers, Waste Storage/Disposal/Dumpsite Managers, Researchers and all professionals in fields involved in groundwater flow characterization. This method is particularly suited to non-confining flow under atmospheric conditions, and detailed layer by layer samples can be used easily in this apparatus. As in all methods involving the use of field samples, the hydraulic conductivity value is as representative as the rigor of the sample collection procedure. With geologic insight and a lucid view of hydrogeological phenomena, an understanding of the flow characteristics of the formations in a region is enhanced.

The PHC apparatus has the following advantages:

i) Simple to use and needs very little maintenance (three components only)

ii) Economic, needing small amounts of water (ten litres)

iii) Light weight (six kilograms) and needs little space (0.16 m^3)

iv) Rapid results. Complete determination for a sample takes minutes.

4.0 THE PATIAL HYDRAULIC CONDUCTIVITY THEORY OF BULK FLOW IN AQUIFERS

4.1.0 INTRODUCTION

The present chapter is based on a laboratory method on the small scale (cm).

4.2.0 RATIONALE

The use of laboratory experiments for the understanding of bulk flow characteristics is based on the principle of scaling from small scale to medium scale and finally to large scale or bulk flow. Up-scaling is the prediction of hydraulic conductivity, based on the understanding of the heterogeneous structure of small-scale conductivities. The converse is down-scaling. Scaling is having an increasingly importance in regional groundwater flow studies because measurements are easier to be quantified at small scale, while the problems that need solutions are at the larger scale (Samouelien, 1999).

Amongst the problems in scaling, is that of size. What should we consider as small scale?

i) On the local groundwater flow.

ii) On the intermediate groundwater flow.

iii) On the regional groundwater flow.

Various methods abound which use measurements and mathematical description. The major ones are;

1) Stochastic Theory. Here, the heterogeneity of the parameter fields are characterized by their second order properties, namely

   i) Mean. ii) Variance and, iii) auto-covariance functions. It is implied that simple averaging of the formations conductivities is possible. Also that high and low permeability bands do exist.

2) Multi-Gaussian Theory. Here, the parameter fields are characterized using the perturbation techniques including the effects of anisotropy.

The effect of anisotropy is not weighted.

3) Homogenization Theory. In this theory the heterogeneous field is considered to be composed of a number of representative cells, containing small-scale heterogeneities. Each unit cell is assumed to be representative of the whole. Like a pixel in a picture representing the whole picture. This can only be if the field is iso-characteristic (all parameters equal every where). This is in contradiction with field observations in aquifers.

4) Power Averaging Theory. Here

   $K_{eff} = [1/V \int K(x)^q dV]^{1/q}$ (Samouelien, 1999)

V is the volume of the domain, K is the local hydraulic conductivity, x is the spatial coordinate and q belongs to the interval [1,-1].

This theory assumes that groundwater flows only through porous media. (no joints, fractures, faults, lineaments, etc).Unlike in field observations.

5) Others;

Use of euler-numbers based on the topology of sub-scale structures to measure connectivity. – Tensorial Renormalisation. – Standard Renormalisation –Simplified Renormalisation – Rameu Formula. – Landau-Lifshitz-Matheron Conjecture. – Dagan Approach. – Maxwell Approach

The above theories and approaches, with their impressive mathematical formulations, are useful and applicable only within the limits of their assumptions. They are however very limiting when applied to groundwater regional (bulk) flow in fractured rock aquifers. According to Toth (1999), irrespective of their great numbers and diversity, groundwater flow hydraulic conductivities comprise a relatively small number of basic types with variations within each type being due to local characteristics of the geohydrological environment. These conductivities are cumulative.

In a regional scale, each water body or each flow regime acts like a different fluid (gas) because its composition imposed by the result of its interaction with the geology at local, intermediate or regional level, gives it a distinct characteristic which govern how it interacts with other fluids (flow regimes) and rocks like how gases mix or chemicals' activity. There being natural laws governing natural phenomena, water, a fluid that exists in three states, gas, liquid and solid, should obey natural laws governing matter in these states; gas laws, fluid miscibility and immiscibility laws, to some extent, at all times.

In the fine scale, chemical characteristics of fluids define their interactions. At the small scale, the characteristics of the medium gradually become more

important. This in turn governs regional flow, which is the result of the interaction of all the water bodies or flow regimes. At the boundaries of groundwater bodies or flow regimes, interactions are similar to those at gas/gas, gas/liquid, miscible (liquid/liquid), immiscible (liquid/liquid) and liquid/solid interfaces, depending on the chemistry, temperature and pressure conditions that avail. Zijl (1998) states that, the parameters of formations in situ are different from the parameters measured in the laboratory samples and on cores and as such, the laboratory scale parameters cannot be used in models on the regional scale without appropriate corrections.

I believe that, regional scale groundwater flow hydraulic conductivities in aquifers can be calculated from measured "point scale" hydraulic conductivities with geologic insight. As such, if all the hydraulic conductivities of the characteristic local aquifers making a regional groundwater flow regime are measured and weighted in relation to their abundance, the weighted sum will make up the regional effective hydraulic conductivity. This is the partial hydraulic conductivity theory.

4.3.0 METHODS

Two hundred and fifty (250) measurements of hydraulic conductivity, using two sets of six (12) samples ranging from fine sand to gravel are done. One set of tests is done with six vertically layered samples, to validate the partial hydraulic conductivity theory. The other set of six sorted samples is used to determine the effects of layering and variation of proportion of layers to hydraulic conductivity.

Each sample is placed alternatively in the sample cell of the hydraulic conductivity apparatus (Figure3.2).

After the determination of the hydraulic conductivity of individual samples, the sample cells are filled with the samples of known hydraulic conductivity arranged in various spatial dispositions; vertically layered (a), horizontally layered (b), vertically stripped (c), and mixed (d) using a stirrer. There is progressive increase in the number of samples per disposition.

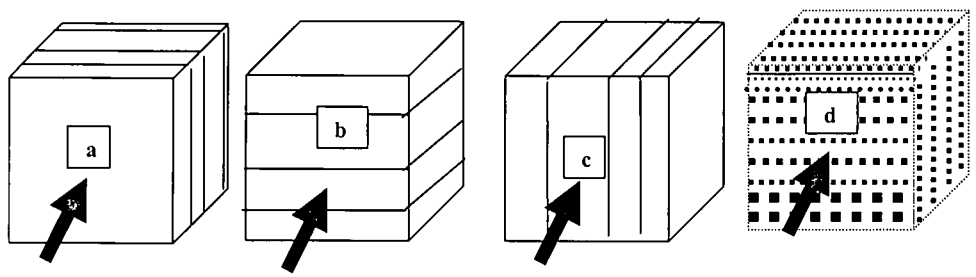

Figuire4.1. Spatial disposition of samples in sample cells of hydraulic conductivity apparatus. Arrow shows direction of flow through sample during measurement.

The hydraulic conductivity for each spatial disposition and proportion is determined, using the Dupuit-Forchheimer formula (1). The condition for using this formula is that the height (Δh) must be at least one tenth the horizontal length of flow path. This condition was satisfied. After this, the value is used in the partial hydraulic conductivity formula (5), to recalculate the hydraulic conductivity for each sample disposition and proportion (Table5.1).

The results of the measured and calculated hydraulic conductivities for the samples in the various dispositions were analyzed (Table5.1). From data analysis that both Dupuit and Darcy formulae give the same results at the small scale as below.

DARCY'S (1856) law is,

$Q = K\ I\ A$ ..... (2)

$I = (h_2-h_1)/L.\ A = W\ (h_2+h_1)/2.$

Q is the flow rate. K is hydraulic conductivity, I is the hydraulic gradient, L is the length, W width and A is area. h_2 and h_1 are the water levels. Replacing the above into (2).

$Q = KW\ [(h_2-h_1)/L][\ (h_2+h_1)/2]$ .....(3)

$(h_2-h_1)\ (h_2+h_1) = (h^2_2 + h_2h_1 - h_1h_2 - h^2_1) = h^2_2 - h^2_1$

The second and third terms cancel out.

Equation (4) becomes,

$Q = K W (h^2_2 - h^2_1) / 2L$ ..... (4)

Equation (4) is the DUPUIT equation (1).

4.4.0 RESULTS

4.4.1 EFFECTS OF LAYERING AND PROPORTIONS OF LAYERS

4.4.1.1 Vertical Layering

When the layers are of varied proportions of different samples, the resultant K goes towards the value of the layer with the higher K value. Three samples layered in proportions of 20% 60% 20% of samples 2, 6 and 1, will be represented as 2:6:1. 20/60/20). (sample number: proportions), Table4.1.

Considering the effect of vertical layering, (1:6.50/50), (1:6:2.30/30/40), Table4.2.

4.4.1.2 Horizontal layering

Considering horizontal layering, (2:5), (1:6:2).Table4.2. The value of the resultant K depends only on the proportion of the layers to one another. The resultant K approaches that of the layer with the largest proportion.

4.4.1.3 Vertical stripping

When the spatial disposition of the layers is in vertical strips, the values of the resultant K approach the harmonic mean. (1:6:2).Table4.1

4.4.1.4 Mixing

When the samples are mixed, the resultant K value approaches the arithmetic mean of the samples, with a slight control of the formation with the larger K value.(1:6mix)Table4.2.

As the number of layers increase, the resultant K value increasingly depends on the proportion of the layers to one another, each layer contributing its quota to the final K value by its partial hydraulic conductivity to the whole.

The partial hydraulic conductivity formulation below was developed with the constant head hydraulic conductivity apparatus for phreatic conditions, to be able to predict the resultant K values of varied layering and proportions of the samples' hydraulic conductivity.

Thus,

$$\mathbf{K}_{\mathbf{eff}} = \sum_{i=1}^{n} KiFi \quad \text{..... (5)}$$

K_{eff} is the bulk or regional hydraulic conductivity.

K_i = Hydraulic conductivity measurement at points in aquiferous formation.

F_i = Formations' weight in the region (Partial).

$F_i = V_i / V_T = V_i / \sum V$

V_i = Volume of formation (i).

V_T = Total volume of all formations in region.

$V_T = \sum V = V_1 + V_2 + V_3 + \text{---} + V_n$

K is measured from the formations' pump-tests, slug test, point dilution test etc.

F is gotten from accurate invasive or non-invasive methods (Geophysics etc), for all the formations in the region.

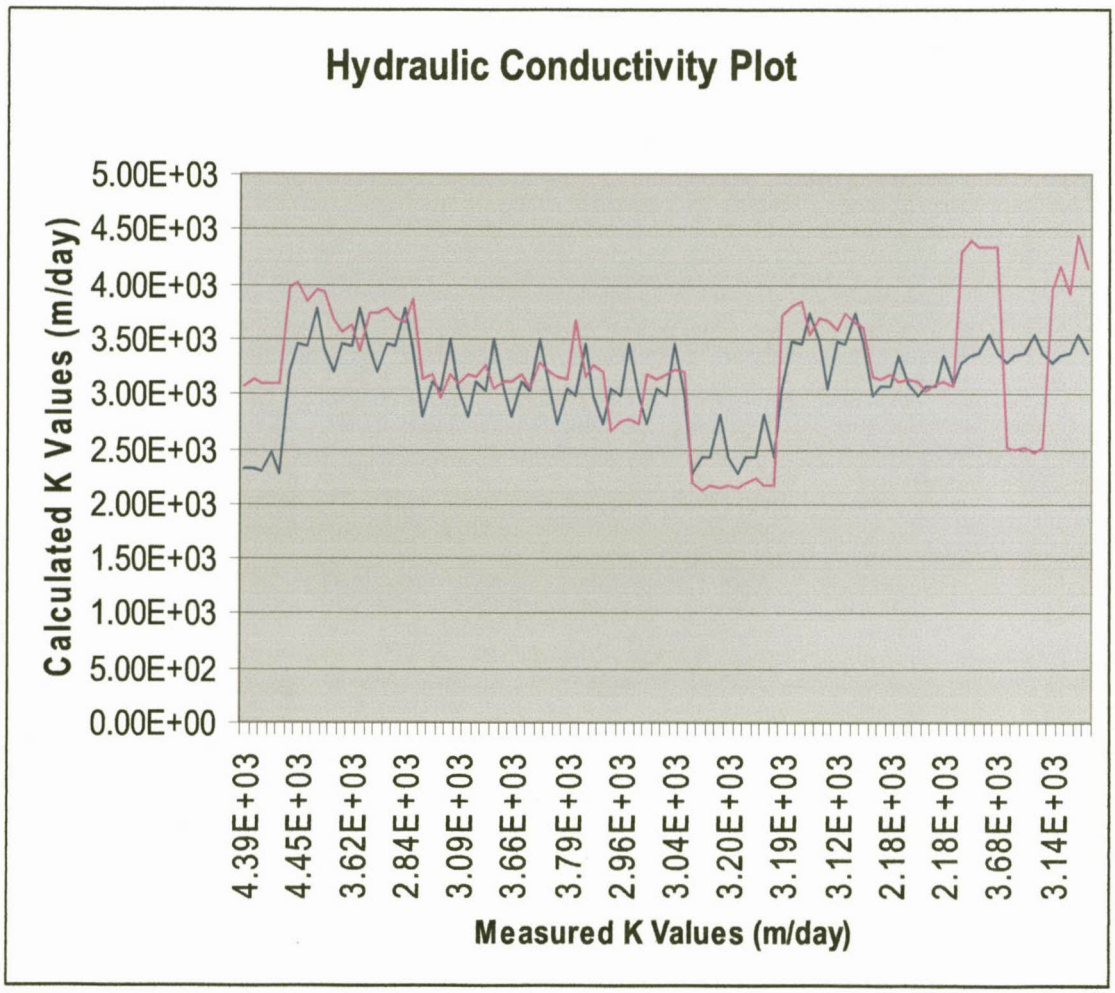

Figure4.2. Plot of measured and calculated hydraulic conductivities. Red curve: measured K values; Blue curve: Calculated K values using partial hydraulic conductivity formula.

Table4.1. Measured and calculated hydraulic conductivities for the first set of tests

Sample	Trial	Measured	Calculated
	3	2.18E+03	2.43E+03
	4	2.15E+03	2.81E+03
	5	2.17E+03	2.42E+03
43 mix(50/50)	1	2.14E+03	2.28E+03
	2	2.19E+03	2.43E+03
	3	2.22E+03	2.43E+03
	4	2.18E+03	2.81E+03
	5	2.16E+03	2.42E+03
1/3(412)	1	3.72E+03	3.04E+03
	2	3.79E+03	3.48E+03
	3	3.84E+03	3.46E+03
	4	3.55E+03	3.74E+03
	5	3.68E+03	3.48E+03
1/3Mix	1	3.68E+03	3.04E+03
	2	3.58E+03	3.48E+03
	3	3.74E+03	3.46E+03
	4	3.65E+03	3.74E+03
	5	3.61E+03	3.48E+03
1/4(4213)	1	3.14E+03	2.99E+03
	2	3.13E+03	3.08E+03
	3	3.18E+03	3.08E+03
	4	3.10E+03	3.36E+03
	5	3.13E+03	3.09E+03
1/4 MIX	1	3.11E+03	2.99E+03
	2	3.02E+03	3.08E+03
	3	3.09E+03	3.08E+03
	4	3.10E+03	3.36E+03
	5	3.08E+03	3.09E+03
1/5(5,2,4, (1/3mix),1)	1	4.30E+03	3.29E+03
	2	4.40E+03	3.36E+03
	3	4.33E+03	3.37E+03
	4	4.33E+03	3.54E+03
	5	4.34E+03	3.37E+03
1/5 (1,(1/3), (4,2,5)	1	2.52E+03	3.29E+03
	2	2.49E+03	3.36E+03
	3	2.50E+03	3.37E+03
	4	2.47E+03	3.54E+03
	5	2.51E+03	3.37E+03
1/5(1,(1/3), (4,2,5) MIX	1	3.94E+03	3.29E+03
	2	4.16E+03	3.36E+03
	3	3.91E+03	3.37E+03
	4	4.45E+03	3.54E+03
	5	4.14E+03	3.37E+03
16(30/70)	1	1.43E+03	2.25E+03
	2	1.41E+03	2.28E+03
	3	1.40E+03	2.31E+03
	4	1.41E+03	2.35E+03
	5	1.40E+03	2.31E+03
61(70/30)	1	4.54E+02	2.25E+03
	2	4.24E+02	2.28E+03
	3	4.28E+02	2.31E+03
	4	4.25E+02	2.35E+03
	5	4.14E+02	2.31E+03
61(7/3) MIX	1	1.17E+03	2.25E+03
	2	1.17E+03	2.28E+03
	3	1.18E+03	2.31E+03
	4	1.17E+03	2.35E+03
	5	1.16E+03	2.31E+03
16(70/30)	1	1.04E+03	3.44E+03
	2	1.03E+03	3.44E+03
	3	1.03E+03	3.49E+03
	4	1.02E+03	3.51E+03
	5	1.03E+03	3.48E+03
61(30/70)	1	1.19E+03	3.44E+03
	2	1.22E+03	3.44E+03
	3	1.20E+03	3.49E+03
	4	1.22E+03	3.51E+03
	5	1.23E+03	3.48E+03
61(30/70) MIX	1	2.10E+03	3.44E+03
	2	2.13E+03	3.44E+03
	3	2.08E+03	3.49E+03
	4	2.14E+03	3.51E+03

SAMPLE	Km/day	Av K	Mean	Type
106um	2.81E-03	2.77E-03		
no 7	2.72E-03			
250um	6.86E-03			
no 6	6.75E-03	6.80E-03		
1000um	1.46E-01			
no 5	1.47E-01	1.47E-01		
1000um	1.09E-01			
no 4	1.12E-01	1.10E-01		
	1.09E-01			
	1.09E-01			
1400um	1.93E-01			
no 3	1.92E-01	1.91E-01		
	1.93E-01			
	1.88E-01			
2000um	4.81E-01	4.81E-01		
no 2	4.79E-01			
	4.82E-01			
4699um	9.42E-01	9.38E-01		
no 1	9.34E-01			
1:6.50/50	5.54E-03			
VLayer	5.40E-03		4.72E-01	Avmean
	4.52E-03	5.00E-03	7.99E-02	Geomean
	4.53E-03		1.35E-02	Harmean
6:1.50/550	5.44E-03			
Vlayer	5.39E-03			
	5.30E-03	5.34E-03		
	5.25E-03			
6:1 mix	1.03E-02			
Layer	9.21E-03	1.07E-02		
	1.16E-02			
	1.16E-02			
6:1.50/50	3.17E-01			
50:50HL	3.01E-01	4.31E-01		
1:6.50/50	5.48E-01			
50/50HL	5.59E-01			
2:5.20/80	1.53E-01			
Hayer	1.54E-01	1.53E-01	3.14E-01	Avmean
	1.54E-01		2.65E-01	Geomean
	1.51E-01		2.25E-01	Harmean

SAMPLE	Km/day	Av K	Mean	Type
5:2.80/20	1.76E-01			
Hlayer	1.78E-01	1.77E-01		
	1.78E-01			
	1.77E-01			
5:2.80/20	2.12E-01			
Mixed	2.12E-01	2.12E-01		
	2.12E-01			
	2.12E-01			
1:6:2.V/L	1.74E-02			
(3/3/4) v	1.70E-02	1.70E-02		
	1.67E-02			
	1.67E-02			
261	1.61E-02		4.74E-01	Avmean
(40/30/30)v	1.61E-02	1.60E-02	1.08E-01	Geomean
	1.60E-02		8.23E-03	Harmean
	1.58E-02			
162Mix	2.78E-02			
	2.77E-02	2.76E-02		
	2.74E-02			
	2.77E-02			
162hstrip	6.21E-01			
25/25/50	6.32E-01	6.27E-01		
	6.25E-01			
	6.29E-01			
261	1.06E-02			
(50/25/25)vs	1.04E-02			
	1.00E-02	1.02E-02		
	9.68E-03			
162	1.10E-02			
(25/25/50)vs	1.12E-02	1.10E-02		
	1.10E-02			
	1.09E-02			
162 Mix	4.95E-02			
	4.78E-02	4.91E-02		
	5.01E-02			
	4.92E-02			
51(162mix)	2.26E+00		3.30E-01	
33/33/33	2.51E+00	2.46E+00	5.04E-02	
	2.55E+00		7.84E-03	
	2.52E+00			

Table4.2. Compositions and layering of samples and the resultant K values second set of tests.

SAMPLE ORDER	LAYERING TYPE	PROPORTION %	AVERGE VALUE	K	Means. Arithmetic(Am) Geometric(Gm) Harmonic(Hm)
1:6	Vertical	50:50	5.0 E-03		
6:1	Vertical	50:50	1.07E-02		
6:1	Mix	50:50	1.07E-02		
6:1	Horizontal	50:50	4.31E-01		4.71E-01 Am 7.92E-02Gm
1:6	horizontal	50:50	1.53E-01		1.35E-02Hm
2:5	Horizontal	20:80	1.53E-01		3.14E-01 Am 2.65E-01Gm
5:2	Horizontal	80:20	1.77E-01		2.25E-01Hm
5:2	Mix	80:20	2.12E-01		
1:6:2	Vertical	30:30:40	1.70E-02		
2:6:1	Vertical	40:30:30	1.60E-02		4.74E-01Am 1.08E-01Gm
2:6:1	Mix	40:30:30	2.76E-02		8.23E-03Hm
1:6;2	Horizontal	25:25:50	6.27E-01		
2:6:1	Vertical Strip	50:25:25	1.10E-02		
1:6:2	Vertical Strip	25:25:50	1.02E-02		4.74E-01Am 1.08E-01Gm 8.23E-03Hm
1:6:2	Mix	25:25:50	4.91E-02		
5:1:(162mix)	Vertical	33:33:33	2.46E+00		3.30E-01 Am 5.04E-02Gm 7.84E-03Hm

Table4.3. Spatial disposition, layering, proportions and various means for the second set of tests.

values may be more accurate. As the number of samples in the layering and proportions increases, the K values vary from arithmetic through geometric and harmonic to power means (Figure 5 & Figure 6).

From the above, the hydraulic conductivity values obtained from laboratory measurement and those determined using the partial hydraulic conductivity formula are the same for all layering and spatial dispositions (Table4.1& Figure4.1).

4.4.1.5 DISCUSSIONS

Various researchers have worked on the problem of spatial variability of hydraulic conductivity. According to De Marsily (1981), the spatial variability of hydraulic conductivity leads to questions of how to compose local hydraulic conductivity values in order to obtain an average regional value. For confined (Darcian) conditions, the composition of uniform blocks placed side by side in space gives; (De Marsilly,1989).

i) A law of harmonic composition if the blocks are in series.

$\Sigma l_i / K_{mean} = \Sigma (l_i / K_i)$

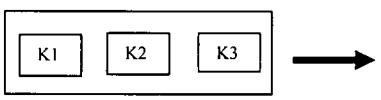

ii) A law of arithmetic composition, if the blocks are in parallel

$K_{mean}\ \Sigma e_i = \Sigma e_i K_i$

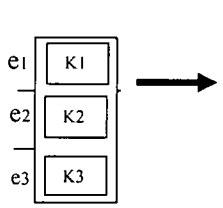

As such in confined conditions if the flow is uniform (parallel flow lines) whatever the spatial correlation of the permeabilities and whatever the number of dimensions of space, the average hydraulic conductivity always ranges between the harmonic mean and the arithmetic mean of the local hydraulic conductivities.

If the flow model is two dimensional (fractures), the average hydraulic conductivity is equal to the geometric mean.

If the flow is not uniform, there is no law of composition.

De Marsily noted that, this is quite worrying since pump tests for the determination of in situ hydraulic conductivities are based on non uniform convergent radial flow. Pump tests force water to flow in ways that would be different under natural conditions since pumping or accelerated perturbations bias flow through paths of higher K values and more often wells penetrate aquifers only partially. Pump test hydraulic conductivities are a measure of the ease with which water flows under pumping conditions and not how water flows naturally in the aquifers.

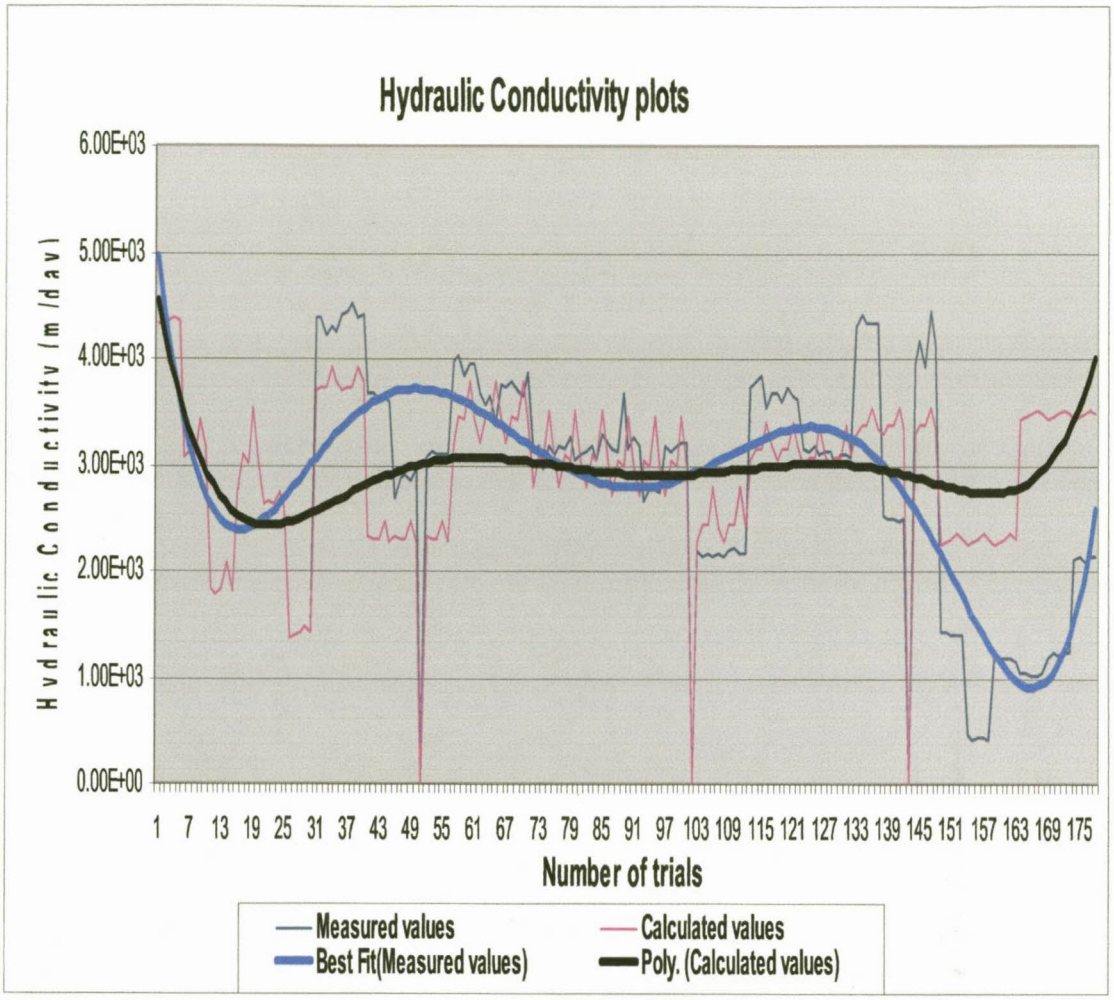

Figure4.3. Best fit plot of measured and calculated hydraulic conductivity values. Note the similarity of the measured best fit curve to that of bulk flow (regional flow) patterns of groundwater table in aquifers as more formations contribute their partial in the hydraulic conductivity characteristics of regional flow.Figure4.6.

Looking at the shape of the polynomial plot of the measured and calculated hydraulic conductivity values of horizontally layered samples, the curves behave as the arithmetic mean, through geometric to harmonic and finally to the power mean as the number of samples through which water flows increases significantly.

Comparing this with the behaviour of the water table in phreatic aquifers from the work of Zijl (1999) (Figure5&6), as the length of flow path increases and number of formations increase in the direction of flow, we see an identical pattern. Since the behaviour of the water table in phreatic aquifers reflect the hydraulic conductivity of such aquifers (Basis for pump tests). We can deduce that the hydraulic conductivity under phreatic conditions obeys the partial conductivity theory.

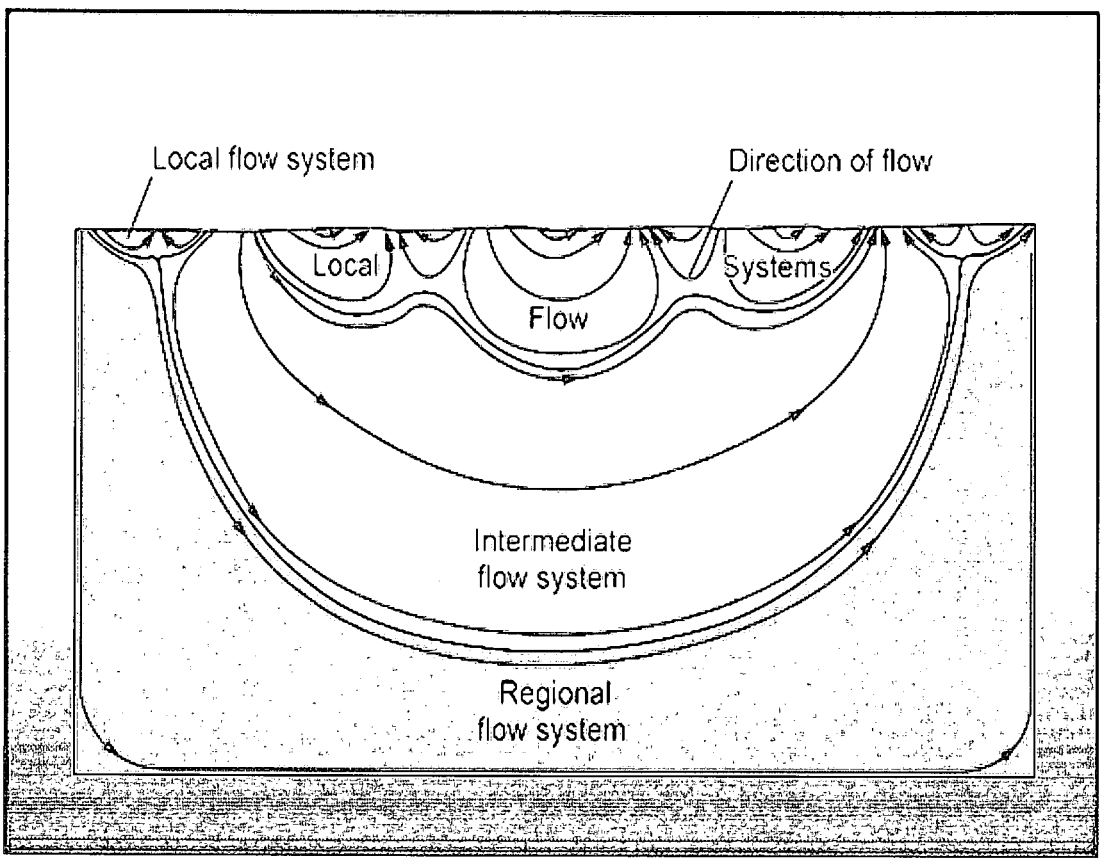

Figure4.5. Local groundwater flows make up local flow systems. Groups of local flow systems make up intermediate flow systems. Groups of intermediate flow systems make up regional flow systems. This is in accordance with the partial hydraulic conductivity theory each system contributes its partial. (culled from Toth, 1999)

4.5.0 CONCLUSION

The partial hydraulic conductivity theory can be used to predict bulk hydraulic conductivity in porous aquifers since the measured hydraulic conductivities of the samples can be interpreted as representative for the hydraulic conductivities of the formations. This has a far reaching implication when we consider the importance of hydraulic conductivity in;

- groundwater exploration,
- groundwater exploitation,
- in regional groundwater management .
- in groundwater pollution,
- investigation of groundwater contaminant transport,
- determine risks caused by the presence of contaminants in the subsurface,
- implementing remedial systems,
- construction of dams,
- calculation of seepage rates for waste facilities (landfills, ponds) and,
- determination of groundwater well field yields.

5.0 THE TRIGGER-TUBE; A NEW APPARATUS FOR MIXING SOLUTES FOR INJECTION TESTS IN BOREHOLES

5.1.0 INTRODUCTION

Borehole dilution is a well-established method for analyzing groundwater velocity. It is a tracer technique that is performed in a section of a well isolated by inflatable packers from the remainder of the well. A small amount of tracer is quickly injected into the isolated test section from a reservoir and is subjected to continual mixing in the borehole by a submerged pump as groundwater gradually replaces the tracer solution in the well. A log normalized concentration-versus-time curve can be plotted allowing for the magnitude of the horizontal velocity of the groundwater flow to be calculated. Testing vertically distinct sections of the well, a picture of the vertical velocity variation in the aquifer (near the well) can be obtained. The measurement of the lateral variability of the flow system depends on the number and distribution of monitoring wells. This method endeavors to account for the flow system distortions through a well screen. However, this accounting requires a calibration test for each well. The groundwater through-flow gradually removes the tracer introduced into the well from the well bore, to produce a time-concentration relationship from which the Darcy velocity is computed. The tracer is not recovered by pumping (Freeze and Cherry, 1979; Lamontagne et al, 2004; Devlin, 2006).

The single-well injection-withdrawal-test (SWIWT), or the Push-pull test. A tracer is introduced to the standing water column of the test well and allowed to drift, under natural gradient, away from the well bore. After a period of time, a few hours to days depending on the velocity of the formation, the test well is pumped to retrieve the tracer plume. Groundwater flow velocity is then calculated, based on the amount of pumping needed to recover the tracer (Leap and Kaplan, 1988).

The faster the groundwater flows, the farther the tracer plume migrates and the more pumping is needed to retrieve the plume. The drift or push phase of the test in such cases is shortened to prevent the tracer from moving too far away or escaping.

Natural gradient tests (multi-well tracer tests). A non reactive tracer is introduced into the standing water column in one well and the time it take to arrive at another borehole at a known distance is used to calculate the natural velocity.

Forced gradient tests (radial convergent test) are carried out between two boreholes by using the one borehole as the point for the introduction of tracer (solute) as in the point dilution tests and the other borehole as an abstraction borehole. For the source borehole the point dilution test will give an estimate of the Darcy velocity q. Fitting the breakthrough curve measured in the abstraction borehole will yield the seepage velocity v from which the effective porosity could be estimated from the equation $v = q/\varepsilon$.

Natural gradient tests, Point dilution tests, Tracer tests, Single well injection withdrawal tests (SWIWT) (Push-pull tests) and Forced gradient tests are all carried out based on a number of assumptions. The most important of these assumptions are,

i) Solutes are injected as well mixed slugs.

ii) The well mixing mechanism does not increase the rate at which the tracer moves out of the well

iii) The injection time is short compared to the overall length of time to carry out the whole experiment. (Neretnieks, 2007; Lamontagne *et al*, 2002).

However, every researcher who has ever carried out one of these tests in the field will attest that, one of the major problems in the use of these tests as a tool for hydrogeological investigations is the field procedure which requires a homogeneous mix of solute in the test well using a pump. The importance of the homogeneity of solute in the test well can never be over emphasized. The very success of getting good data and consequently good results from all these tests depends on it. It has always been the field nightmare, irrespective of which type of tracer or test method is being applied. In fractured rock aquifers, where the tests are carried out with the fracture in continuous flow field with the pump mixing method, it is exceedingly difficult to completely eliminate the influence of pumping on the rate at which the tracer moves into the fracture. This gives higher or lower velocities than would have been otherwise.

Also, on our campus test site, where groundwater velocities in the larger fractures are high (Hundreds of meters per day), and as such the overall time for tests are shorter (Tens of minutes), the injection time by using the method of pumping and mixing at the surface in a chamber by Lamontagne *et al* (2002), becomes long compared to the overall time needed for the experiments. It is difficult technically to get good data and accurate results.

Lamontagne *et al* (2002) in their very instructive paper came to one major conclusion that, the potential for the well-mixing mechanism (by pump circulation)

to increase the rate at which tracer mixes and moves out of the well is the main technical difficulty associated with the point dilution tests designs at present. And that future research on point dilution tests should quantify this problem and seek to develop instrumentation that would limit this potential bias. Neretneiks (2007) noted that, the notion of Taylor dispersion is valid for the case when the traced solution is collected and mixed at the "outlet" of the fracture. If there has not been time to even out the concentration between the streamlines the "dispersion" would not be seen if the fluid was rapidly pulled back as in a SWIW test.

Devlin (2002) affirmed that, the chief disadvantage of the borehole dilution method by pump-mixing is the need for mixing in the well; that down-hole mixers have not proven reliable and recirculation of the tracer solution from the well to the surface and back limits the depth at which the measurements can be made.

The difficulties associated with calibration for an in-ground well screen are also non-trivial though necessary for calculations for groundwater velocity from pump-mixing point dilution tests.

5.1.1 Aim

After many botched tests and ambiguous results from field tests due to the above assumptions not being met. We undertook to develop a new apparatus aimed at;

i) Mixing the solute inside the borehole homogeneously on injection.

ii) Instantaneously introduce solute inside the borehole within seconds.

iii) Introduce the solute inside the borehole without perturbations.

5.2.0 APPARATUS

5.2.1 The trigger tube

The trigger tube was designed and built after laboratory experimentation. It is made up of a fifty centimetre length of polyvinylchloride (PCV) piping with a lid and trigger mechanism at one end and a threaded coupling joint at the other. The trigger mechanism consists of a lid, a larger retractor spring, a trigger disc, a smaller retractor spring and a circular rubber seal (Figure5.1).All round the lid, is glued a circular rubber seal to make the assembly leak proof .The lid which is hinged at one end of the tube is opened by the larger retractor spring attached to it. At the opposite end to the hinge is the lock which is L-shaped with a small bearing at the tip (Figure5.2). To close the lid, pull the chord (blue) attached to the trigger disc to align the slit to the bearing, Plate2b, while simultaneously, the chord attached to the lid (yellow chord) is pulled, bringing the lids' lock bearing into the trigger discs through the slit. Release the discs chord (blue) and the small retractor spring rotates the trigger disc anti clockwise, locking the lid in place. Then release the lids chord (yellow) . (To close; p*ull blue, pull, yellow: release blue, yellow*).

To open the lid, pull the chord (blue) attached to the trigger disc. The trigger disc is rotated clockwise by the small retractor spring which aligns the discs slit to the lids' bearing and the large retractor spring then retracts, pulling the lid open . (To open; *Pull blue*) This trigger tube has been tested to pressures equivalent to down-hole pressures of up to one hundred meters (100m) depth below the water table and it opened and closed smoothly. It is coupled with segments of PVC tubes of same diameter to make up the trigger tube assembly. Fourteen PVC tubes of two meter lengths where used for the field tests to a depth of 28m.

Figure5.1. Trigger-tube apparatus for injecting solutes into wells for point dilution tests

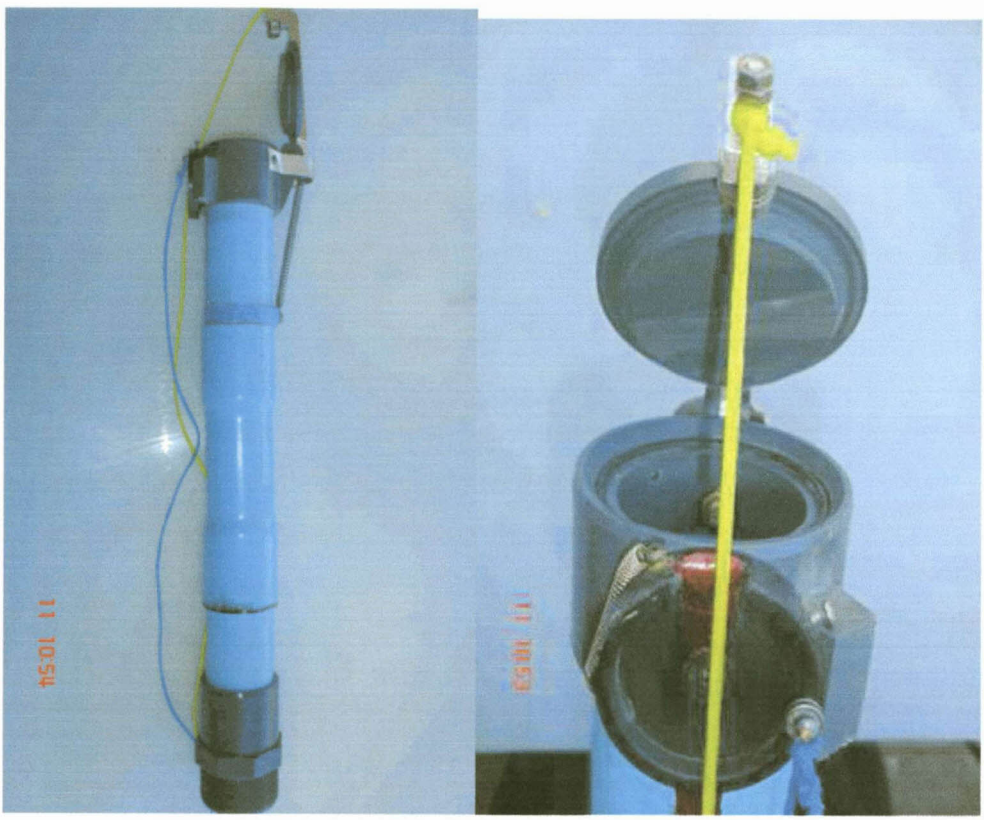

(a) (b)

a) Trigger-tube. Full view, with the trigger mechanism (top) and threaded end for coupling. (Bottom). b) Trigger tube. With lid opened by pulling the blue chord. (Lower right) and releasing lid chord (yellow).Hinge spring pulls the lid opened.

Figure5.2. Opening and closing trigger-tube apparatus

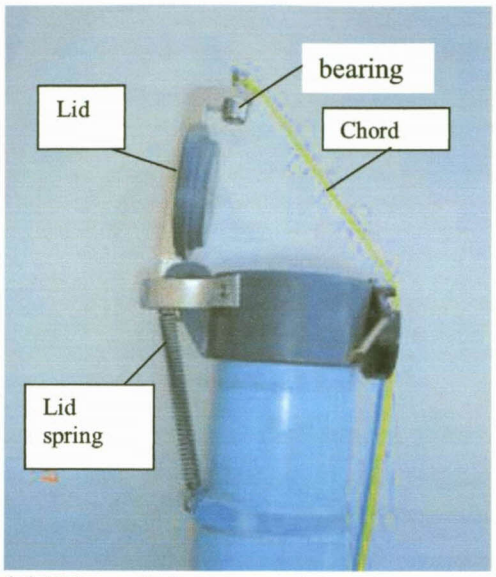

(a) Trigger-tube apparatus

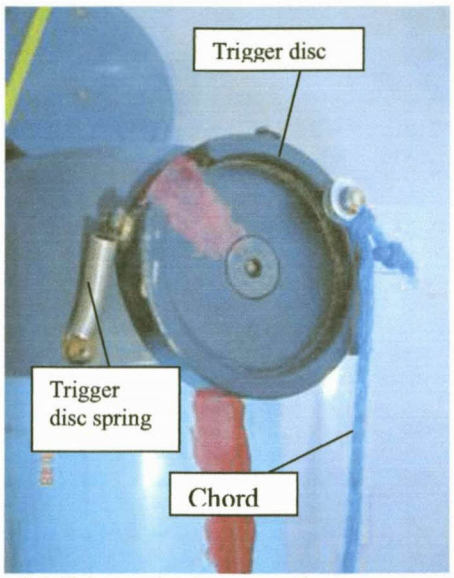

(b) Trigger lock-open disc.

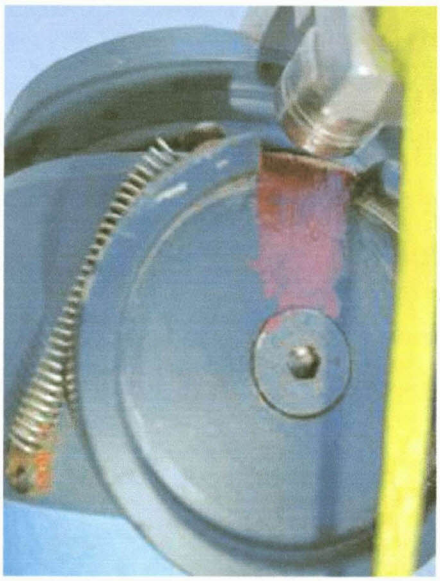

(c)

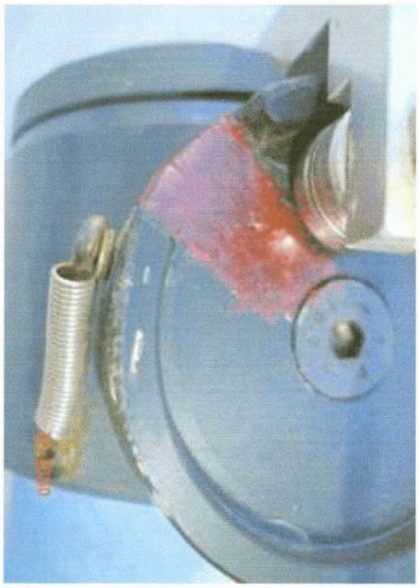

(d)

. c) Trigger disc in closing position with trigger chord being pulled (blue chord) With the yellow lid chord pulled down and lid bearing entering slit .d) Lid bearing in place.

5.2.2 Solute (Homogeneous mixing)

The determination of the test solute concentration is calculated by taking into consideration the concentration of the borehole water (Background EC), the total volume of water in the borehole, the volume of water outside the trigger tube and its concentration, the volume of the trigger tube and the solute concentration in the trigger tube, using the formulae below.

From laboratory experimentation, the concentrations for various trigger tube sizes and EC values were gotten from;

$$EC_T V_T = EC_b V_b + EC_t V_t \quad \text{..... (1)}$$

$$V_T = \pi r_T h \quad \text{..... (2)}$$

$$V_t = \pi r_t h \quad \text{..... (3)}$$

$$V_b = \pi (r_b - r_t) h \quad \text{..... (4)}$$

EC_T = Solute EC required for carrying out test in the whole borehole (Test EC)

EC_t = Trigger tube EC (Premixed solute EC in trigger-tube). Input EC.

EC_b = Borehole background EC

V_T = Total borehole volume

V_t = Trigger tube volume (*includes volume due to thickness of tubes*)

V_b = Borehole volume outside trigger tube

h = Length of test segment

r_b = Radius of borehole

r_t = Radius of trigger tube

Laboratory tests were carried out using trigger tubes of 30 mm, 63mm, 100mm, 110mm and 120mm diameter, to determine the input solute concentrations and the required volumes of fluid, for any desired initial solute concentration for the test, using trigger tubes of different borehole sizes. The calculated values are given in Figure5.3.

5.2.3 EC meters

These were of two types;

a) Solinst Temperature/Level/Conductivity (TLC) meter.

b) A multi-parameter probe.

This was used to measure water levels and profile the borehole.

These measured EC

5.2.4 Winch

A winch was used to lower and raise the trigger tube assembly into the borehole. It was made up of a solid tripod, pulley, gear and sprocket and a 5mm diameter stainless steel cable.

5.2.5 Clamps

A set of three clamps to hold the trigger tube assembly unto the borehole casing and to couple and decouple the PVC tubes during insertion and withdrawal from the borehole were used. It is very important to clamp the trigger tube assembly firmly attached to the borehole casing, to resist the enormous buoyancy forces that come into play, pushing upward when the

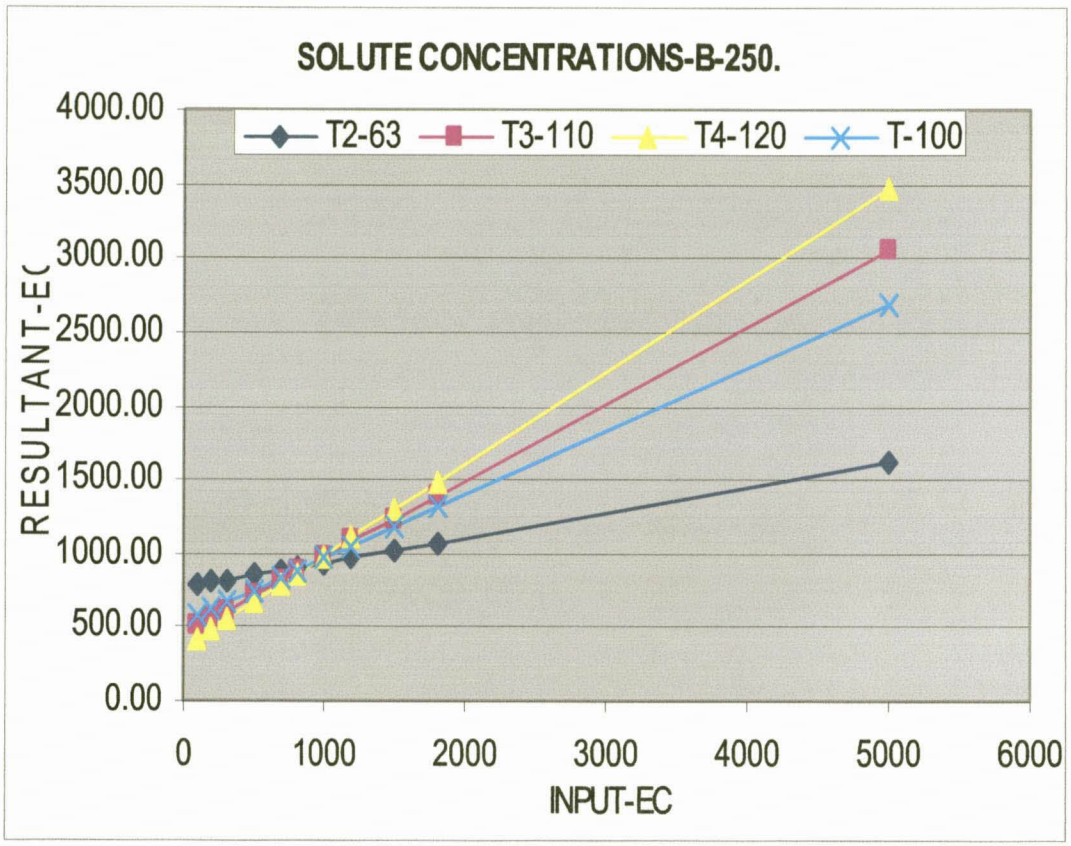

Figure5.3. EC calculator for various trigger-tube sizes from laboratory experimentation; each solute input from a given trigger-tube size gives a resultant EC mixture value in the borehole of a given background EC (250 µS).

tube assembly becomes empty, after all the water has been pumped out of the trigger tube assembly before the introduction of the solute into the trigger tube assembly. This may present a hazard if the trigger tube assembly is not firmly attached.

5.2.6 Submersible pump

A 0.5 horse power, 4cm diameter 2l/min submersible pump was used to pump water out of the trigger tube assembly. No pumping takes place inside the borehole itself thus there are no perturbations in the borehole.

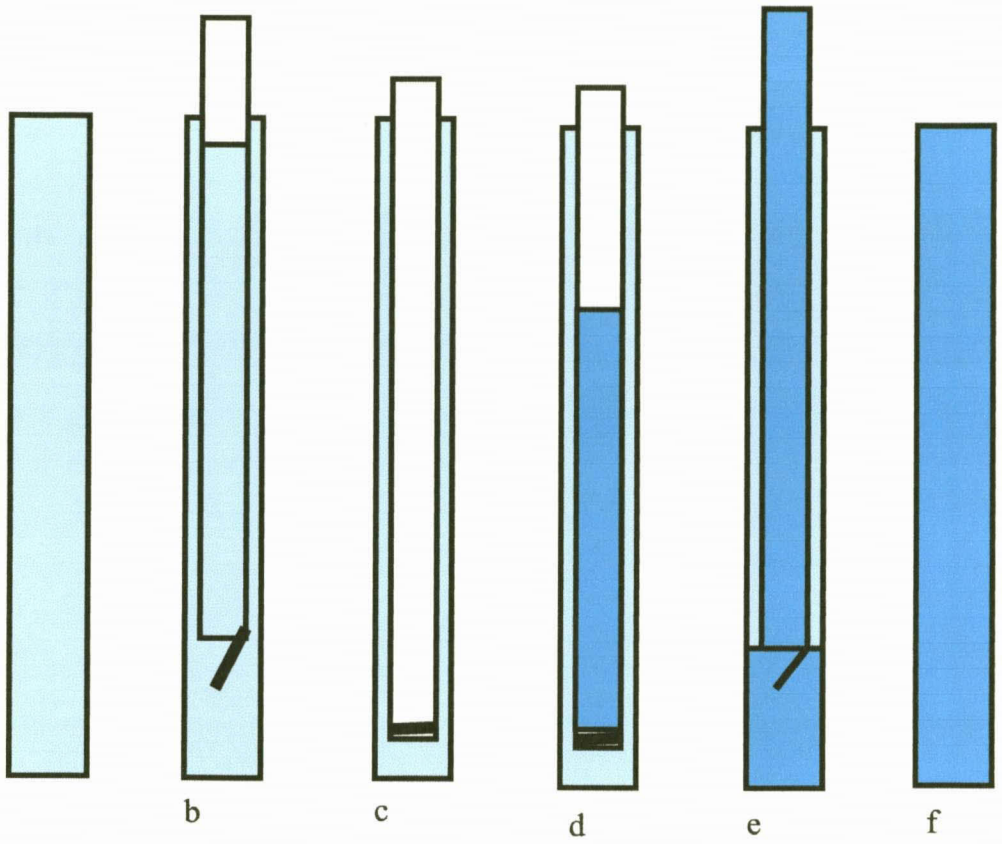

Figure5.4. Steps in carrying out the thermal dilution test; (a) Borehole with water, (b) Insertion of trigger tube with valve open, (c) Trigger tube assembly with valve closed and water pumped out. (d) Solute filled into trigger tube assembly with valve closed. (e) Trigger tube assembly with valve opened, being withdrawn. (f) Borehole now filled with homogeneously premixed solute (trigger tube withdrawn). Only the saturated section of borehole is shown.

5.3.0 Test procedure

The procedure to carry out the test (Figure5.4) using the trigger tube assembly is as follows;

- The multi-parameter EC probe is placed down-hole below the water table at the required test depth for the investigation 21m. (Point dilution test) The probe is activated to start taking readings.
- The test well is profiled from top to bottom using a Solinst temperature-level-conductivity (TLC) probe, to get the background values of EC and temperature with depth. While the multi-parameter probe was placed at the fracture at a depth of 21m.
- The trigger tube is inserted into the borehole down to the required depth by coupling six meter length PVC pipes to the trigger tube, with its lid opened Figure5.4a.
- At the required depth, the chords of the lid and the trigger disc are then pulled simultaneously to close the lid, with water inside the tube (Figure5.4b). The water in the tube and that in the borehole are at the same level. Static water level.
- The submersible pump is lowered to the bottom of the closed tube, and the water in the tube is pumped out Figure5.4c.
- The submersible pump is withdrawn from the now empty trigger tube assembly.

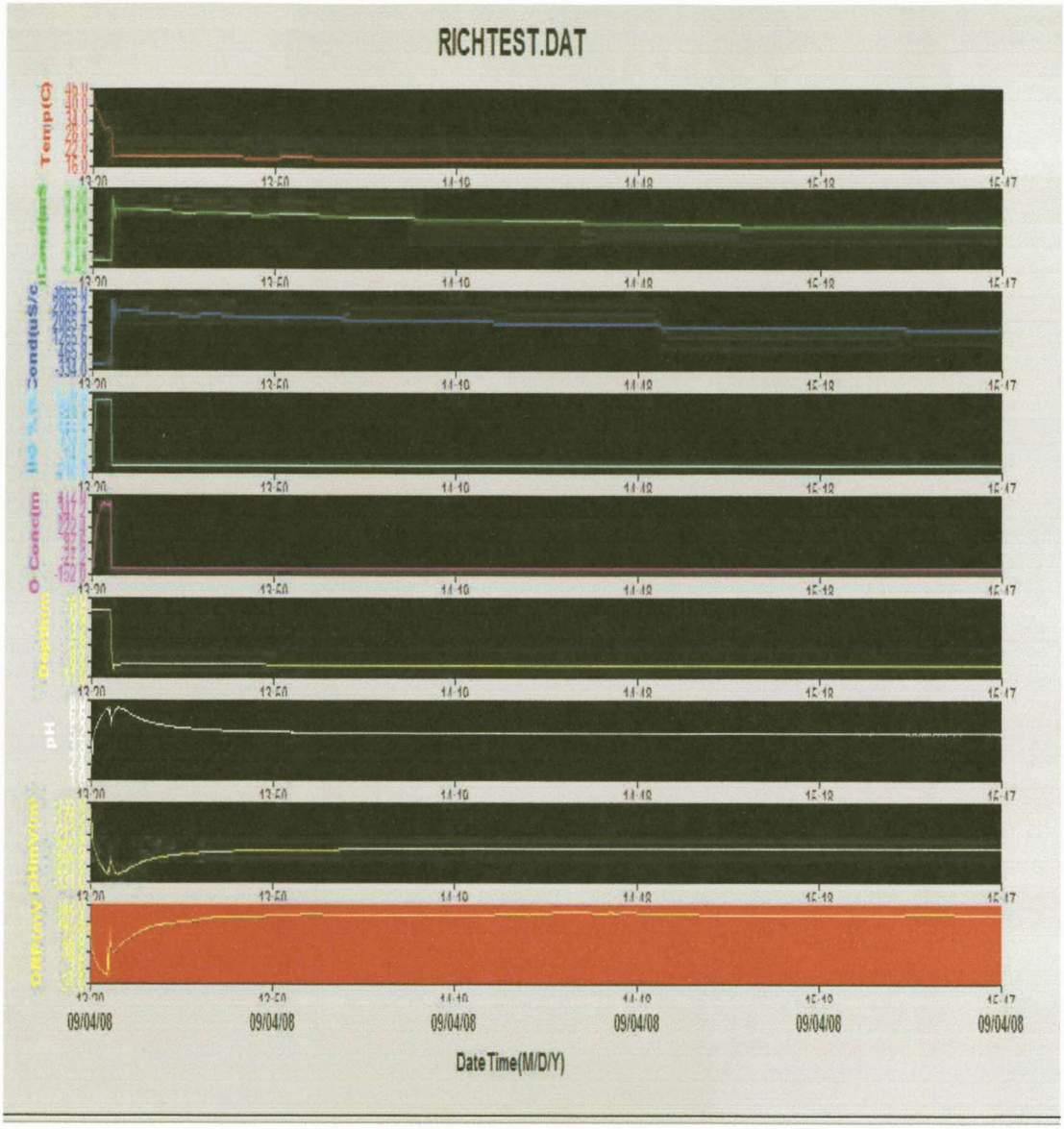

Figure5.5. Point dilution test showing instantaneously mixed solute using trigger tube apparatus

- With the lid of the tube closed, the water pumped from inside the trigger tube assembly is poured into three 20 litre containers and is mixed with an appropriate mass of salt (in our case NaCl) to the required concentration for the trigger tube (EC_t). The well mixed solute of predetermined concentration (Point dilution test, Natural gradient test), is poured into the tube up to the static water level Figure5.4d.
- Using the EC calculator Fig5.3, 500 μS Ect was appropriate to give us an EC_T of 366 μS in the borehole, using the EC calculator, Figure5.3. The three 20 litres plastic containers were enough to fill the trigger tube assembly to the required test length of 16m (depth of 12m-28m below water level). 14 PVC pipes of 63 mm diameter at 2m lengths and 3.56 l/m volume of solute. 56.96 litres of solute in three 20 litre plastic containers was used.
- The chord of the trigger disc is then pulled to open the lid and the trigger tube assembly with the lid now opened is withdrawn at a constant rate of one meter every five seconds, to avoid disturbing the water in the borehole Figure5.4e.
- The borehole is immediately profile by the pull-up and lowering method at depths of fifty centimetres intervals, using the TLC probe while the multi parameter probe is placed at a depth of 21m measures the EC until the EC of the well returns to over ninety percent of its background EC value.
- At the observation borehole UO7, another TLC probe is lowered simultaneously to the fracture at a depth of 21m, and readings are taken at one minute intervals. Passive test.

The combined readings from the two probes make up the natural gradient tracer test.

5.4.0 RESULTS

5.4.1 Darcy velocity

The Darcy velocity q, for point dilution tests is given by;

$q = -\frac{V}{\alpha A t}\log(\frac{C}{C_0})$ (Drost and Neumaier, 1974) ..... (5)

Where;

V = Volume of fluid contained in the test section

A = cross sectional area normal to the direction of flow

C_0 = Tracer concentration at t = 0

C = Tracer concentration at time = t

α = Borehole distortion factor (between 0.5 and 4; =2 for an open well)

t = Time when the concentration is equal to C

$q\alpha = \nu$, where ν = apparent velocity inside well.

In practice either the radial flow solution or the parallel plate model is used to estimate the cross sectional area A (Novakowski, *et al.*, 1998);

- For the radial flow model,

$A = \pi r_w b$ ..... (6)

r_W = well radius

b = the length of the tested section in the borehole.

- For the parallel plate model

$A = \pi r_w(2b)$ ..... (7)

where

2b = equivalent aperture of the fracture rock.

5.4.2 Natural flow velocity

The natural flow velocity is given by,

$V = x / t$ ..... (8)

x = Distance of observation borehole UO7 from test well UO5.

t = is the time taken for the tracer to travel from test well to observation well.

The results from tests using the trigger tube for a point dilution test on borehole UO5 and a natural gradient test on borehole UO5/UO7 at the University of the Free State test-site shows that, the solute was instantaneously mixed to the desired EC within a minute of withdrawal of the tube assembly from the borehole (Table5.1).

The data from the passive natural gradient test from the TLC probe was plotted on an x-y scatter using an excel spreadsheet and this shows the arrival of the peak of a pulse of EC 82 minutes after the release of the tracer (solute) in UO5. Figure5.3. Using equation (8), a natural flow velocity of 123 m/days was determined.

The data from the multi-parameter probe for the point dilution test in borehole UO5 was analyzed using equation (5) in SOLVER, from which effective porosity, Darcy velocity and seepage velocities were calculated. This gave a Darcy velocity of 4.06 m/day, an effective porosity of 0.033 (3.3%) and a seepage velocity of 122.89 m/day (Table5.2). From these results, the natural flow velocity of 123 m/day from the natural gradient test and the seepage velocity of 122.89 m/day from the point dilution are equal. This shows that the trigger tube test results are accurate. Comparing these results with those for the same fracture at 21m from tests carried out on the campus site by Van Tonder et al (2000) using the pumping mixing mechanism, (Table5.4), they have the same value of 0.03 for the effective porosity but different values of seepage velocity and Darcy velocity for radial convergence tests and injection withdrawal tests.

Table5.1 EC calculator for solute concentration using various types of trigger tube sizes

V-bhole	E C-bh	V1-bh63	V2-bh110	**V3bh-120**	V3-tt120	V2-bh110	V1- t-63	V4-t-100	V4-bh100
18.24	900	15.51	11.31	9.5	9.13	7.32	3.12	7.85	10.78
18.24	900	15.51	11.31	9.5	9.13	7.32	3.12	7.85	10.78
18.24	900	15.51	11.31	9.5	9.13	7.32	3.12	7.85	10.78
18.24	900	15.51	11.31	9.5	9.13	7.32	3.12	7.85	10.78
18.24	900	15.51	11.31	9.5	9.13	7.32	3.12	7.85	10.78
18.24	900	15.51	11.31	9.5	9.13	7.32	3.12	7.85	10.78
18.24	900	15.51	11.31	9.5	9.13	7.32	3.12	7.85	10.78
18.24	900	15.51	11.31	9.5	9.13	7.32	3.12	7.85	10.78
18.24	900	15.51	11.31	9.5	9.13	7.32	3.12	7.85	10.78
18.24	900	15.51	11.31	9.5	9.13	7.32	3.12	7.85	10.78
18.24	900	15.51	11.31	9.5	9.13	7.32	3.12	7.85	10.78
18.24	900	15.51	11.31	9.5	9.13	7.32	3.12	7.85	10.78
Tt-input	EC-63	**EC-110**	EC-120	EC-100	diff 63-t	**diff 110-t**	diff-120-t	diff-100-t	
100	782.40	502.58	423.19	574.95	-117.60	-397.42	-476.81	-325.05	
200	799.51	554.66	485.20	617.98	-100.49	-345.34	-414.80	-282.02	
300	816.61	606.74	547.20	661.02	-83.39	-293.26	-352.80	-238.98	
500	850.82	710.91	671.22	747.09	-49.18	-189.09	-228.78	-152.91	
700	885.03	815.08	795.23	833.17	-14.97	-84.92	-104.77	-66.83	
800	902.14	867.16	857.24	876.21	2.14	-32.84	-42.76	-23.79	
1000	936.35	971.33	981.25	962.28	36.35	71.33	81.25	62.28	
1200	970.56	1075.49	1105.26	1048.36	70.56	175.49	205.26	148.36	
1500	1021.88	1231.74	1291.28	1177.47	121.88	331.74	391.28	277.47	
1800	1073.19	1387.99	1477.30	1306.58	173.19	487.99	577.30	406.58	
5000	1620.56	3054.66	3461.51	2683.77	720.56	2154.66	2561.51	1783.77	
10000	2475.822	5658.827	6561.842	4835.636	1575.822	4758.827	5661.842	3935.636	

Table5.2. Natural gradient test from boreholeUO7

Time	EC mS
0	745
1	745
2	745
3	745
4	745
5	745
6	745
7	745
8	745
9	745
10	745
11	745
12	745
13	745
14	745
15	745
16	745
17	753
18	757
19	757
20	760
21	760
22	762
23	766

Time m	EC mS
24	768
25	769
26	771
27	773
28	773
29	773
30	773
31	773
32	776
33	776
34	776
35	776
36	776
37	776
38	776
39	776
40	776
41	776
42	776
47	779
52	782
82	798
87	780
92	769
97	761

Table5.3. Tests on borehole UO5 using trigger tube. Point dilution and natural gradient test

Point dilution test UO5

Flow Dimension	Distortion Factor	Section Tested	Interval	Tracer	Effective Porosity	Darcy Velocity	Seepage Velocity
n = 2	2	20.5-21.5m	1m	NaCl	0.033	4.06 m/day	122.89 m/day

Natural gradient test UO7

DISTANCE (m)	TIME (minutes)	NATURAL VELOCITY(m/day)
7	82	123

Table5.4. Comparative time frame for carrying out a point dilution test using trigger-tube and pump mixing of solute in test well

a. Trigger tube test time frame.

ACTIVITY	Inserting tube assembly	Inserting pump and Pumping out water	Filling tube assembly with solute	Withdrawing tubes and Releasing tracer
TIME	3minutes	5mins (2 l/sec)	2 minutes	3 minutes
Total time	13 minutes			

b, Pump Mixing test time frame

ACTIVITY	Insertion of pump and mixing mechanism	Recirculation and mixing for homogenization of solute	Withdrawal of pump and mixing mechanism
TIME	5 minutes	At least 15 minutes	5 minutes
Total time	At least 25 minutes		

Point Dilution Test: Natural Gradient - Single-well test

Source Borehole	UO5	Enter values in yellow cells			Tracer used	NaCl
Date of test	01-Sep-08					
Radius of BH (m)	0.08	Section volume	0.020096		Section tested	20.5-21.5m
Interval length (m)	1(20.5-21.5)	Effective porosity	0.033	#DIV/0!	Mass injected (kg)	
BH Distortion factor	2	Flow dimension n	2	1.85	area =	0.050
Geology		Sandstone	0.2	0.16		

		Method 1	Darcy velocity q_v (m/d) =	4.06	☑ Yes
Co - background	-84	Method 2	Darcy velocity q_v (m/d) =	12.53	☐ Yes #####
		84	Darcy velocity q_n (m/d) =	4.06	click both for average
			Seepage velocity v_n (m/d) =	122.89	

Time	Conc C	Background value =
(minutes)	mS/m	C-backgr
0.00	366.1	282.1
0.08	361.6	277.6
0.17	329.6	245.6
0.25	300	216
0.33	295.7	211.7
0.42	235.1	151.1
0.50	295.4	211.4
0.58	297.9	213.9
0.67	297.6	213.6
0.75	297.3	213.3
0.83	297.5	213.5
0.92	297.9	213.9
1.00	298.2	214.2
1.08	298.4	214.4
1.17	298	214
1.25	298.3	214.3
1.33	298.5	214.5

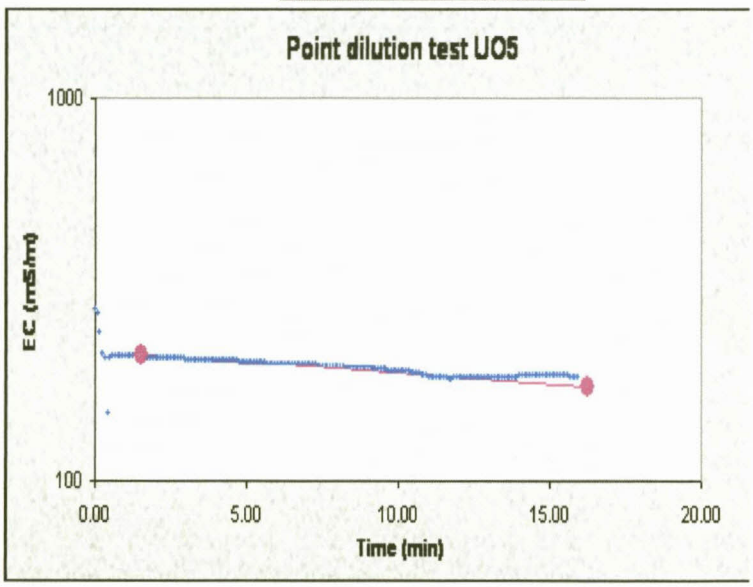

Figure5.6. Point dilution test (Natural gradient) of borehole UO5 analysis using SOLVER

5.5.0 DISCUSSION

By comparing the results from the tests on the campus test site using the trigger tube to those over the years by other researchers using the pump mixing mechanism (Table5.4, Figure5.6). The total time for set up and introduction of tracer is shorter than that for the other method. The smoothness of the plotted data is better, the seepage velocity and natural velocity are the same while that of the other method are not equal. (Figure5.7&5.8). This shows that the trigger tube method is accurate.

5.6.0 CONCLUSION

From the results of the field tests carried out on the campus test site, we can conclude that the trigger tube apparatus for the mixing of solutes for injection tests in wells was successful. It satisfies the three most important assumptions for; Point dilution, Single well injection withdrawal tests, Natural gradient and forced gradient tests (Figure5.7).

Namely;

i) Solutes are injected as well mixed slugs.

ii) Introduction of solute by the trigger tube does not increase the rate at which the tracer moves out of the well

iii) The injection time is short compared to the overall length of time to carry out the whole experiment.

Thus, a very useful apparatus for carrying out field tests that involve the injection of homogeneously mixed solutes in tests wells has been developed. The development of the Trigger-tube which is of great importance for use in well injection tests' as a user friendly, cost effective and accurate apparatus.

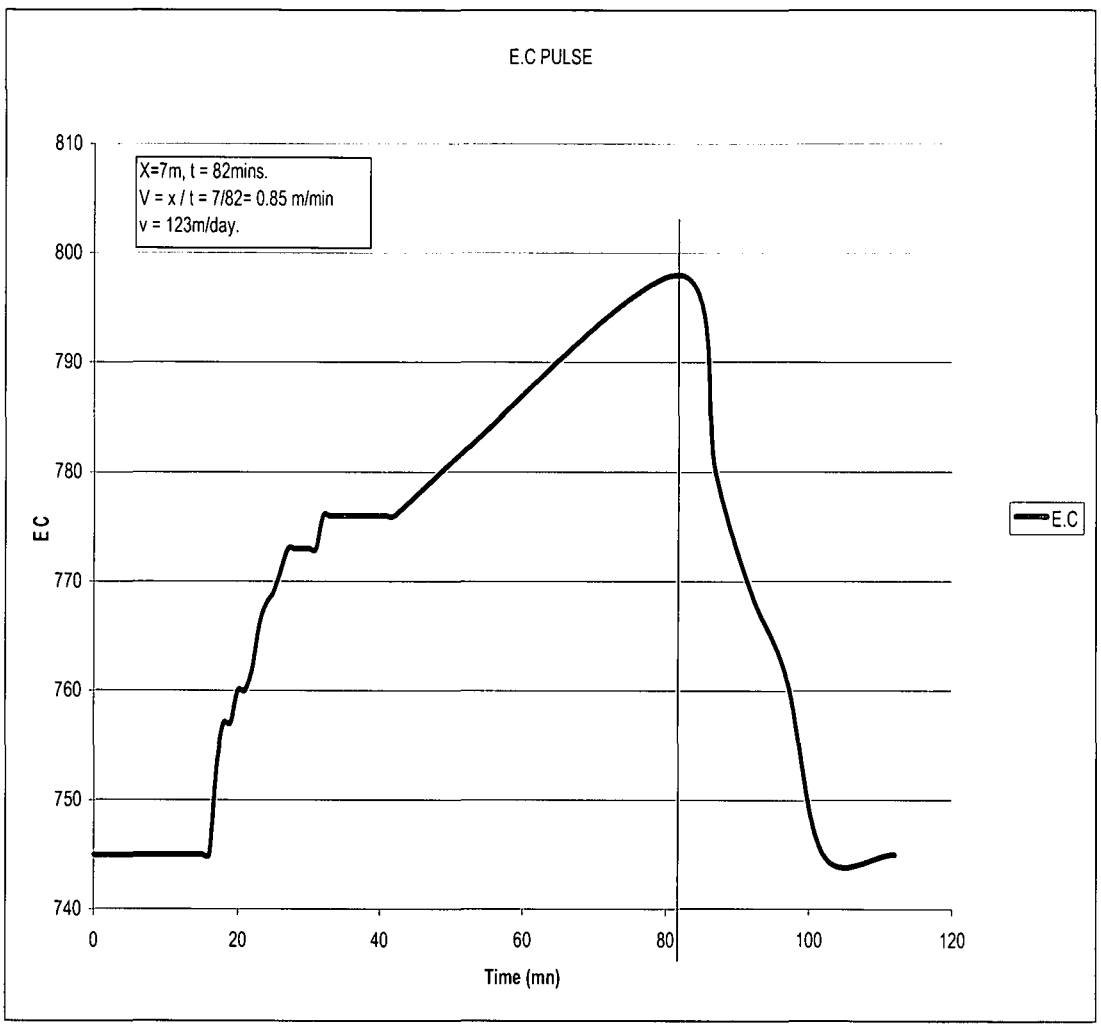

Figure5.7. EC pulse of natural gradient test using trigger tube; Note arrival time of 82 minutes at observation borehole UO7.

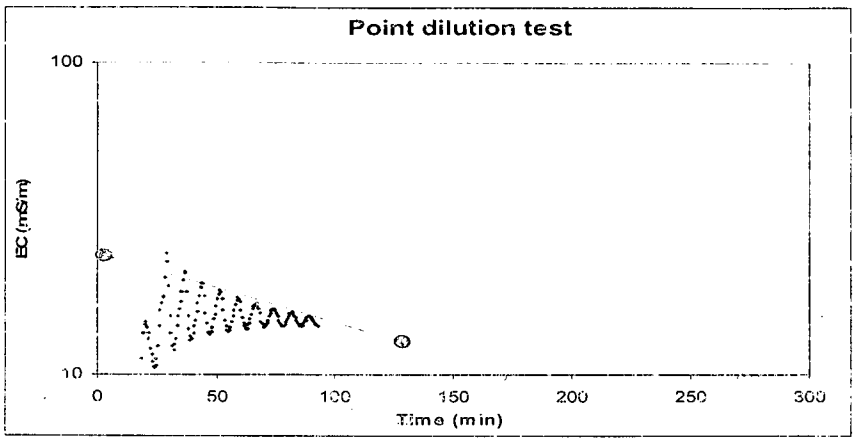

(a) Point dilution test on UO5 using pump mixing mechanism. (Bangoy. 1998)

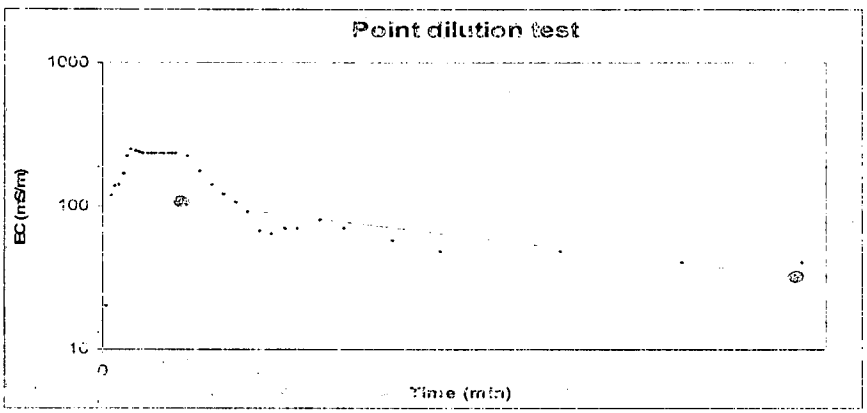

(b) Point dilution test on UO5 using pump mixing mechanism. (Charl 2008)

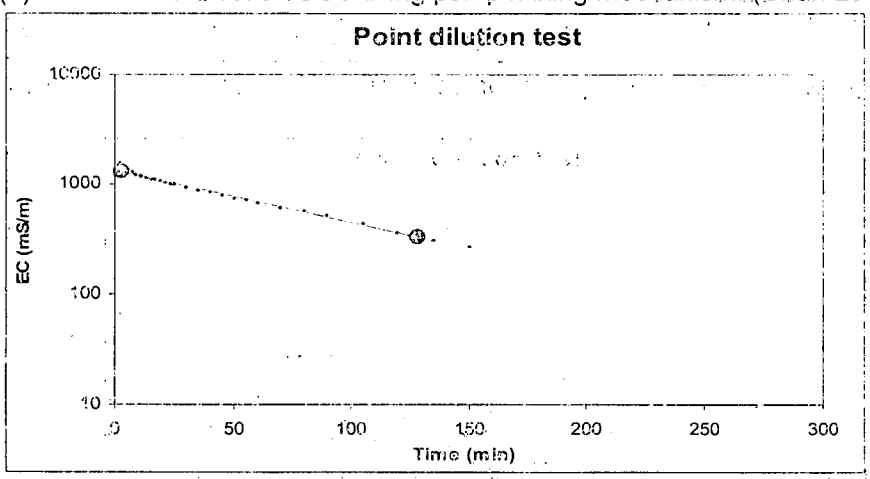

(c) Point dilution test on UO5 using trigger tube (2008).

Figure5.8. Comparing results of tests using trigger tube (c) and pump mixing methods (a & b). Note the oscillating data points in the pumping mixing tests due to the effect of the pump.

The use of this apparatus has advantages over using the pumping and mixing mechanisms.

5.6.1 Advantages

These are;

- No perturbation of well since there is no pumping in the well
- No specialized pump (Peristaltic etc)
- No isolation of test section or use of packers.
- No recirculation of borehole water which can affect the rate of tracer entry into test well.
- Better control of solute concentration (predetermined).
- No mechanism for mixing of solute down hole since the solute is more homogenously pre-mixed.
- The whole length of the borehole can be tested at once.
- This test method uses few instruments and as such is quicker to set up and carry out.
- The solute is released at once (instantaneously).
- Simple equipment to transport and handle.
- Economical. The trigger tube is cheap to construct.
- Accurate data acquisition.

5.6.2 Disadvantage

The pipes for the trigger tube assembly are bulky to carry for very deep boreholes. Also, there is a hazard during the transition between emptying the trigger tube and filling it with a tracer if the tube assembly is not well attached in place. The empty tube becomes buoyant with a tremendous lifting force.

6.0 THERMAL DILUTION TEST: A NEW METHOD FOR THE DETERMINATION OF FRACTURE POSITIONS, FLOW ZONES AND GROUND WATER VELOCITIES IN AQUIFERS, USING TEMPERATURE AS A TRACER IN SINGLE WELLS.

6.0.0 INTRODUCTION

In boreholes drilled in fractured rock aquifers, the position and the number of fractures present, the flow zones and relative flow contributions of the fractures present is very important for the characterization of these aquifers.

Acoustic scanners, callipers and borehole cameras can determine the position and number of fractures in a borehole. These are very expensive equipment that is not within the reach of every investigator. Their use also takes time and a certain level of technical know-how. These methods cannot tell you which and to what extent the fractures present contribute to the flow of ground water in the aquifer.

Pump-tests, Tracer tests, point dilution tests and single well injection withdrawal tests are used to determine aquifer and fracture hydraulic characteristics. However in most situations where fractures are so closely-spaced that packers and other grouting techniques used to isolate fractures for characterization are difficult to use, it becomes extremely difficult to tell which fracture has what characteristic flow properties. Thus, the use of terms such as, test segments; test section, test zone, etc to denote bulk properties of a number of inseparable fractures. The use of packers and grouting techniques to isolate fractures for tests, is complicated and equipment intensive. There was the need therefore for a new apparatus and technique to determine the groundwater

velocity, flow zones and fractures in fractured rock aquifers. We decided under the "Bulk flow project", to develop such an apparatus and technique called the Thermal Dilution Test (TDT).

6.2.0 AIM

The aim of this part of the research was;

i) Develop a technique to determine zones and fractures with flowage.

ii) Develop an appropriate apparatus to use such a technique.

iii) Develop a method to determine groundwater velocity without the need of a fore knowledge of the aquifer's effective porosity.

6.2.1 PRINCIPLE

It has been known for a long time that, heat transfer, water movement, and solute transports are coupled (Constanz *et al*, 2003). Various studies have been carried out using heat as a tracer.

The use of temperature in groundwater studies can be divided into two groups;

a) Passive methods. Here the natural temperature of the earth (Geothermal gradient) and ground water is used to elucidate aquifer characteristics.

b) Active methods. Here thermal perturbations are imposed on the system by heating the water in the borehole and the variations of temperature resultant thereof are measured to determine aquifer parameters.

The above approaches use temperature either of the groundwater (geothermal) or generated, as a tracer to determine horizontal flow through the fractures, vertical infiltration of water through soils, flow patterns in regional or

basin studies, recharge and discharge zones. An exhaustive discussion of heat as a tracer can be found in the review paper by Anderson (2005). The present method is on the use of active temperature in the form of cold water to identify fractures and delineate flow zones, in a single well test, analogous to a point dilution test. Here, the cold of the water introduced into the borehole is carried away by the warmer groundwater flowing through the borehole and the formation.

Heat flows in three ways: Radiation, conduction and advection. Heat flow by groundwater takes place by heat conduction and advection.

Heat radiation is the process by which regions of higher molecular kinetic energy pass their thermal energy to regions with less molecular energy without direct collision of molecules. Radiation takes place at temperatures above zero Kelvin.

Heat conduction (Thermal diffusion) is the process by which regions of higher molecular kinetic energy pass their thermal energy to regions with less molecular energy by direct collision of molecules.

Heat advection (Thermal advection) or forced advection (since it requires a hydraulic head gradient to drive the fluid motion, which is responsible for the thermal advection) is flow of heat due to the movement of groundwater which transports it and to which it is coupled.

Heat transport in groundwater is through conduction (Thermal diffusion) and forced advection.

6.6.0 TRANSPORT OF HEAT

6.6.1 Heat conduction

In the theory of heat conduction, an assumption is made that heat flows in the direction of decreasing temperature. Another assumption is that the time rate at which heat flows across a surface area is proportional to the component of the temperature gradient in the direction perpendicular to the surface area (Mathews and Howell, 2006).

If the temperature at a point is T(x, y), then the heat flow at that point (x, y) is given by the vector

$$\vec{V}(x,y) = -KgradT(x,y) = -K(T_x(x,y) + iT_x(x,y) \quad \text{..... (1)}$$

Where K is the thermal conductivity of the medium and is assumed to be constant. If Δz denotes a straight-line segment of length Δs, then the amount of heat flowing across the segment per unit of time is

$$\vec{V} \bullet \vec{N} \Delta s \quad \text{..... (2)}$$

Here, $\vec{N}$ is a unit vector perpendicular to the segment.

If we assume that no thermal energy is created or destroyed within the region, then the net amount of heat flowing through any small rectangle with sides of length Δx and Δy is identically zero (see Figure6.1). This leads to the conclusion that T(x,y) is a harmonic function. The following heuristic argument is often used to suggest that T(x,y) satisfies Laplace's equation. Using equation (2) we find that the amount of heat flowing out of the right side of the rectangle in Figure6.1 is approximately

$$\vec{V}_1 \bullet \vec{N}\,\Delta s = -K(T_x(x+\Delta x, y) + iT_x(x+\Delta x, y) \bullet (1+0i)\Delta y \quad \text{..... (3)}$$

and the amount of heat flowing out of the left edge is;

$$= -KT_x(x+\Delta x)\Delta y \quad \text{.....(4)}$$

If we add the contributions in Equations (3) and (4), the result

$$-K(\frac{T_x(x+\Delta x, y) - T_x(x, y)}{\Delta x})\Delta x\Delta y \approx KT_{xx}(x, y)\Delta x\Delta y \quad \text{..... (5)}$$

Similarly, the contribution for the amount of heat flowing out of the top and bottom edges is

$$-K(\frac{T_x(x, y+\Delta y) - T_x(x, y)}{\Delta y})\Delta x\Delta y \approx KT_{yy}(x, y)\Delta x\Delta y \quad \text{.....(6)}$$

Adding the quantities in Equations (5) and (6), we find that the net heat flowing out of the rectangle is approximated by the equation,

$$-K(T_{xx}(x, y) + T_{yy}(x, y)\Delta x\Delta y = 0$$

Which implies that?

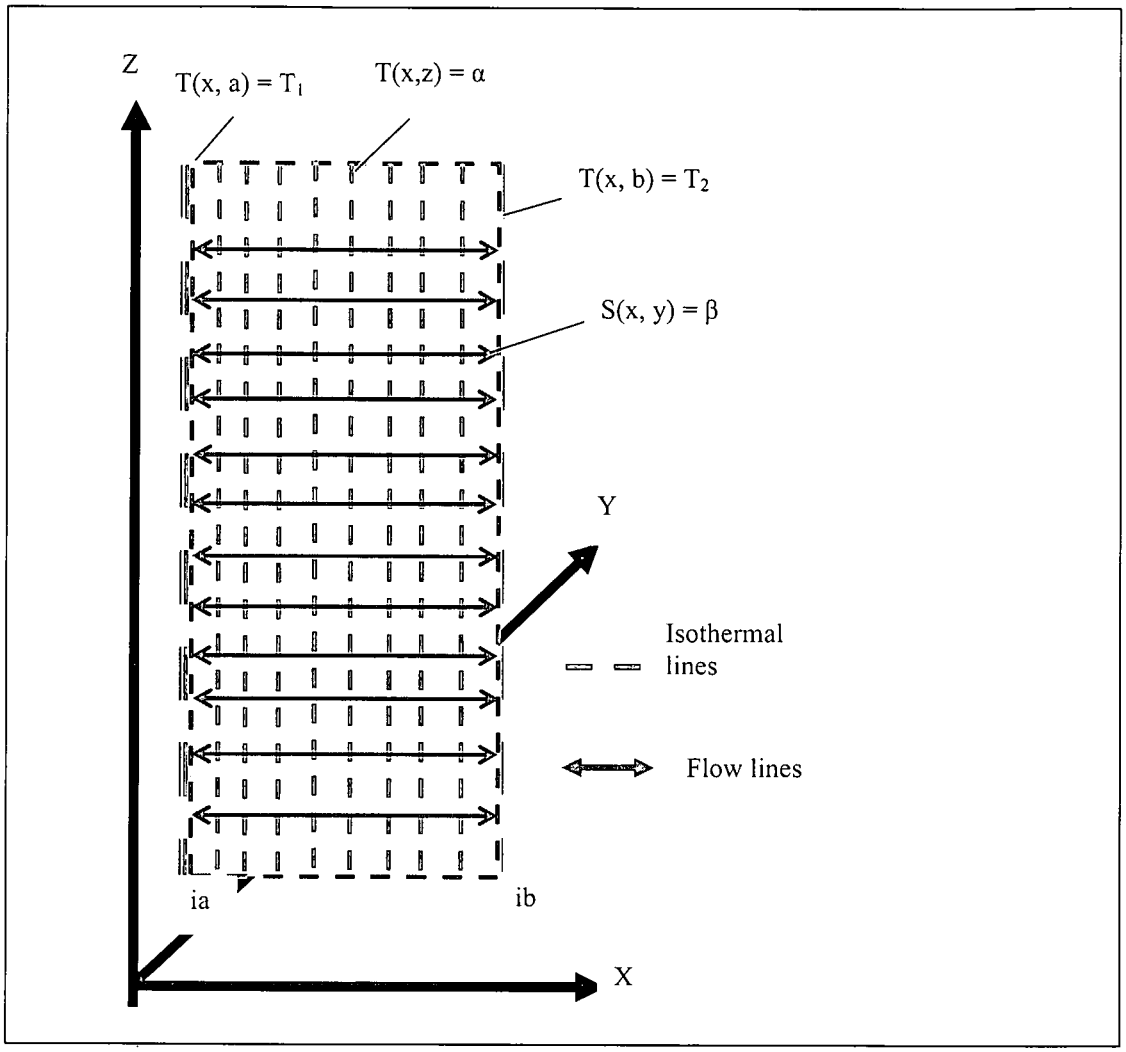

Figure6.1. Temperature between parallel planes (ia) and (ib) where $T_1 > T_2$ or $T_2 > T_1$.Showing flow lines and isothermal lines in conductive heat transfer in a borehole with cold water with warmer groundwater all round.(Adapted from Mathews and Howell,2006)

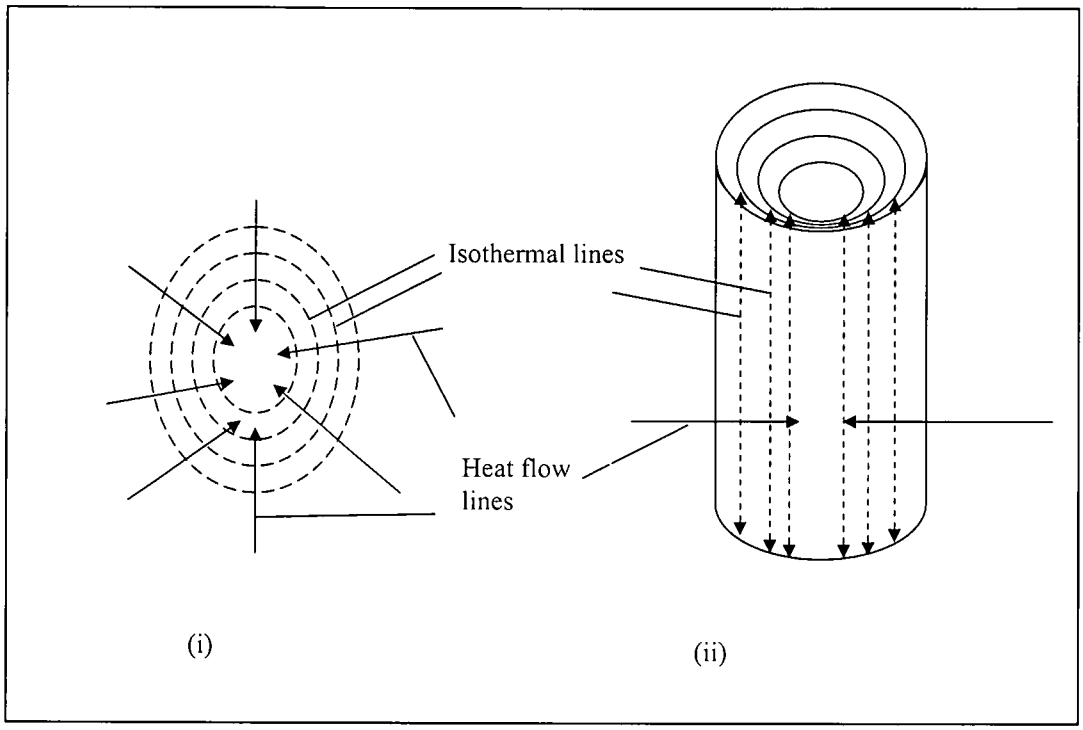

Figure6.2. Borehole isothermals Top (i) and side view (ii) (in the vertical, z-direction) and flow lines (horizontal, x-direction, concentric inwards) due to heat conduction from warmer groundwater all round a water column of cold water inside the center of a borehole,.

$$T_{xx}(x,y)+T_{yy}(x,y)=0$$

Hence $T(x,y)$ satisfies Laplace's equation and is a harmonic function.

If the domain in which $T(x,y)$ is defined is simply connected, then a conjugate harmonic function $S(x,y)$ exists, and

$$F(x)=T(x,y)+iS(x,y) \quad \text{.....(7)}$$

F(x) is an analytic function. The curves $T(x,y)=K_1$ are called isothermals and are lines connecting points of the same temperature. The curves $S(x,y)=K_2$ are called the heat flow lines, and heat flows along these lines from points of higher temperature to points of lower temperature. The situation is illustrated in Figure6.1. Boundary value problems for this type of steady state temperatures are realizations of a Dirichlet problem where the value of the harmonic function T(x, y) is interpreted as the temperature at the point (x, y).

Taking two parallel planes perpendicular to the y-plane (like the walls of borehole UO5) that pass through the vertical lines x = a, and x = b, and that the temperature is held constant at the values T(x, a) = T_1 and T(x, b) = T_2, respectively, on these planes at the time of the introduction of the cold water at two degrees Centigrade instantaneously using the trigger tube apparatus. Then T(x, y) is given by,

$$T(x,y) = T_1 + \frac{T_2 - T_1}{b-a}(y-a) \quad \text{..... (8)}$$

The two-dimensional solution is constructed at points in the vertical strip $a < lm(x) < b$ in the complex plane, and within the time taken to change from initial to final temperature, $T_1 < lm(T) < T_2$. A reasonable assumption is that the temperature at all points on the plane passing through the line x = x_o is constant (isothermal). Hence, T(x, y) = t(x), where t(x) is a function of x alone. Laplace's equation implies that t''(x) = 0, and an argument similar to that in (6) above, shows that the solution T(x, y) has the form given in the preceding equation (8).

The isotherms $T(x,y) = \alpha$ are approximately vertical lines (within 2 °C) Figure6.3. This means that, the heat as groundwater flows into the borehole will be conducted in the horizontal direction, which is also the direction of groundwater flow. The conjugate harmonic function of heat flow and groundwater flow is;

$$S(x,y) = \frac{T_1 - T_2}{b-a}x, \quad \text{.....(9)}$$

and the heat flow lines $S(x,y) = \beta$ are horizontal segments between the vertical lines. If $T_1 > T_2$, then the heat flows along these segments from the plane through x = a, to the plane through x = b, as illustrated in Figure6.1 and figure6.2 (i&ii). Heat can flow only perpendicular to isothermals and not along isothermals by conduction because there must be a gradient.

From the above, a major part of the heat transported by warmer groundwater flowing through the colder water will be in the horizontal direction as that transported by forced advection, within the period of the test. As such, a measure of the change in temperature with time in the cold water, will give a good estimation of the groundwater velocity, and show where there are fractures and flow zones. The method uses cold water at two degrees Celsius throughout the full length of the well or any section of interest, released instantaneously by use of a trigger tube designed for this purpose. The warmer groundwater, flowing into the borehole increases the temperature of the cold water at a rate proportional to the groundwater velocity from fractures or flow zones. These flow zones and fractures are then identified from their thermal signatures along the length of the borehole. The rate of temperature rise in the cold water in the borehole could be used to estimate the groundwater velocity. The method is analogous to the point dilution test (Drost et al, 1968).

6.6.2 Heat convection (Forced convection)

The standard one-dimensional transport equation below for heat, or rather, for the change of temperature, is identical to the advection-reaction-dispersion equation for a chemical substance (De Marsily, 1986):

$$(\theta\rho_w k_w)\frac{\partial T}{\partial t} + (1-\theta)\rho_s k_s \frac{\partial T}{\partial t} = -(\theta\rho_w k_w)v\frac{\partial T}{\partial t} + \kappa\frac{\partial^2 T}{\partial x^2} \quad \text{..... (9)}$$

where T is the temperature (℃), θ is the porosity (a fraction of total volume, unit less), ρ is the density (kg/m ^{3}), k is the specific heat (kJ℃ $^{-1}$ kg $^{-1}$), κ is a term

which entails both the dispersion by advective flow and the heat conductivity of the aquifer (kJ℃ $^{-1}$ m $^{-1}$ s $^{-1}$), and subscripts *w* and *s* indicate water and solid, respectively. The temperature *T* is assumed to be uniform over the volume of water and formation.

Dividing equation (1) by $\theta\rho_w k_w$ gives:

$$R_T \frac{\partial T}{\partial t} = -v\frac{\partial T}{\partial t} + \kappa\frac{\partial^2 T}{\partial x^2} \quad \text{..... (10)}$$

where, $R_T = 1 + \frac{(1-\theta)\rho_s k_s}{\theta\rho_w k_w}$ is the temperature retardation factor (unit less), and

$\kappa_L = \frac{\kappa}{\theta\rho_w k_w}$ is the thermal dispersion coefficient. The thermal dispersion coefficient contains a component for pure diffusion, and a component for dispersion due to advection: $\kappa_L = \kappa_e + \beta_L v$, similar to the hydrodynamic dispersion coefficient. This analogy permits the use of the same numerical scheme for both mass and heat transport.

6.6.3 Application

De Marsily (1986) suggests that the thermal dispersivity β_L and the hydrodynamic dispersivity α_L (**6.6.2** above) may be equal, whereas the thermal diffusion coefficient κ_e is orders of magnitude larger than D_e. Thus, dispersion due to advection can be calculated with the same algorithm for both mass and heat.

Assuming this is true, then, we can consider the segment of a borehole as in the diagram below. With a radius r, a vertical cross-sectional area through its center, A. (Area in blue). If the initial Temperature of the water was T_o, the

temperature after a period of time t is T and the volume of the cylindrical segment is V.

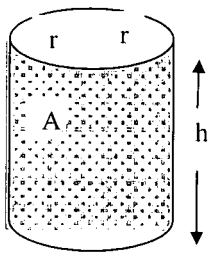

The change in temperature of the water with time in the borehole is given by;

$$\frac{dT}{dt} = A\bar{v}\frac{T}{V} \quad \text{..... (11)}$$

The cross-sectional area A = 2 r h, the surface area of the cylindrical section S = 2π r h and the volume of the segment V = π r ^{2} h and $\bar{v}$ is the velocity of flow. Replacing (A) and (V) in equation (1)

$$\frac{dT}{dt} = 2\pi rh\bar{v}\frac{T}{\pi r^2 h} \quad \text{giving,} \quad \frac{dT}{dt} = 2\bar{v}\frac{T}{r} \quad \text{.....(12)}$$

Intergrating (12) above, $\frac{r}{2}\int\frac{dT}{T} = \bar{v}\int dt$ gives $\frac{1}{2}r$ ln (T) + B = $\bar{v}$t ..... (13)

At time 0, t = 0, $\bar{v}$t = 0 and T = T_o

$\frac{1}{2}r$ ln (T_o) = -B ..... (14)

Replacing the (B) in (3) with (4)

$\frac{1}{2}r$ ln (T) - $\frac{1}{2}r$ ln (T_o) = $\bar{v}$t ; $\frac{1}{2}r$ [ln (T) – ln (T_o)] = $\bar{v}$t

$$\frac{1}{2} r \ln \left(\frac{T}{To}\right) = \bar{v} t$$

$$q\alpha = \bar{v} = \frac{1}{2t} r \ln \left(\frac{T}{To}\right) \quad \text{..... (15)}$$

q is the Darcy velocity which is equal to $\bar{v}$ when α =1(parallel plate model for fracture has porosity as 1 at the fracture in the borehole using Thermal dilution test (TDT). Analogous to point dilution test of solute transport by Drost *et al* (1968).

The value of K can then be determined, using the groundwater gradient I, and this Darcy velocity.

Considering the segment of the borehole as above, if the initial temperature and volume of the segment is known, we can calculate how much volume of water will be necessary to change the temperature to the final temperature from thermodynamics, using the specific heat capacity of water within 10-20 degrees Centigrade which is C_v = 4.184 (constant volumes).

Thus,

$$T_1 V_1 / T_2 V_2 = C_V \quad \text{..... (17)}$$

$$\Rightarrow V_2 = T_1 V_1 / T_2 C_V \quad \text{..... (18)}$$

$$q = V_2 / At \quad \text{..... (19)}$$

Since area A = 2rh; $V_1 = \pi r^2 h$; $T_1 = T_i$; $T_2 = T_f$ $q = V_2 / 2rht$

$q = \frac{1}{2} V_2 / rht$ ..... (20)

Replacing V_2 in (20) by V_2 in (18),

$$q = \frac{\pi}{2t} r * \frac{nT_i}{C_v T_f} \quad \text{..... (21)}$$

C_v = Heat capacity of water (at constant volumes). C_v = 4.184

n = Flow dimension. Here, n = 2. Flow is in the x-y plane.

q = Darcy velocity

r = Radius of borehole

h = Length of segment

t = Time elapsed after introduction of cold water by trigger tube to get from

T_i to T_f

T_i = Initial temperature after introduction of cold water by use of trigger tube.

T_f = Temperature at end of test after time t.

During the test, the water level in the borehole is constant. The volume of water is constant since inflow = outflow across the centre of the borehole in the direction of flow. Change in temperature due to advection, is proportional to rate of change of inflowing volume of ground water in the borehole. Heat exchange between the water in the borehole and the formation is negligible since the ground water causing the change in temperature is at same temperature as the formation. The two systems A (Groundwater) and B (Formation), are in thermal equilibrium with one another. Thermal diffusion may require an additional calculation when it

exceeds hydrodynamic diffusion. The temperature retardation factor and the thermal diffusion coefficient are important. Both parameters may vary in time, but are uniform (and temperature independent) over the flow domain since the cold water cannot lose heat to the formation or groundwater.

The similarity assumed here between thermal and hydrodynamic transport is an approximation which may fall short because, diffusion of mass is by some orders of magnitude larger in water than in the rock formations in the borehole, whereas diffusion of heat is comparable in the water and in the formation, although often anisotropic in the formation. This difference in thermal diffusivity may lead to complicated heat transfer at phase boundaries which is not accounted for here. We could not consider the convection that may have developed in response to temperature gradients during our experiment.

6.4.0 APPARATUS

6.4.1 The trigger tube

A trigger tube for injection tests in wells (described in the preceding chapter) was used. Five PVC tubes of six meter length where used for this test to a depth of 28m.

6.4.2 Test-temperature determination (Cold water)

The determination of the test water temperature, is calculated by taking into consideration the temperature of the borehole water (Background temperature T_b), the total volume of water in the borehole V_T, the volume of water outside the

trigger tube V_b and its temperature T_b, the volume of the trigger tube V_t and the temperature of the water in the trigger tube T_t, using the formulae below.

From laboratory experimentation, the input temperatures for various trigger tube sizes and resultant temperature for the thermal dilution tests' values were gotten from;

$$T_T V_T = T_b V_b + T_t V_t \quad \text{..... (22)}$$

$$T_T = (T_b V_b + T_t V_t)/V_T \quad \text{..... (23)}$$

$$V_T = \pi r_T h \quad \text{..... (24)}$$

$$V_t = \pi r_t h \quad \text{..... (25)}$$

$$V_b = \pi(r_b - r_t)h \quad \text{..... (26)}$$

T_T = Temperature required for carrying out test in the whole borehole (Test temperature)

T_t = Trigger tube Temperature, input temperature of cold water.

T_b = Borehole background temperature (background temperature)

V_T = Total borehole volume

V_t = Trigger tube volume (*includes volume due to thickness of tubes*)

V_b = Borehole volume outside trigger tube

h = Length of test segment

r_b = Radius of borehole

r_t = Radius of trigger tube

Laboratory tests carried out using trigger tubes of 63mm, 100mm, 110mm and 120mm diameter, to determine the input temperature and the required volumes of cold water, for any desired initial cold water temperature for the test, using trigger tubes of different sizes were used to derive a temperature calculator. Figure6.3

In the field test water was cooled to a temperature of two degrees Celsius. Using110mm diameter PVC pipes at 9.6 litres of cold water per meter length of pipe. A total of 267 litres of cold water from the twelve 25 litre plastic containers filled with water that was cooled at the biochemistry laboratory cold room II. The water temperature was two degrees Celsius, with an EC of 196 micro siemens.

6.4.3 EC meters

These were of two types;

a) Solinst Temperature/Level/Conductivity (TLC) meter.

b) A multi-parameter probe (Ecowatch)

These were used to measure water levels and profile the borehole for EC and temperature

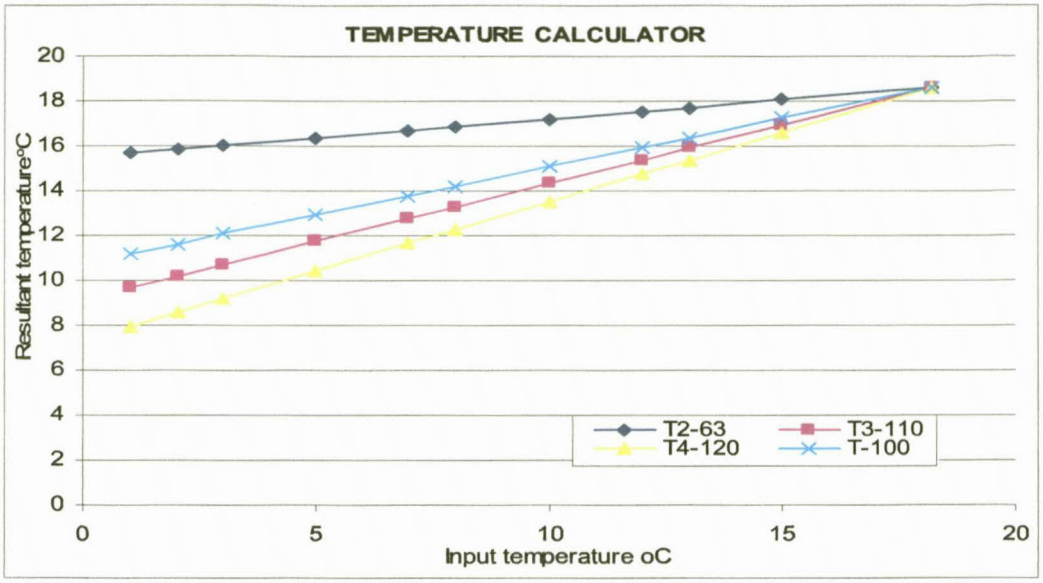

a) For each input water temperature for any particular trigger tube size, a resultant temperature was measured instantaneously on introduction into the borehole simulator as the water from the trigger tube and that in the borehole mix.

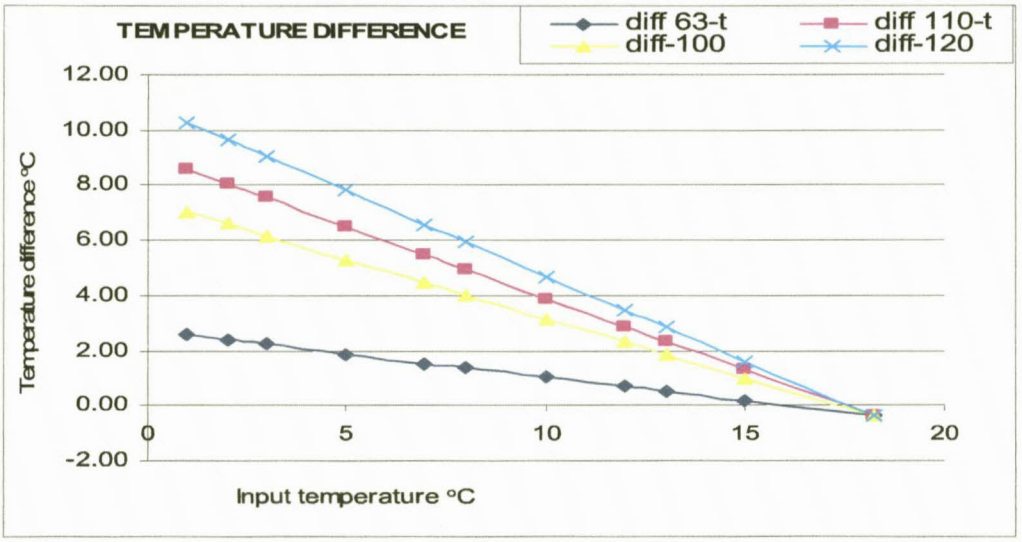

b) Temperature difference between the cold water introduced into the borehole using each trigger tube size and the resultant final borehole water temperature.

Figure6.3. Temperature calculator for thermal dilution tube method for various sizes of trigger tube

6.4.4 Winch

A winch was used to lower and raise the trigger tube assembly into the borehole. It was made up of a solid tripod, pulley, gear and sprocket and a 5mm diameter stainless steel cable.

6.4.5 Clamps

A set of three clamps to hold the trigger tube assembly unto the borehole casing and to couple and decouple the PVC tubes during insertion and withdrawal from the borehole were used. It is very important to clamp the trigger tube assembly firmly attached to the borehole casing, to resist the enormous buoyancy forces that come into play, pushing upward when the tube assembly becomes empty, after all the water has been pumped out of the trigger tube assembly before the introduction of the solute into the trigger tube assembly. This may present a hazard if the trigger tube assembly is not firmly attached.

6.4.6 Submersible pump

A 0.5 horse power, 4cm diameter 2l/min Grumfos submersible pump was used to pump water out of the trigger tube assembly. No pumping takes place in the borehole itself thus any perturbations.

6.5.0 Test procedure

The procedure to carry out the test using the trigger tube assembly is as in **5.3.3** in the chapter above.

6.6.0 RESULTS

6.6.1 Thermal profile and Fracture Positions

The cold water at 2 degrees mixed instantaneously with the borehole water at 19.45 degrees to a temperature of 9.98 degrees. And the change in temperature with time was recorded. Data from the thermal dilution test, table6.1 & 6.2, were normalized by subtracting the initial test temperature at the time recording commenced, T_o, from the final temperature at end of test T_f, to get the total change in temperature ΔT during the test. (Figure6.4), and then subtracting the least value of ΔT from the other ΔT values, to determine the difference of the difference in temperature within the test period and within the set of values from the surface to the bottom of the borehole since the measurements were carried out by the dropdown lift method which creates a time lag in successive measurements. The normalized values were then plotted, Figure6.6.

Table6.1. EC and temperature measurements from the field thermal dilution test on borehole UO5.

Depth m	Time sec	Temp °C	EC µS	Time sec	Temp °C	EC µS	Time sec	Temp °C	EC µS	Time sec	Temp °C	EC µS
12	0	12.4	248	663	12.4	241	1488	13	271	2129	13.6	284
12.5	12	12.3	221	668	12.4	228	1493	12.9	238	2120	13.5	240
13	21	12.3	203	672	12.2	207	1499	12.7	216	2112	13.5	224
13.5	27	12.2	213	677	12.4	200	1505	12.7	212	2102	13.6	217
14	35	12	243	682	12.5	196	1511	12.9	205	2086	14	211
14.5	44	12.1	226	691	12.6	195	1519	13.1	202	2075	14	205
15	51	12	205	697	12.7	195	1523	13.1	199	2067	14.1	206
15.5	65	12.1	199	702	9.8	169	1530	13.1	197	2058	14.6	211
16	72	12.2	192	721	9.6	169	1543	13.1	198	2048	14.9	214
16.5	79	12.2	202	726	9.4	169	1551	13.2	198	2041	15	220
17	85	12.3	192	731	9.2	171	1559	13.2	208	2031	15.2	228
17.5	93	12.5	189	739	9.2	171	1584	14.4	213	2024	15.4	243
18	101	12.6	202	746	9.4	169	1594	14.7	205	2014	15.6	266
18.5	108	13	192	753	9.4	171	1600	14.7	208	2003	15.7	289
19	113	13.1	196	756	9.5	171	1605	15	208	1900	16	334
19.5	121	13	205	759	9.8	169	1610	15.1	276	1892	16.6	364
20	128	13.2	196	765	9.8	170	1615	15.4	335	1887	17.1	431
20.5	137	13.4	207	770	9.7	171	1622	15.5	329	1880	17.6	593
21	145	13.9	215	773	9.9	169	1628	15.6	510	1872	17.9	635
21.5	157	14.5	233	777	10	171	1635	16.5	565	1841	17.9	704
22	162	14.5	250	781	10.4	169	1641	16.7	547	1834	17.9	720
22.5	170	14.6	270	790	10.4	169	1648	16.7	560	1827	18	740
23	175	15	289	795	10.5	171	1650	19.9	619	1817	18.1	842
23.5	244	15.6	323	800	10.7	170	1685	17	585	1811	18.2	841
24	253	15.6	422	804	10.9	169	1689	17.9	892	1806	18.2	941
24.5	257	15.6	418	808	11	171	1694	18	876	1800	18.2	940
25	262	15.9	418	815	11.2	172	1700	18	922	1784	18.2	944
25.5	266	16	420	820	11.2	170	1706	18.1	933	1764	18.2	1054
26	270	16	446	826	11.2	170	1712	18.2	908	1756	18.2	1054
26.5	282	16	458	830	11.2	170	1717	18.2	1148	1748	18.2	1066
27	288	16	461	833	11.4	170	1721	18.2	1147	1743	18.2	1094
27.5	306	16	469	838	11.4	171	1725	18.2	1145	1739	18.2	1156
28	314	16.1	459	841	11.6	169	1728	18.2	1130	1735	18.2	1162

Table6.2. EC and temperature measurements from the field thermal dilution test on borehole UO5. (Continued)

Depth m	Time sec	Temp °C	EC µS	Time sec	Temp °C	EC µS	Time sec	Temp °C	EC µS	Time sec	Temp °C	EC µS
12	2148	14.1	255	2470	14.5	281	5136	16.6	274	5429	15.5	285
12.5	2158	14	243	2478	14.4	251	5141	16.3	279	5439	15.7	272
13	2164	14.6	243	2786	14.4	245	5149	15.9	258	5448	15.7	260
13.5	2173	13.9	222	2494	14.4	241	5158	15.5	254	5457	15.7	254
14	2182	14	217	2505	14.4	227	5164	15.5	246	5466	15.9	252
14.5	2191	14	210	2514	14.4	223	5176	15.4	243	5477	15.9	245
15	2198	14	207	2523	14.1	208	5182	15.5	240	5491	16	244
15.5	2215	11.9	174	2531	13.2	179	5194	15.5	239	5500	16	243
16	2223	10.9	170	2539	11.6	177	5207	15.6	241	5512	16	243
16.5	2230	10.6	170	2550	11.1	171	5214	15.6	243	5524	16	247
17	2236	10.6	170	2562	11.1	170	5224	15.7	245	5537	16.1	253
17.5	2243	10.6	170	2578	11	169	5235	16	255	5551	16.5	260
18	2255	10.6	169	2587	11.1	169	5244	16	259	5563	16.6	279
18.5	2261	10.6	170	2598	11.2	169	5254	16.1	332	5572	16.7	303
19	2268	10.7	170	2607	11.4	170	5262	16.5	396	5576	17.1	355
19.5	2277	10.7	170	2620	11.4	169	5274	16.7	397	5615	17.4	456
20	2282	10.9	169	2627	11.7	169	5282	17	484	5631	17.6	492
20.5	2293	11.2	169	2638	12	168	5292	17.4	556	5637	18.4	630
21	2301	11.4	170	2651	12.2	169	5302	17.6	679	5642	18.5	708
21.5	2311	11.6	169	2661	12.4	169	5309	17.9	641	5652	18.2	693
22	2322	11.9	170	2678	12.5	169	5317	17.9	688	5663	18.2	707
22.5	2333	12.1	169	2693	12.6	169	5324	18	704	5672	18.2	726
23	2341	12.2	169	2703	12.6	169	5329	18.2	713	5676	18.4	772
23.5	2353	12.4	169	2716	12.9	168	5342	18.2	666	5686	18.1	688
24	2365	12.5	169	2724	12.9	169	5351	18.1	637	5711	18	657
24.5	2379	12.5	172	2732	13	171	5356	18	632	5721	17.9	623
25	2386	12.6	171	2741	13	171	5368	17.9	618	5728	17.9	613
25.5	2394	12.7	171	2761	13	171	5376	17.9	608	5744	17.9	594
26	2401	12.9	172	2771	13	171	5385	17.9	589	5752	17.7	592
26.5	2408	12.9	173	2790	13.1	170	5396	17.9	575	5759	17.6	589
27	2441	13.1	171	2796	13.2	170	5406	17.6	568	5769	17.6	576
27.5	2445	13.2	170	2806	13.2	170	5409	17.6	570	5773	17.6	566
28	2449	13.2	170	2816	13.2	170	5418	17.6	589	5783	17.6	575

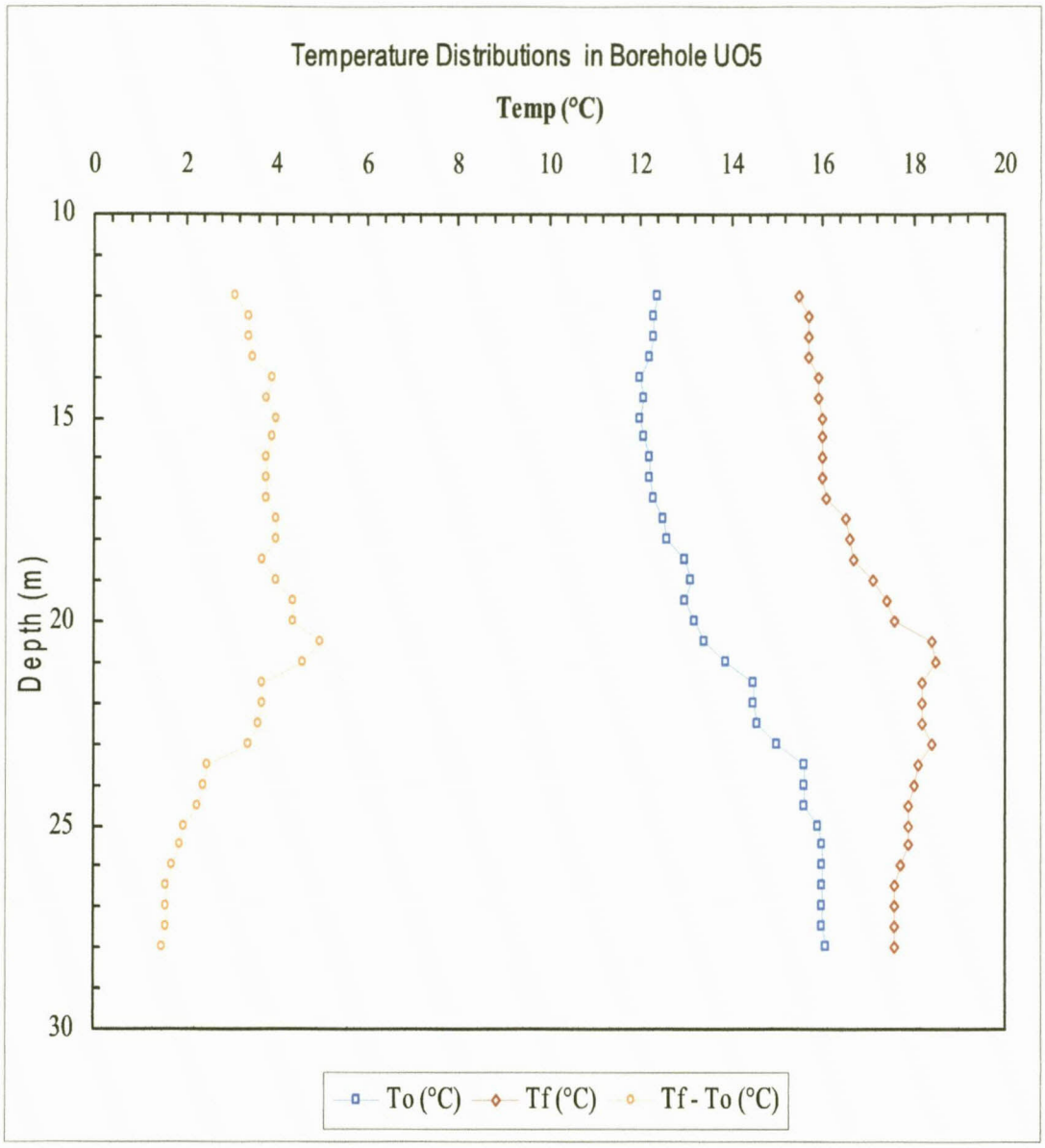

Figure 6.4 Temperature distributions for the thermal dilution test carried out in borehole UO5. T_o represents the initial temperature measurements, T_f represents the final temperature measurements and $\Delta T = T_f - T_o$ represents the change in temperature during the test.

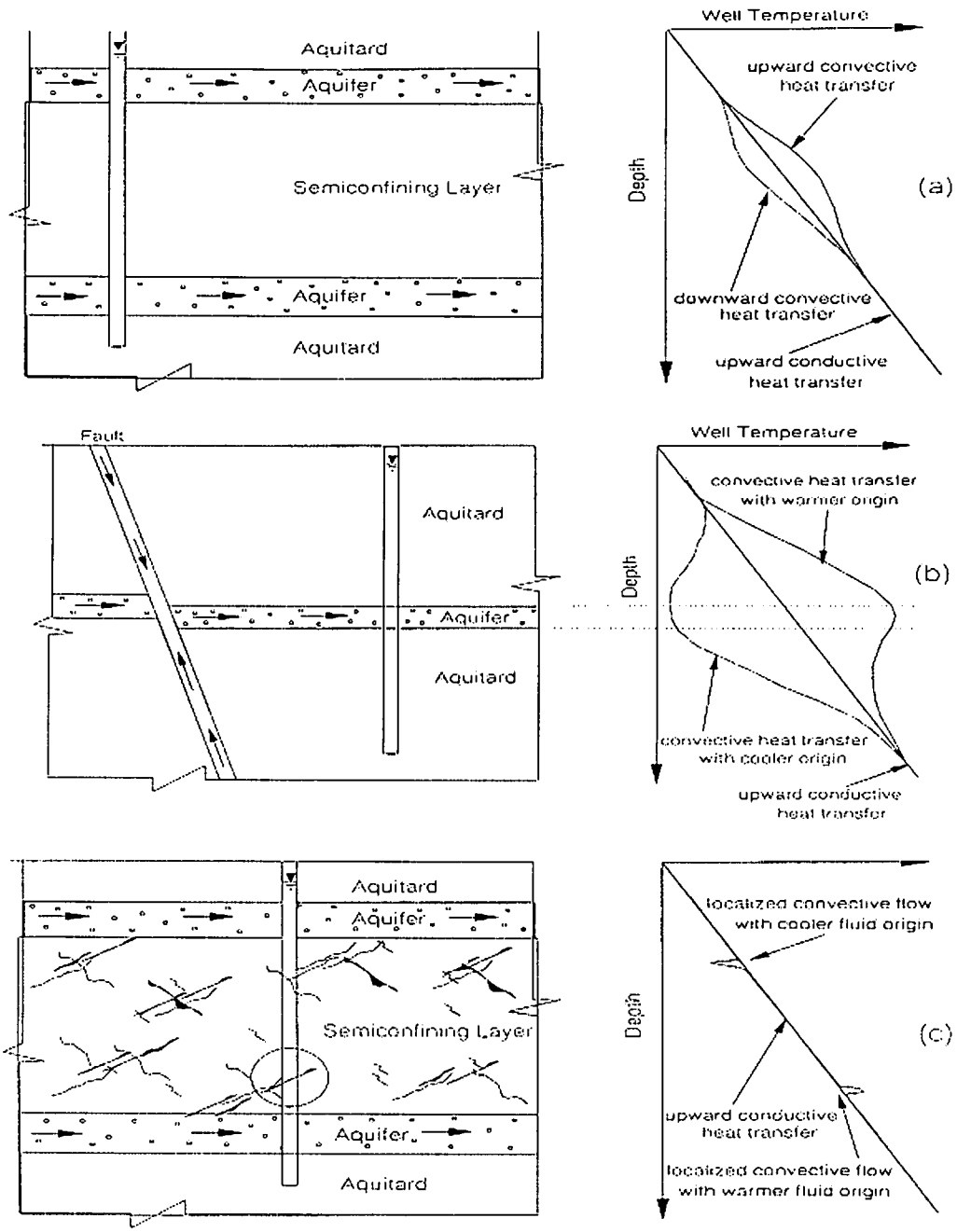

Figure6.5 Patterns of non-conductive temperature profiles in different hydrothermal settings: a. temperature profile affected by vertical groundwater movement; b. temperature profile affected by horizontal groundwater flow of either warmer or cooler origins, Shemin Ge (1998).

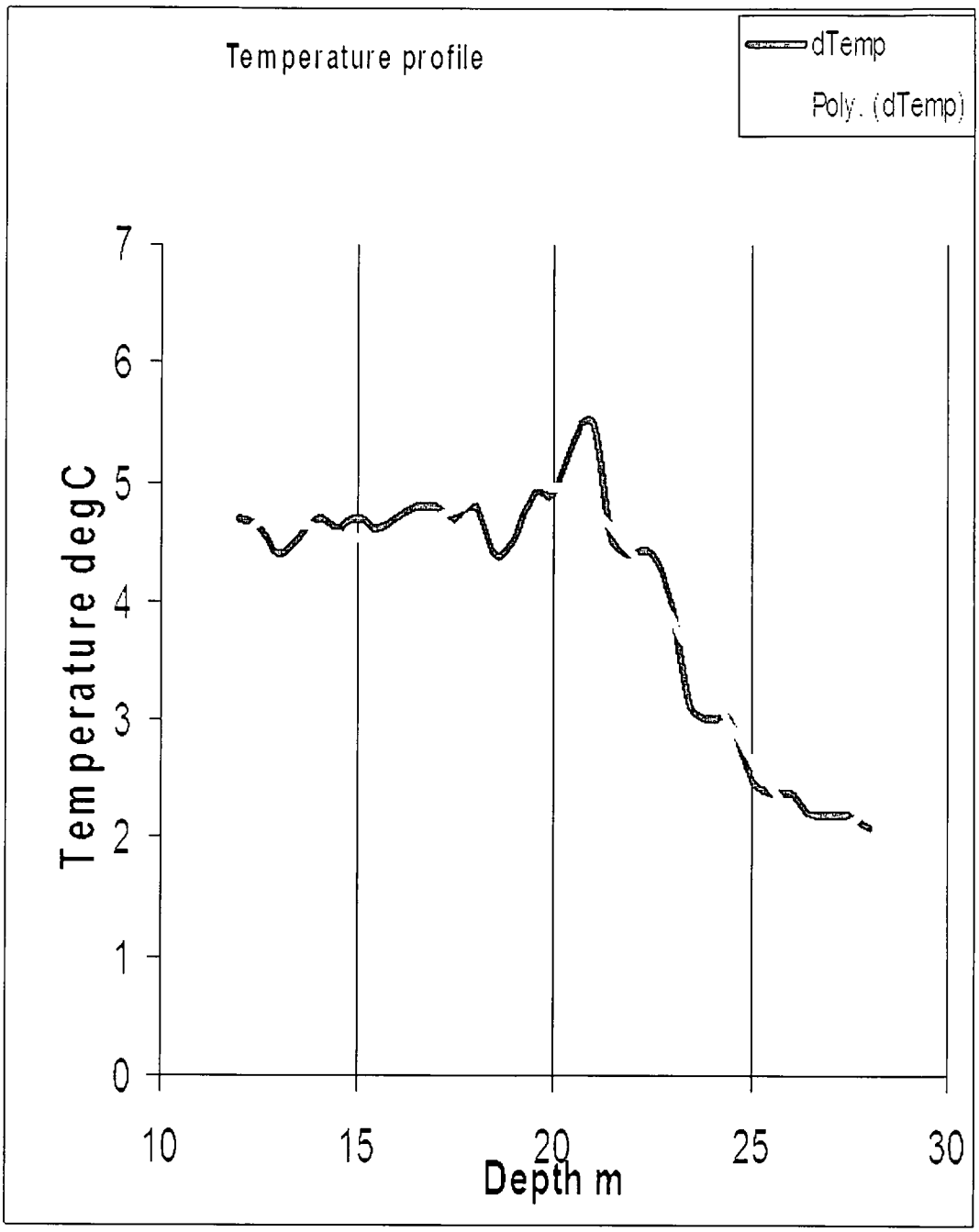

Figure6.6. Temperature profile of borehole UO5. Plot of temperature against depth. The profile given by the polynomial fit is characteristic of a fracture affected by horizontal groundwater flow with convective heat transfer of a warmer origin in figure6.4 (b), as was the case in the setup of the field test.

$\Delta T = T_i - T_f$ ..... (7)

T_i is the initial test temperature after introduction of cold water into borehole.

T_f is the final test temperature at the end of the test in the borehole.

The resultant temperature profile shows spikes at 14.0m, 15.0m, 16.8m, 18.2m, 19.8m, 21m, 22.4m, 24.0m, 26.1m and 27.4m. Comparing these spikes to the acoustic scan and lithological section (Figure6.8) of borehole UO5, with depth (Figure6.9) shows that, the spikes correspond to some of the fractures. The largest spike corresponded to a depth of 21m which is where the major fracture is found. This shows that the thermal dilution test detects fractures in which ground water flows and the relative size of the spikes show the relative contribution to flow in the borehole of each fracture. The fractures which did not have corresponding thermal spikes were those in which there was very little or no ground water flow, and therefore no thermal hotter water inflow) signatures.

6.6.2 Darcy velocity (q)

From the field test data at 21m (Tables6.1&6.2),

T_o = 13.9 °C.

T = 19.4 °C.

t = 0.01 days

r = 0.08 m

π = 3.14

ln (T/ T_o) = ln 1.4 = 0.38.

Using equation (21)

q = (2x3.14x0.08x13.9) / (0.02x4.184x19.4)

q = 4.23 m/day

Also,

C_v = 4.184

N = 2

Using equation (15)

q = (3.14x0.08x0.38) / 0.02

q = 4.77 m/day.

These values tally with other estimates of Darcy velocity from other works on the UO5, using cross packer pump-tests by Botha et al, (1998) v = 4.86 m/day; Single well injection withdrawal tests by Van Tonder et al, (2000) v = 4.67 m/day and natural gradient tests by Akoachere Van Tonder (2008) v = 4.06 m/day.

Darcy velocity profile (values) for borehole UO5 from static water level to bottom where thus calculated, Figure6.11.

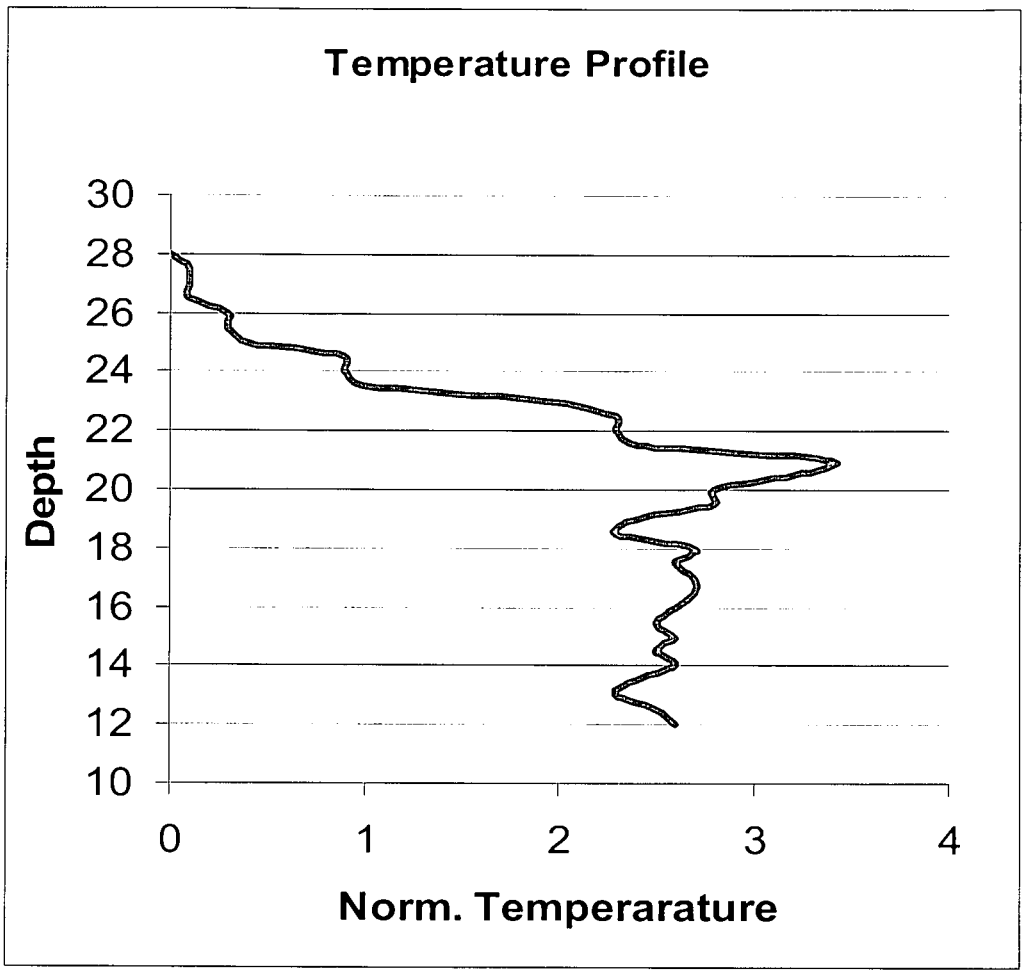

Figure6.7, Normalized temperature profile showing peaks denoting fractures, their relative velocities and groundwater flow contribution, Note the distinct spiked peaks.

6.7.0 DISCUSSIONS

The temperature profile in Figure6.6 shows that the flow is that of warmer water, inferring from Figure6.5. This confirms that during the test, warmer ground water flows into and then through the colder injected water in the borehole.

Placing the borehole log by the normalized temperature profile from the thermal dilution tests, the fractures from the logs corresponded to some of the spikes on the profile (Figure6.9). Also these same fractures were identified by the packer tests by Botha *et al* (1998) as those contributing to the flow of ground water in this aquifer, figure6.10. The major fracture determined by acoustic scan Figure6.8, borehole calliper and borehole camera imagery, is that found at the depth of twenty-one meters. It has been confirmed as the major contributor to the ground water flow in the aquifer at the test site, by pump-tests using packers (Botha et al, 1993) and this thermal dilution test.

A number of workers have carried out work on wells using temperature, notably, Grace et al (2005) who used 2.5 meter long heating probes to heat sections of the water in wells and the flow around in-situ heat based flow sensors by inverting thermistor temperature evolutions and using numerical simulations to obtain estimates of ground water flow velocity. Also, Tsang et al, (1990) replaced well bore water with de-ionized water and then profiling the well's electrical conductivity through time in his hydro-physical method. The results were then used in numerical simulations to estimate fracture parameters. These methods however are different from the new method developed here which replaces well-bore water with ice cold water and then the heat influx of the formation water is

used to determine directly, the fracture depth, fracture positions, number of fractures and the Darcy velocity of the fractures.

This method uses ice cold water which acts as a thermal insulator and has distinctly different heat conducting properties from heated water using various probes by Grace et al (2005) where heat moves from the probe's heater to the water and formation. While in the thermal dilution test, the ice-cold water insulates the cold water and does not release heat into the groundwater and formation. The hydro-physical method is a variation of well bore dilution test.

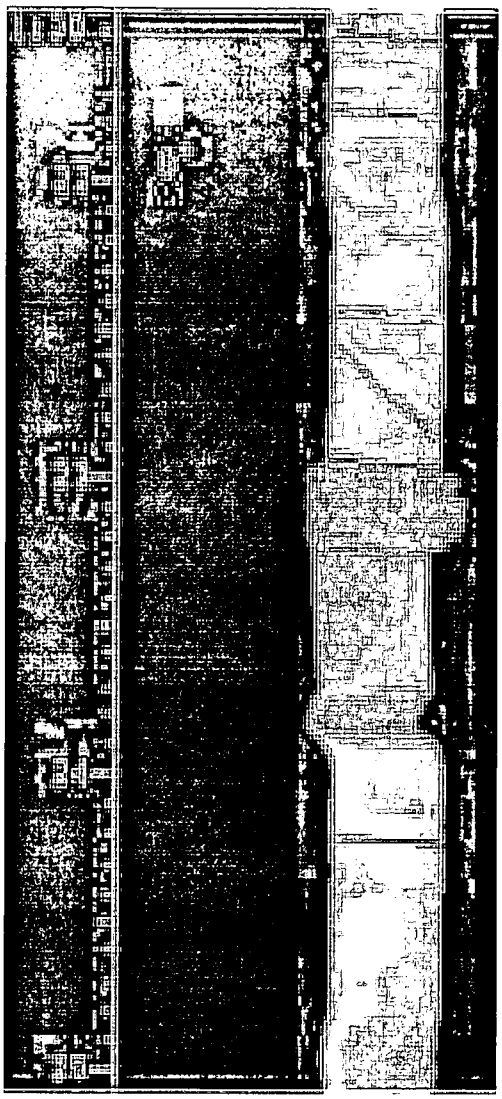

Figure6.8. Acoustic scan of borehole UO5, showing fractures at various depths (Botha et al, 1998). Some of these fractures correspond to the fractures detected by using the thermal dilution test. Those not detected are those with insignificant flow or no flow.

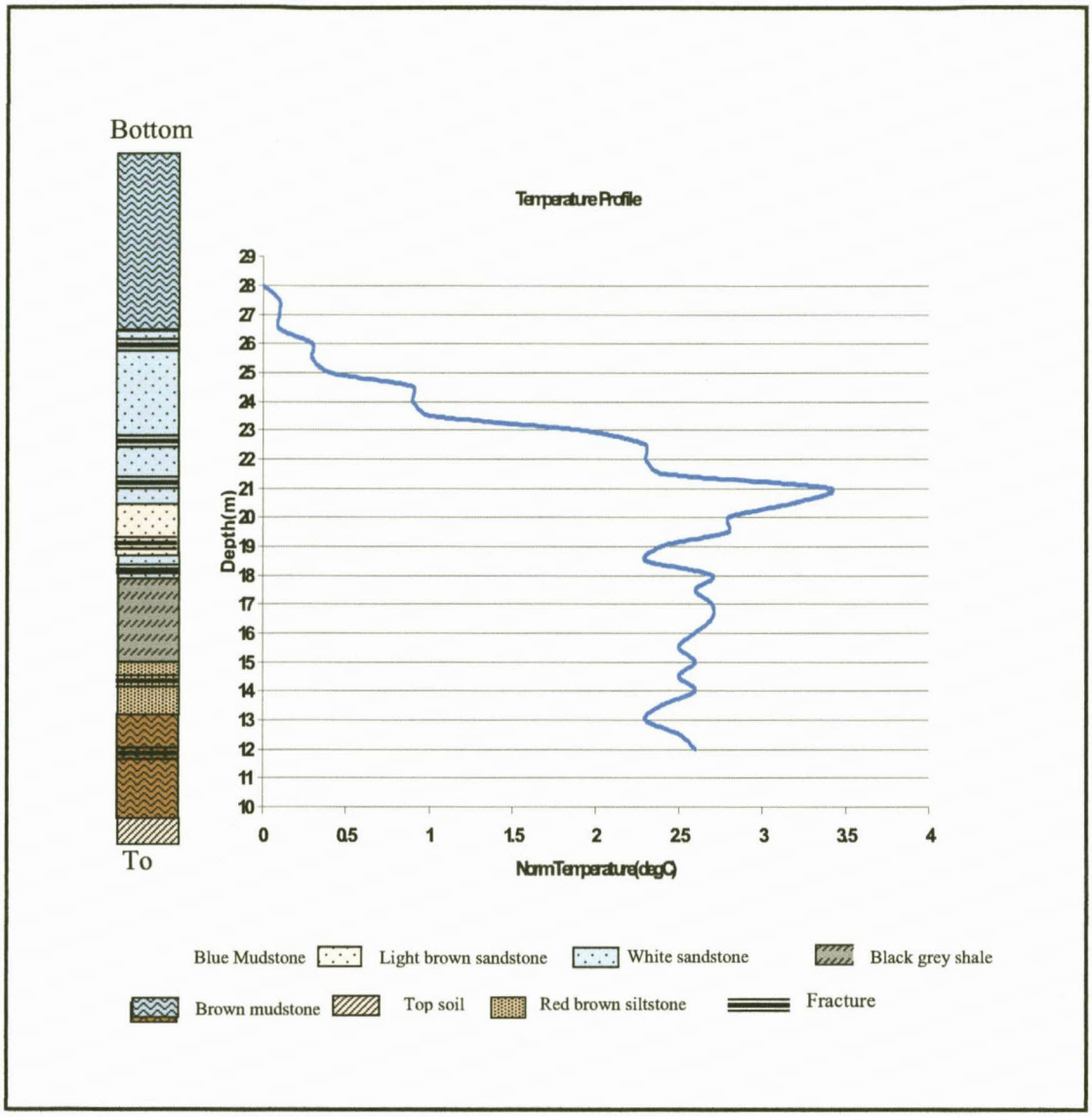

Figure6.9. Temperature profile and litho logical section of borehole UO5, showing fractures in the borehole and the corresponding spikes on the temperature profile from the thermal dilution test. (The borehole log is drawn topside down). Only fractures where there is flow and flow zones are reflected by the spikes in the thermal dilution tests' profile.

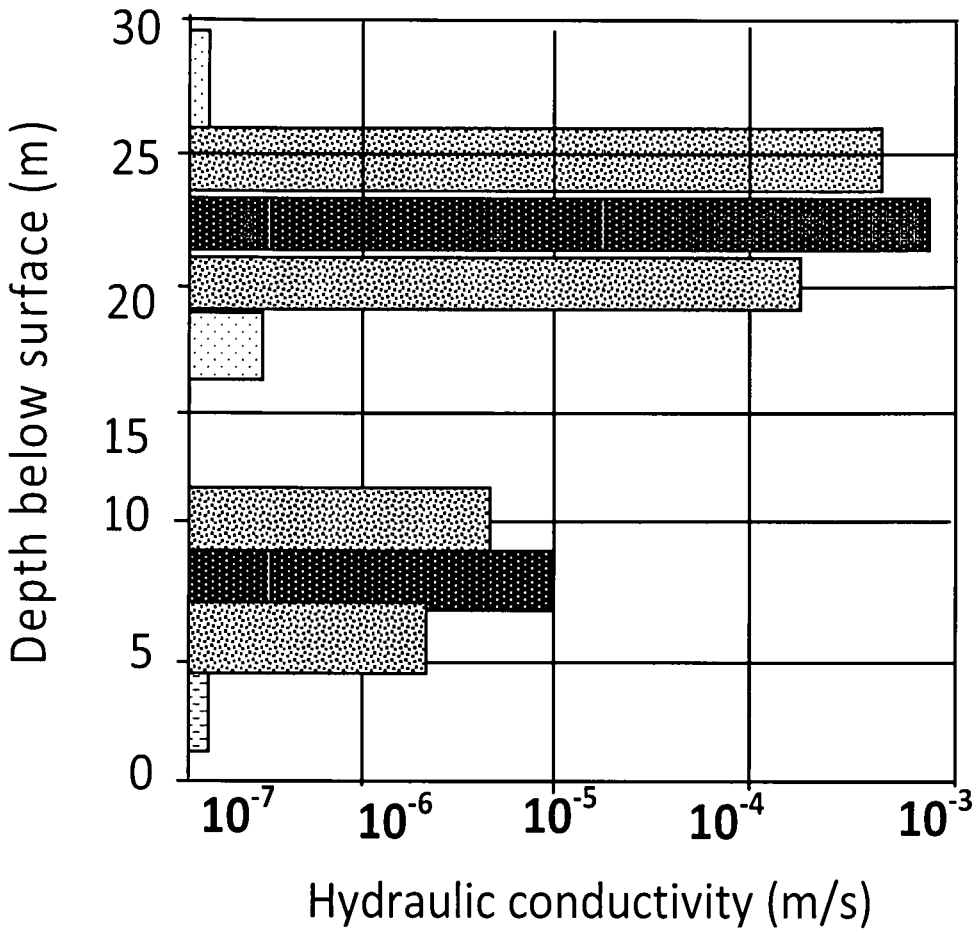

Figure6.10. Hydraulic conductivity values for UO5 cross packer tests (Redrawn after Botha et al, 1998) Note that the high hydraulic conductivity values correspond to the fractures at the depths depicted by the profile of the thermal dilution test.

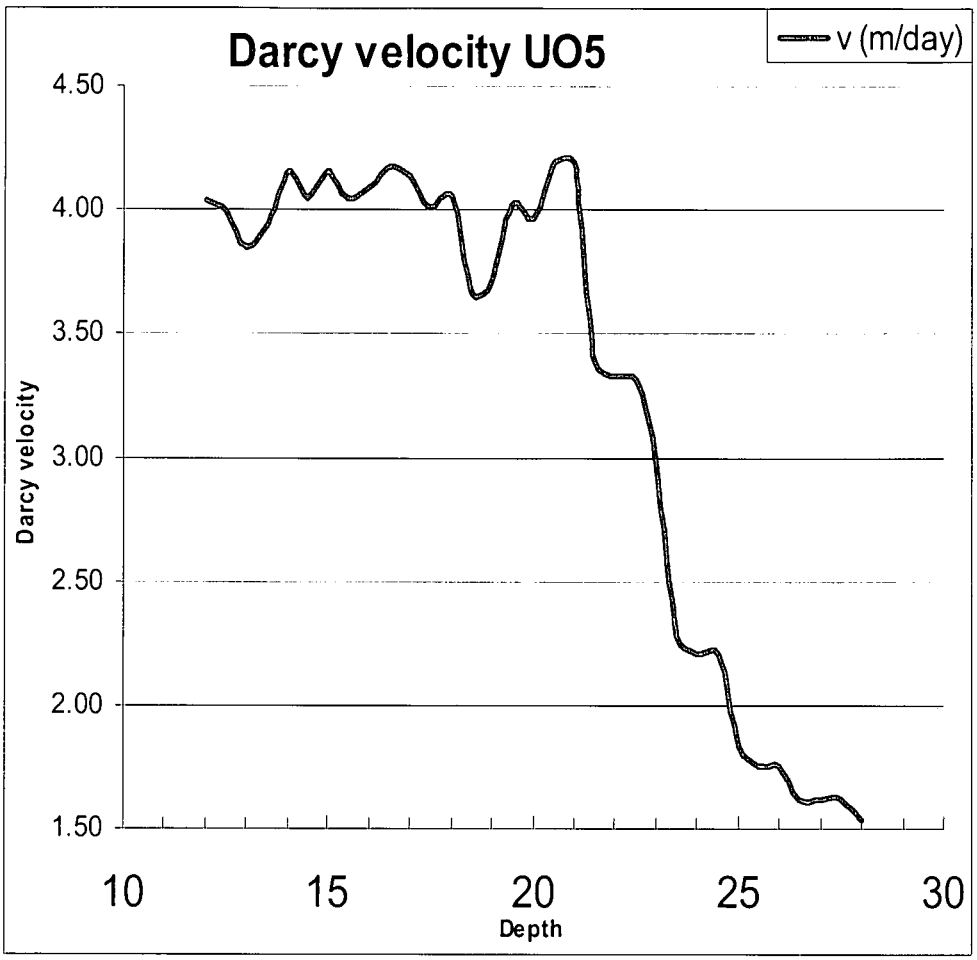

Figure6.11 Darcy velocity profile of borehole UO5 determined using the thermal dilution test method. The major fracture is at 21m.

s

6.8.0 CONCLUSION

The need for an apparatus and technique that can be used to determine fracture positions down hole and flow zones in fractured rock aquifers, together with the groundwater velocity (Darcy velocity) abounds. The thermal dilution test accurately determines the position and relative flow contribution of these fractures in fractured rock aquifers using a single borehole. Of importance also is the fact that, the determination of the Darcy velocity does not require a pre-knowledge of the aquifer porosity or effective porosity.

This test method also confirms that, solute and thermal transport in groundwater are coupled. The thermal dilution test is therefore a very important tool to be added to the field investigators kit for the characterization of fractured rock aquifers.

Advantages

- No need for a pre-knowledge of effective porosity.
- Detects fracture with flow.
- No specialized pump (Peristaltic etc)
- No isolation of test section or use of packers.
- Better control of water temperature (predetermined).
- The whole length of the borehole can be tested at once to give hydraulic characteristics from a single test in a single borehole.
- This test method uses few instruments and as such is quick to set up and carry out.

Disadvantages

- Values are for areas within the reach of the single well. Point values (small scale).
- Does not determine characteristics of vertical fractures in vertical boreholes.
- Does not detect fracture with no flow.

However, if the fractures are not parallel to the vertical borehole and many of such tests are carried out in a reasoned manner over an area, such data could become a powerful tool for the modelling of fractured rock aquifers.

7.0 CONCLUSION

From the work presented in the chapters above, I conclude that the results of this research, from the laboratory and field experiments gave two new apparatus and five new methods that are very useful in the characterization of fractured rock aquifers. These are;

i) Two new methods for the determination of mechanical and hydraulic fracture apertures in fractured rock aquifers.

ii) A new phreatic hydraulic conductivity apparatus for the determination of hydraulic conductivity.

iii) The partial hydraulic conductivity theory of bulk flow in aquifers. A new method for the determination of bulk flow hydraulic conductivity.

iv) The Trigger tube; a new apparatus for mixing solutes for injection well tests in boreholes.

v) The thermal dilution test; a new method for the determination of fracture positions, flow zones and groundwater velocities in fractured rock aquifers, using temperature as a tracer in single wells.

These methods and apparatus are innovative in the characterization of fractured rock aquifers and will go a long way to make studies in groundwater in all scales easier. The results from these tests using these methods and apparatus are accurate. Their use will go beyond the field of hydrogeology.

7.1 RECOMMENDATIONS

As in all research that have limited funding, time frame and scope, a PhD research cannot solve all the problems in the complex task of characterizing fractured rock aquifers. Future research in these domains should focus on the following ;

- Field testing of laboratory methods for aperture determination
- Development of computer programmes that will make computation of data fast and easy for the partial hydraulic conductivity theory.
- Develop wire line multi-parameter probe for the thermal dilution test.
- Design trigger-tube for small diameter drill holes to make tests in them much easier.
- Focus on research methods that can determine fracture parameters directly other than indirect methods.

REFERENCES

Akoachere, RA and Van Tonder, GJ (2008a) The trigger tube; a new apparatus for mixing solutes for injection tests in boreholes. (Unpublished).

Akoachere, RA and Van Tonder, GJ (2008b) A new method for the determination of phreatic hydraulic conductivity (Unpublished)

Akoachere, RA., Van Tonder, G., Yaya, OO & Menghistu, MT (2007) Partial hydraulic conductivity theory of bulk flow in aquifers. Paper presented at the 19th Annual conference; "Port Harcourt 2007" of the Nigerian Association of Hydrogeologists (NAH), 18th-23rd November 2007. Port Harcourt, Nigeria.

Alayamani, MS & Sen, Z (1993) Determination of hydraulic conductivity from complete grain-size distribution curves. Ground Water 31 (4) 551-555.

Allen, TT (1998) Field Laboratories in environmental Geology and Hydrogeology. Geological Society of America, Abstracts with Programs, 30 (7): A 306.

Almkvist, G & Berndt, B (1998) "Gauss, Landen, Keppler, Ramajuan, the Arithmetic-Geometric mean, Ellipse, π, and the Ladies' Diary". The American Mathematical Monthly., Vol. 95, No.7 p.585-608

ANCID (2000) Open channel seepage and control. Vol. 1.1 Literature reviews of channel seepage identification and measurement. Australian National Committee on Irrigation and Drainage. Prepared by Sinclair Knight Merz.

Anderson, MP (2005) Heat as a groundwater tracer. Groundwater. 43 (6): 951-968.

Botha, JF., Verwey, JP., Van der Voort, I., Vivier, JJP., Colliston, WP and Loock JC (1998) *Karoo Aquifers. Their Geology, Geometry and Physical Behavior* WRC Report No 487/1/98. Water Research Commission, P.O. Box 824, Pretoria 0001

Brassington, R (1988) Field Hydrogeology, Geological Society of London Handbook Series. Open University Press

Cey, EE., Rudolph, DL., Parkin, GW & Aravena, R (1998) Quantifying groundwater discharge to a small perennial stream in southern Ontario, Canada. Journal of Hydrology 210 :21-37.

Constanz, J., Tyler, SW and Kicklis, E (2003) Temperature methods for Estimating Percolation rates in Arid Environments Vadose Zone Journal 2:12-24

Cook, PG (2003) A guide to regional groundwater flow in fractured rock aquifers. CIRO, Land and water, Glen, SA . Australia. pp.108.

Cook, PG and Simmons, CT (2000) Using environmental tracers to constrain flow Parameters in fractured rock aquifers; Clare Valley, South Australia In: Faybishenko B., Witherspoon P.A. and Benson S.M. (ed.) *Dynamics of Fluids in Fractured Rock* Geophysical Monograph 122, American Geophysical Union, 337–347

Cook, PG., Solomon, DK., Sanford, WE., Busenberg E., Plummer, LN and Poreda, RJ (1996) Inferring shallow groundwater flow in saprolite and fractured rock using environmental tracers. Water Resources Research 32(6):1501–1509.

Darcy, H (1856) Les Fontaines Publique de la Ville de Dijon, V. Dalmont, Paris 647pp.

De Marsily, G (1989) Quantitative hydrology; groundwater hydrology for engineers Academic Press Inc, New York 440pp

Devlin, JF (2002) The Groundwater Velocity Probe. US Patent 6393925

Dijk, P., Berkowitz, B & Bendel, P (1999) Investigation of flow in water-saturated rock fractures using nuclear magnetic resonance imaging (NMRI). Water Resources Research 35, No. 2, 347–360.

Drost, WD., Klotz, A., Koch, H., Moser, F., Neumaier & Rauert (1968) Point dilution methods for investigating ground water flow by means of radio isotopes. Water. Resources Research 4: 125-146.

Dupuit J (1863) Etudes théoriques et pratiques sur le mouvement des eaux dans les canaux découverts et à travers les terrains permeables.2eme édition ; Dunot, Paris 304pp.

Duwelius RF (1996) Hydraulic conductivity of the streambed, East Branch Grand Calumet River, Northern Lake County, Indiana US Geological Survey Water-Resources Investigations Report 96-4218

Freeze, RA & Cherry, JA (1979) Groundwater. Prentice-Hall; Englewood Cliff inc, NJ. 604p.

Grace, WS., Barry, MF., Curtis, MO., Preston, DJ & Daley PF (2005) Interpreting velocities from heat based flow sensors by numerical simulations. Groundwater 44; 3. 386-393

Ge, S (1998) Estimation of groundwater velocity in localized fracture zones from well temperature profiles. Journal of Volcanology and geothermal research, 84; 93-101

Hakami, E & Larsson, E (1996) Aperture measurements and flow experiments on a single natural fracture. Int. J. Rock Mech. Mining Sci. Geomech., Abstr. 33, No. 4, 395–404.

Halevy, E (1968) Direction and velocity Guide book on nuclear techniques, Chapter IV B3, Technical report series: 139-155.

Hazen, A (1893) Some physical properties of sands and gravels. Massachusetts State Board of Health, 24th Annual Report

Hinsby, K., McKay, LD., Jorgensen, P., Lenczewski, M & Gerba, CP (1996) Fracture aperture measurements and migration of solutes, viruses, and immiscible creosote in a column of clay-rich till. Ground Water 34, No. 6, 1065–1075.

Hvorslev, MJ (1951) Time lag and soil permeability in groundwater observations Waterways Experiment Station Bulletin No. 36 Vicksburg, MI: US Army Corps of Engineers.

Jaleigh, B (2000) what is the formula for the perimeter of an ellipse?

Jorgensen, PR, Broholm, K, Sonnenborg, TO & Arvin, E (1998) DNAPL transport through macro-porous, clayey till columns. Ground Water 36, No. 4, 651–660.

Keller, A (1998) High resolution, non-destructive measurement and characterization of fracture apertures, Int. J. Rock Mech. Mining Sci. 35, No. 8, 1037–1050.

Konzuk, JS & Kueper, BH (2004) Evaluation of cubic law based models describing single-phase flow through a rough walled fracture. Water Resources Research 40, No. 2, 1–17.

Labaky, W, Devlin, J & Gilham R (2007) Probe for measuring groundwater velocity at the centimeter scale. American Chemical Society/ Environmental science and technology.vol.41, no 24.2007.pp8453-8458

Lamontagne, S., Dighton, J & Ullman, W (2002) CIRO, Land and water technical report.14/02, Australia

Lee, DR & Cherry, JA (1978) A field exercise on groundwater flow using seepage meters and mini-piezometers. Journal of Geological Education 27:6-10.

Lindgren, RJ & Landon, MK (2000) Effects of groundwater withdrawals on the Rock River and associated valley aquifer Eastern Rock County, Minnesota US Geological Survey Water-Resources Investigation Report 99-4157.

Love, A.J., Herczeg A.L., Armstrong D., Stadter, F and Mazor, E (1993) Groundwater flow regime within the Gambier Embayment of the Otway Basin, Australia: evidence from hydraulics and hydrochemistry. *J. Hydrol.* 143:297–338.

Love, AJ, Cook, PG., Harrington, GA and Simmons, CT (2002) Groundwater flow in the Clare Valley. Department for Water Resources, South Australia Report DWR02.03.0002, 43pp

Malkki, E & Wihuri, H (1983) Utilisation de traceurs pour mesurer la conductivité hydraulique. Bulletin de l'association internationale de Géologie de l'Ingénieur numéro 26-27. 473-476.

Mc Mahon, PB., Tindall, JA., Collins, JA., Hull, KJ & Nuttle, JR (1995) Hydrological and geochemical effects, on oxygen uptake in bottom sediments of an effluent-dominated river. Water Resources Research 31(10) 2561-2569.

Mathews, JH and Howell, RW (2006) Complex analysis for Mathematics and Engineering. Jones and Bartlett pub Inc, London W6 7PA, U K. pp 648

National Research Council (1996) Rock fractures and fluid flow: Contemporary understanding and applications. Washington, DC: National Academy Press.

Neretnieks, I (2007) Single well injection withdrawal tests (SWIW) in fractured rock. Swedish Nuclear and Waste Co (SKB); Rapport, R-07-54 Stockholm, Sweden

Nicholl, MJ., Rajaram, H., Glass, RJ & Detwiler, R (1999) Saturated flow in a single fracture: evaluation of the Reynolds equation in measured aperture fields. Water Resources Research 35, No. 11, 3361–3373

O'Hara, SK., Parker, BL., Jorgensen, PR & Cherry, JA (2000) Trichloroethene DNAPL flow and mass distribution in naturally fractured clay: evidence of aperture variability. Water Resources Research 36, No. 1, 135–147.

Panchrow, JF and Cherry, JA (1996) Dense Chlorinated Solvents and other DNAPL's in Groundwater; history, behavior, and remediation: Potland, Oreg.Waterloo Press, 522p.

Reitsma, S & Kueper, BH (1994) Laboratory measurement of capillary-pressure saturation relationships, in a rock fracture. Water Resources Research 30, No. 4, 865–878.

Renshaw, CE (1995) The relationship between mechanical and hydraulic apertures in rough-walled fractures. J. Geophys. Res. Solid Earth 100, No. B12, 24629–24636.

Rosenberg, DO (2000) Unsaturated-zone wedges beneath a large natural lake. Water Resources Research 36(12) 3401-3409.

Rutqvist, J (1996) Hydraulic pulse testing of single fractures in porous and deformable hard rocks. Q. J. Eng Geol. 29, No. 2, 181–192.

Samouelien, A., Vogel HJ & Ippisch (2006) Up-scaling the hydraulic conductivity based on topology of the Sub-scale structure. Advances in water resources Doi:10.1016/j.advwatres

Springer, AE., Petroutson, WD & Semmens BA (1999) Spatial and temporal variability of hydraulic conductivity in active reattachment bars of the Colorado River, Grand Canyon. Ground Water 37(3) 338-344.

Steele, A., Reynolds, DA., Kueper, BH & Lerner, DN (2006) Field determination of mechanical apertures, entry pressure and relative permeability of fractures using NAPL injection. Geotechnique 56, No 1, 27-38.

Toth, J (1999) Groundwater as a geologic agent: An overview of the causes, processes, and manifestations. Hydrogeology journal (7):1-14.

Tsang C.F., Hufschmied, P & Hale, FV (1990) Determination of fracture inflow parameters with a borehole fluid conductivity logging method. Water Resources Research 26(4):561–578.

Tsang, YW (1992) Usage of equivalent apertures for rock fractures, as derived from hydraulic and tracer tests. Water Resources Research 28, No. 5, 1451–1455.

U.S. Department of Interior Bureau of Reclamation (USDIBR) (1985) Groundwater manual; a guide for the investigation, development, and management of groundwater resources, Water resources technical publication.480pp

U.S. Department of the Army Corps (USDAC) (1970) Engineering and Design: Laboratory Soil Testing, EM1110-1906. U.S. Army Corps of Engineers, Washington D,C.

USEPA (2001) The State-of-the-Practice of Characterization and Remediation of Contaminated Ground Water at Fractured Rock Sites. EPA 542-R-01-010. United States Environmental Protection Agency.

Van der Kamp, G (1992) Evaluating the effects of fractures on solute transport through fractured clayey aquitards. Proc. 1992 Conf. of the International Association of Hydrogeologists, Canadian National Chapter, Hamilton, Ontario

Van Der Merwe, CJ (2008) Hydraulic Assessment of Low-yield Boreholes in Fractured Rock Aquifers, M.Sc. Thesis. University of The Free State (in Press)

Van Tonder, GJ., Botha, JF., Chiang, W-H., Kunstmann, H and Xu, Y (2001) Estimation of the Sustainable Yields of Boreholes in Fractured Rock Formations. *Journal of Hydrology*.241,70-90

Van Wyk, AE., Xu, Y., De Lange, SS., Van Tonder, GJ and Chiang, W-H (2000) Utilization of tracer experiments for the development of rural water supply management strategies for secondary aquifers. *WRC Report*, Pretoria, South Africa.

Van Wyk, AE (1998) Tracer Experiments in Fractured Rock Aquifers. M.Sc. Thesis. University of the Free State (unpublished)

Vukovic, M & Soro, A (1992) Determination of hydraulic conductivity of porous media from grain-size composition, Water Resources Publications, Littleton, Colorado

Wihuri, H & Malkki E (1980) Studying the ground water flow conditions. 3, Aqua. Scientific and technical Review Pp 0090-0091.

Yeo, I W., DeFreitas, M H & Zimmerman, R W (1998) Effects of shear displacement on the aperture and permeability of a rock fracture Int. J. Rock Mech. Mining Sci. 35, No. 8, 1051–1070.

Zijl, W (1999) Scale aspects of groundwater flow and transport systems Hydrogeology journal (7): 37-150.